Dissertation

SPECIFIC COILED COIL ASSEMBLY THROUGH SIZE-COMPLEMENTARITY

Submitted by

Nathan A. Schnarr

Department of Chemistry

In partial fulfillment of the requirements for the

Degree of Doctorate of Philosophy

Colorado State University

Fort Collins, Colorado

Summer 2004

Colorado State University

May 13, 2004

WE HEREBY RECOMMEND THAT THE THESIS PREPARED UNDER OUR SUPERVISION BY NATHAN A. SCHNARR ENTITLED

SPECIFIC COILED COIL ASSEMBLY THROUGH SIZE-COMPLEMENTARITY

BE ACCEPTED AS FULFILLING IN PART REQUIREMENTS FOR THE DEGREE OF

Doctorate of Philosophy

Committee on Graduate Work

Prof. Louis Hegedus

Prof. C. Michael Elliott

Prof. Gary Maciel

Prof. Robert Woody

Advisor: Prof. Alan Kennan

Department Head: Prof. Anthony Rappé

Abstract of Dissertation

Specific Coiled Coil Assembly through Size-Complementarity

The α-helical coiled coil is a ubiquitous protein structural motif formed by the supercoiling of two or more α-helices. The high regularity in amino acid sequence renders it particularly attractive from a molecular recognition standpoint. Specifically, coiled coil primary structure exhibits a three-four hydrophobic repeat known as the heptad repeat, with residues designated *abcdefg*. The hydrophobic core is comprised of nonpolar *a* and *d* residues while core-flanking *e* and *g* positions contribute to electrostatic interactions at the hydrophilic interface. Positions *b*, *c*, and *f* are solvent exposed and generally contain amino acids with high helix propensity.

Hydrophobic contacts are widely considered the main driving force in strand association. We sought to establish an approach toward specificity in the hydrophobic core using a non-natural amino acid, cyclohexylalanine (Chx), as a steric complement to two opposing alanine (Ala) residues. A specific 2:1 heterotrimer was demonstrated where a central core layer juxtaposed these residues, thereby specifying both strand orientation and stoichiometry. The isolated Chx peptide, however, displayed higher stability than the designed complex, which would become a problem when more demanding assembly problems were addressed. To circumvent this, a cooperative

approach was employed whereby three consecutive core residues were modified to either Ala or Chx such that each strand of a 1:1:1 heterotrimer donates a single large Chx residue to the core structure. All competing assemblies suffer from at least one destabilizing all-alanine core layer. Analysis of the designed system and all component strands revealed the 1:1:1 heterotrimer as the most stable species formed.

With a well-behaved core structure in hand, efforts turned toward manipulation of hydrophilic interface residues which could serve as an orthogonal recognition domain. Persubstitution of these positions with either glutamic acid (Glu), lysine (Lys), or a combination of the two resulted in two stable complexes at neutral pH. The first contained a core alignment as described above with electrostatically matched hydrophilic interfaces. The second bore the same core structure but suffered from Lys-Lys interactions at a single interface. At lower pH, a similar complex could be obtained bearing a Glu-Glu interface. Subjection of the latter two complexes to varying pH revealed differential stability at pH extremes which prompted us to consider the possibility of specific strand exchange. Starting with the Lys-Lys complex, it was shown that adding an appropriate acidic peptide at low pH could effect formation of a specific Glu-Glu complex by ejection of a basic component strand. We then demonstrated sequential exchange of either two or all three component strands from an initial assembly.

The exchange strategy was then exploited in both the formation and dissolution of a set of crosslinked trimers. Addition of a preformed disulfide-linked dimer to a susceptible trimer at varied pH produced a pentamer containing the newly introduced linkage. Reversal of the process was achieved by addition of monomeric peptide to a preformed pentamer at appropriate pH. This process represents a novel approach to

chemical crosslinking where the covalent bond is introduced via an exchange process. This level of control is only achievable through incorporation of orthogonal recognition elements.

Having demonstrated size complementarity as a viable assembly mechanism, we sought to extend complexation-control to include orientation state specificity. By simply reversing the sequence of a peptide from previous dual-interface work, we were able to successfully design an antiparallel heterotrimer. Equilibrium disulfide-exchange experiments provided strong evidence for the expected strand arrangement. Direct competition between analogous parallel and antiparallel structures resulted in an initial kinetic preference for the antiparallel orientation. However, given sufficient equilibration time, a slight thermodynamic preference for the parallel arrangement appeared. With this work, we were now able to specify both oligomerization and orientation through simple steric matching of hydrophobic core side chains, lending access to the entire series of native-like, trimeric coiled coil structures.

More recently, we have focused efforts on understanding coiled coil surface-binding events. Several viral entry mechanisms have been shown to include helix bundle formation through peptide binding at a hydrophobic pocket presented on a coiled coil exterior. Our designed heterotrimer would serve as an appropriate model system to test various design requirements to effectively inhibit this event.

The N-terminal portion of gp41, an HIV envelope protein, forms a parallel, trimeric coiled coil. Binding of three C-terminal strands to the exterior of the trimer results in a six-helix bundle thought to facilitate host-cell infection. We designed an N-terminal trimer mimic which contained a single hydrophobic binding interface to study

C-terminal peptide affinity. Analysis of N- and C- terminal peptide mixtures resulted in strong evidence suggesting our heterotrimer as an appropriate gp41 mimic. Control experiments verified a stable and specific binding event between a short C-terminal gp41 peptide and the exterior of our N-terminal gp41 trimer mimic. With initial characterization of this complex completed, future experiments aimed at uncovering important interactions required for coiled coil surface-binding may be executed.

Nathan A. Schnarr
Department of Chemistry
Colorado State University
Fort Collins, Colorado 80523
Summer 2004

Acknowledgements

I certainly would not be writing this document without the loving support of my family. My mother and father always demanded the highest level from me and placed my education above all else. Getting me to this point on a policeman's and teacher's salary demonstrates the amount of personal sacrifice that my family has been willing to exhibit for my betterment. My brother, Nick, has always been there when I needed to vent from a stressful day at work or just wanted to discuss what kind of car I should buy when I get out into the real world. I wish him all the best as he finishes his doctorate degree in pharmacy.

My soon-to-be-wife, Katie....where do I begin. I could not have enjoyed this arduous experience without her. The fact that we were able to remain best friends through a very demanding and nerve-racking time in our lives gives me all the confidence that we are meant for each other. Congratulations on your Ph.D. and your new job....I am extraordinarily proud of you.

Finally, Alan Kennan has been the best teacher and advisor that I could have had. Thanks for helping me sharpen my skills at tabletop hockey and initiating me into the wonderful world of Scotch. I will certainly miss the "business" lunches and hallway games of bucket-top Frisbee. I look forward to the weekly phone calls wondering where things are or how I did this or that.

For Mom, Dad, and Nick

Table of Contents

Chapter 1

Background

1-1 Molecular Recognition and Biological Assemblies

Controlled assembly of biologically inspired macromolecules remains a formidable task in the area of molecular design. Generation of well-defined, three-dimensional structures may provide insight regarding complex recognition problems.

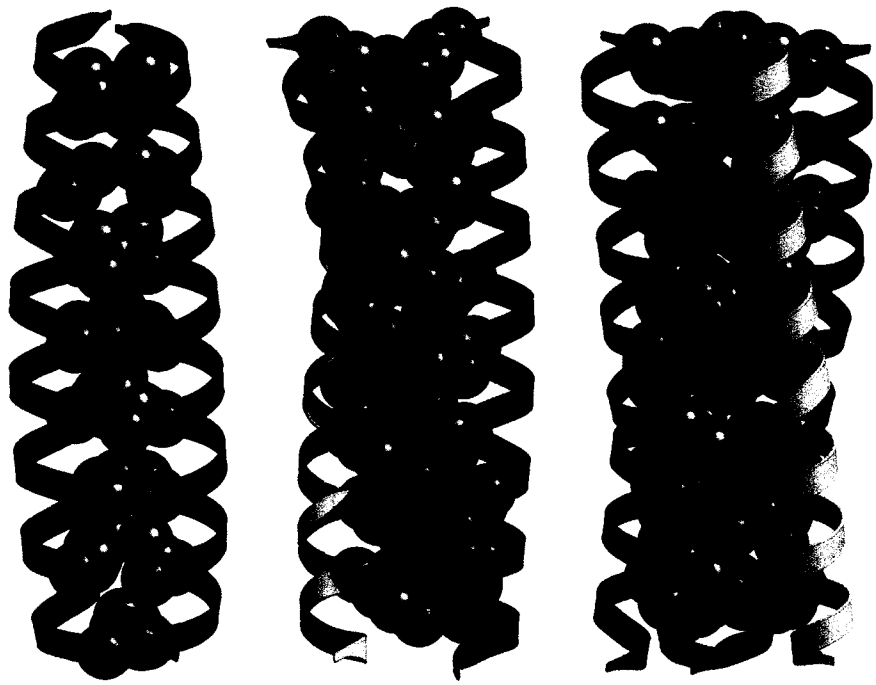

Figure 1. Coiled Coil structures for dimer, trimer, and tetramer. Helix backbones as colored ribbons. Interior residues as grey spheres. Exterior residues omitted for clarity.

The recent spate of literature concerning the behavior of biopolymer mimics has underscored the importance of finding new avenues to study macromolecular interactions. In addition to backbone-modified structures such as β-peptides[1] and other foldamers, incorporation of unnatural amino acids into well-understood peptide scaffolds

should result in novel folding and assembly mechanisms.[2] Protein recognition elements, including β-sheets and α-helical coiled coils, are promising candidates for the introduction of this design strategy as their manipulation, detection, and significance are well documented.[3]

1-2: The α-Helical Coiled Coil

The α-helical coiled coil is a prominent structural motif found as the dominant configuration of both fibrous proteins and a variety of oligomerization and recognition domains.[4] Coiled coils consist of two or more supercoiled α-helices aligned in a parallel

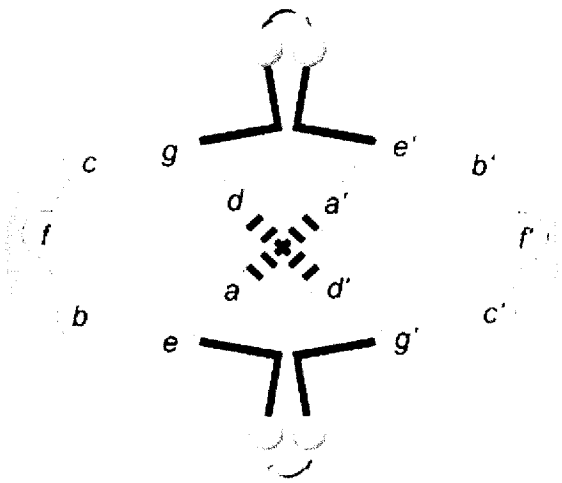

Figure 2. Schematic representation of coiled coil heptad positions. Hydrophobic core residues at *a* and *d* positions control assemby. Core flanking *e* and *g* positions contribute to specificity (interaction depicted by grey spheres). *b*, *c*, and *f* are exposed to solvent in lower order oligomers.

or antiparallel orientation (Figure 1). Their primary sequence

contains a heptad repeat (*abcdefg*) with a tightly packed hydrophobic core consisting of *a* and *d* residues as the primary contributors to assembly (Figure 2).[5] Core flanking *e* and *g* residues impart specificity primarily through avoidance of destabilizing electrostatic

repulsion. Positions *b*, *c*, and *f* are generally occupied by helix-promoting residues (Ala, Lys, Gln, etc.) in lower order oligomers and do not play a specific role in helix recognition. This sequence regularity renders the coiled coil highly predictable and therefore a particularly attractive template from a molecular recognition standpoint.

As stated, the main driving force for helical assembly is hydrophobic core

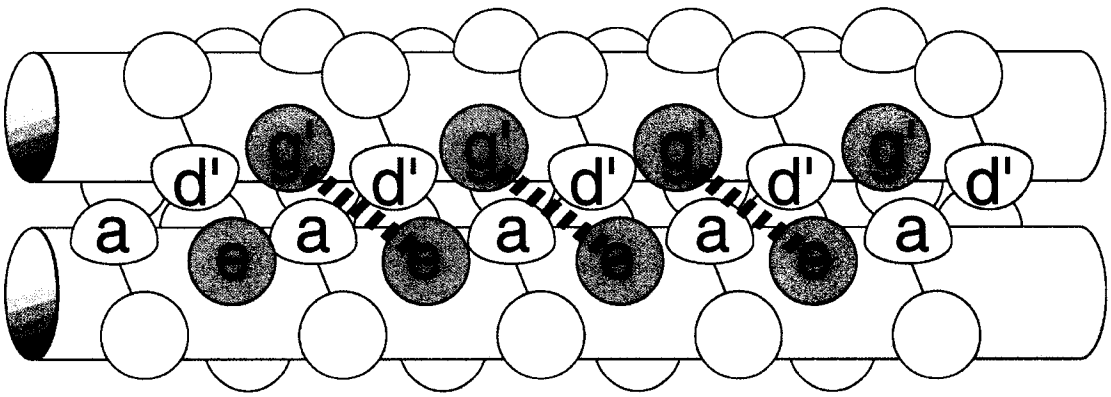

Figure 3. Schematic Diagram depicting "knobs into holes" core packing. Cylinders represent helical backbone. Hydrophilic interface interactions shown as a slotted line. Solvent exposed residues are unlabeled.

assembly. Specifically, alternating *a* and *d* layers exhibit a "knobs into holes" packing arrangement where, in the parallel orientation, hydrophobic *a* residue side chains pack tightly against the same positions on an opposing strand in a hole formed by flanking *d*, *e*, and *g* residues (Figure 3).[6] The antiparallel orientation follows a similar mechanism but requires mixed core layers where *a* packs against *d* on opposing strands. This core configuration provides the basis for coiled coil design and will be discussed in depth (*vide infra*).

In contrast to the well-defined role of the hydrophobic core, the hydrophilic interface (*e* and *g* residues) role is much less understood. This interface has been implicated as a strong specificity determinant in numerous cases including both natural and rationally designed systems.[7] However, its role in complex stability has been vigorously debated.[7] It is clear that the stability contribution from these residues, if any, is small in comparison to that of the hydrophobic core. Therefore, the hydrophilic interface may be treated primarily as an important specificity element. Again, precise assembly strategies employing this interface will be discussed at length in subsequent chapters.

Coiled coils have attracted much recent attention and their importance in critical biological assemblies is well documented. Their simplicity and regularity lends itself very well to studying direct effects of specific design principles on complex formation. The remainder of this chapter will highlight several principal examples of coiled coil design leading to the current state of the art in this area.

1-3: Coiled Coil Design – Oligomerization

There have been numerous reports aimed at specifying oligomerization state. Arguably, the largest contributions to this area have come from empirical analyses where researchers simply substituted known coiled coil sequences with carefully selected hydrophobic amino acids and assessed the effects. The bZIP transcription factor, GCN4, has been a particularly powerful template for probing the influence of amino acid substitutions on both oligomerization and orientation. The natural coiled coil region of this protein (denoted GCN4-p1) exists as a stable, parallel dimer directed by a simple

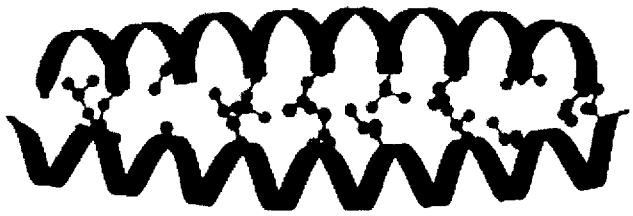

Figure 4. GCN4 coiled coil region structure. Central core asparagine is shown in color. Exterior residues omitted for clarity.

mechanism.[8] A normally hydrophobic, central *a* position contains an asparagine residue which can be partially solvated in the dimeric state as its hydrophobic core is more solvent accessible than those for the trimer and tetramer (Figure 4). Mutation of this asparagine to alanine results in a non-specific mixture of oligomerization states.

Table 1. Oligomerization dependence on hydrophobic pattern.

Position *a*	Position *d*	Tm (deg C)	No. Helices
GCN4-p1	GCN4-p1	53	2
I	L	>100	2
I	I	>100	3
L	I	>100	4
V	I	73	NA
L	V	81	3
V	L	95	(2,3)
L	L	>100	3

This strong dependence on core makeup has allowed researchers to directly ascribe preferred three-dimensional structures to particular hydrophobic patterns.

Alber and coworkers performed an extensive core manipulation study of the GCN4 coiled coil domain.[9] By simple persubstitution of *a* and *d* positions with natural hydrophobic amino acids, a variety of structures could be accessed (Table 1). Interestingly, these two heptad positions exhibited differential behavior when substituted with the same amino acid. For instance, substitution at *a* with isoleucine and *d* with leucine yielded dimers where the opposite configuration gave tetramers. The trimeric state was accomplished with isoleucine at both positions.

Analysis of crystal structures revealed that different modes of the "knobs into holes" packing could readily explain the apparent oligomerization preference described above. Specifically, the Alber team noticed the presence of different packing angles at hydrophobic positions for dimers, trimers, and tetramers (Figure 5). A packing angle was defined as the angle between the Cα-Cβ bond of one hydrophobic core side chain and a vector connecting the alpha carbons of the residues it packs between on the opposing strand. Perpendicular (90 deg) packing angles were observed at the *d* position of dimers and the *a* position of tetramers. Conversely, parallel (180 deg) packing angles were seen at the *a* positions of dimers and *d* positions of tetramers. They hypothesized that bulky, beta-branched residues could not exist in a perpendicular packing arrangement, rendering them important determinants of three dimensional structure. In addition, the trimer possessed intermediate packing angles, termed acute, at both core positions which explained the oligomerization preference when both *a* and *d* were substituted with isoleucine. These findings allowed researchers to accurately predict the three-dimensional structure of simple coiled coils based solely on hydrophobic patterning.

More importantly, this was the first definitive demonstration of hydrophobic components as specificity elements in coiled coil assembly.

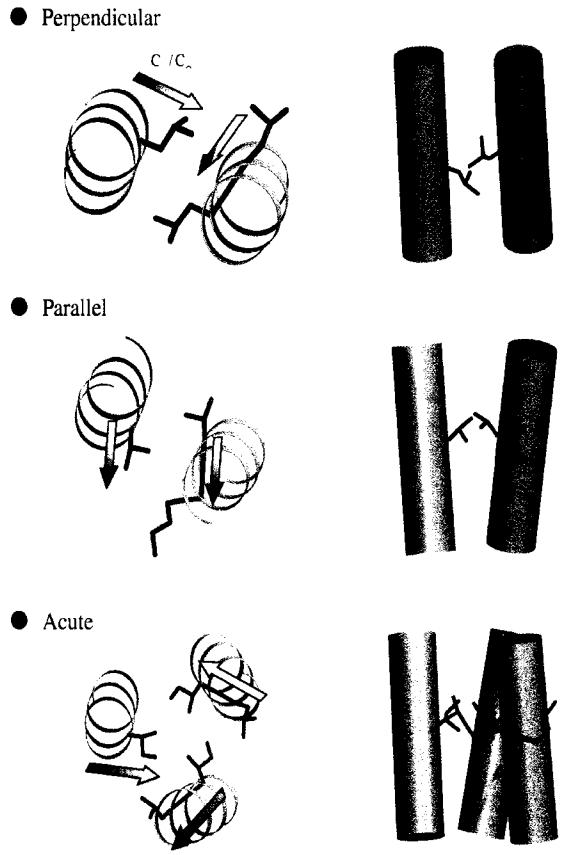

Figure 5. Hydrophobic core packing angles. Residues of interest shown both from a top-down and side view. Hydrophobic side chains are shown in red and blue. Vectors of interest are in green.

The remarkable oligomerization preference exhibited by a buried asparagine in the native coiled coil region of GCN4 and structurally related leucine zippers prompted Alber and coworkers to further investigate this phenomenon.[10] GCN4-based mutants containing glutamine, lysine, or norleucine in place of asparagine were prepared. Analysis of the glutamine mutant revealed a mixture of dimers and trimers. Interestingly,

neither structure allowed for direct hydrogen bonding between glutamine side chains. As a result, a single water molecule in the dimer and two in the trimer core were observed which seemed to participate in a sort of "hydrogen bonding network". In spite of a large penalty taken in oligomerization specificity, the glutamine assembly displayed thermal stability and α-helical content comparable to that of natural GCN4.

Comparison of the lysine and norleucine mutants led to several intriguing observations. The norleucine-modified peptide yielded a melting temperature above 100 degrees Celsius. However, much like alanine and valine, it did not specify a particular oligomerization state. In contrast, lysine mutants produced a less stable but specific dimeric species. The crystal structure of the lysine dimer revealed a unique packing arrangement which directed the side chain away from the core, exposing the ε-amine to solvent. Consequently, the aliphatic side chain methylenes made no specific contacts with each other. On the contrary, the norleucine dimer structure showed efficiently packed side chains which were almost entirely contained in the core. Therefore, lysine adopted its unusual conformation, at the expense of packing, solely for ε-amine solvation. The complex behavior of buried polar residues in the hydrophobic core is extremely evident in this study as subtle changes in side chain functionality resulted in significant structural alterations.

Controlling specific composition of coiled coil species has been a different story altogether. Little success has derived from employing hydrophobic side chains to form heteromeric species.[11] Conversely, implementation of electrostatics has resulted in an abundance of information regarding control over this event.[7] Coupled with core specificity elements, the hydrophilic interface becomes a very powerful design tool. By

simply adjusting the electrostatic arrangement at these core flanking positions, one can select for a precise association event from more complex peptide mixtures.

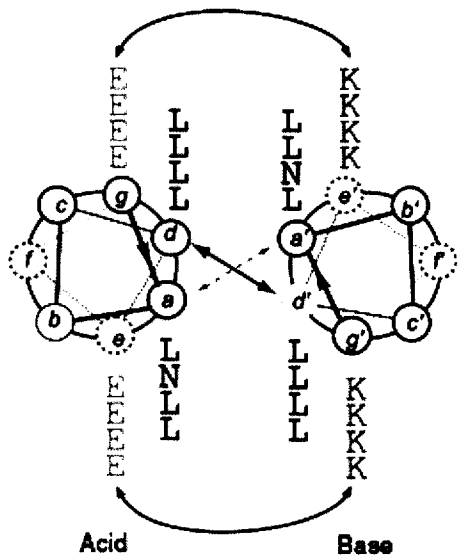

Figure 6. "Peptide Velcro". Helical wheel diagram depicting the 1:1 acid:base heterodimer. Arrows indicate electrostatic interactions at the hydrophilic interface. Solvent exposed residues have been omitted for clarity.

Kim and coworkers successfully designed a coiled coil heterodimer with specificity solely derived from electrostatics based on the known GCN4 coiled coil sequence.[12] This system, denoted "peptide Velcro", preferentially formed the heterodimer to avoid electrostatic repulsion in the parent homomeric species. The *e* and *g* heptad positions of GCN4 were persubstituted with either lysine (Base peptide)

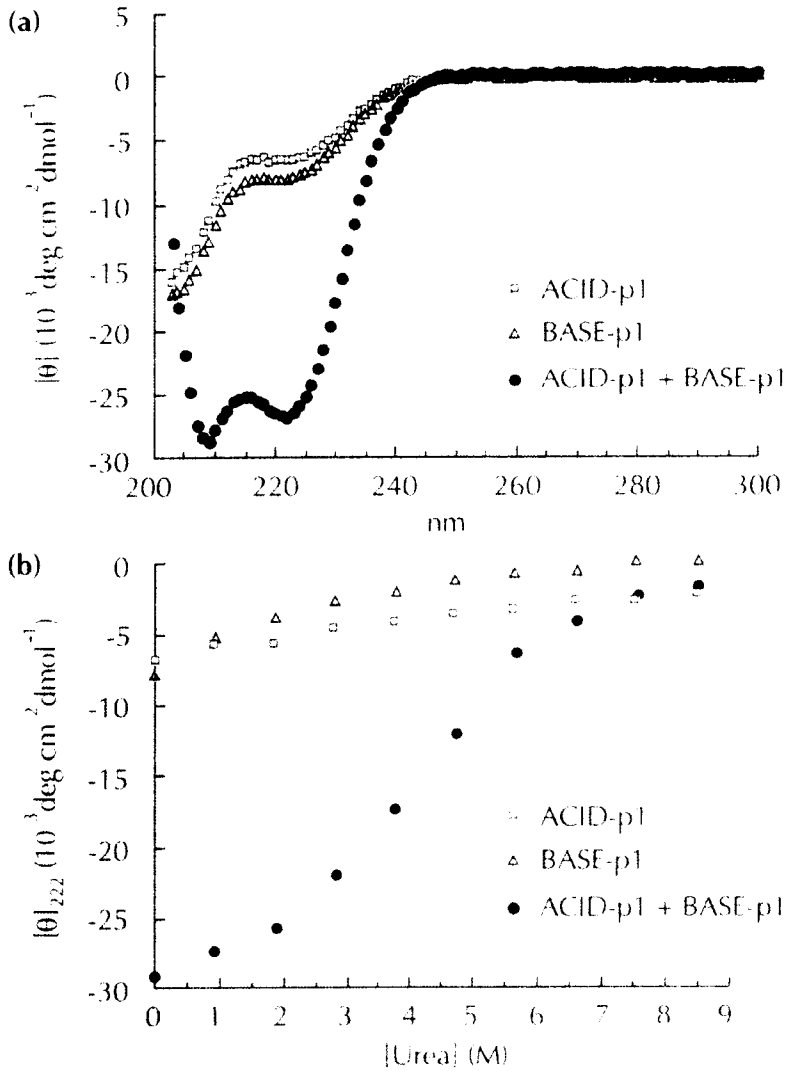

Figure 7. CD analysis of "peptide Velcro". (a) wavelength scans for pure Acid, pure Base, and a 1:1 mixture of Acid and Base. (b) chemical denaturation (urea) of pure Acid, pure Base, and a 1:1 mixure of Acid and Base. All experiments were performed at 37 degrees (pH = 7.0). (Figure from O'Shea *et al.*, 1993)[12]

or glutamic acid (Acid peptide) (Figure 6). Homodimers suffered largely from like charges in close proximity as evidenced by the lack of thermal stability. An equimolar mixture of the Acid and Base peptides yielded a marked increase in the helical CD signal and stability indicating the formation of a new species determined to be the 1:1 heterodimer (Figure 7).

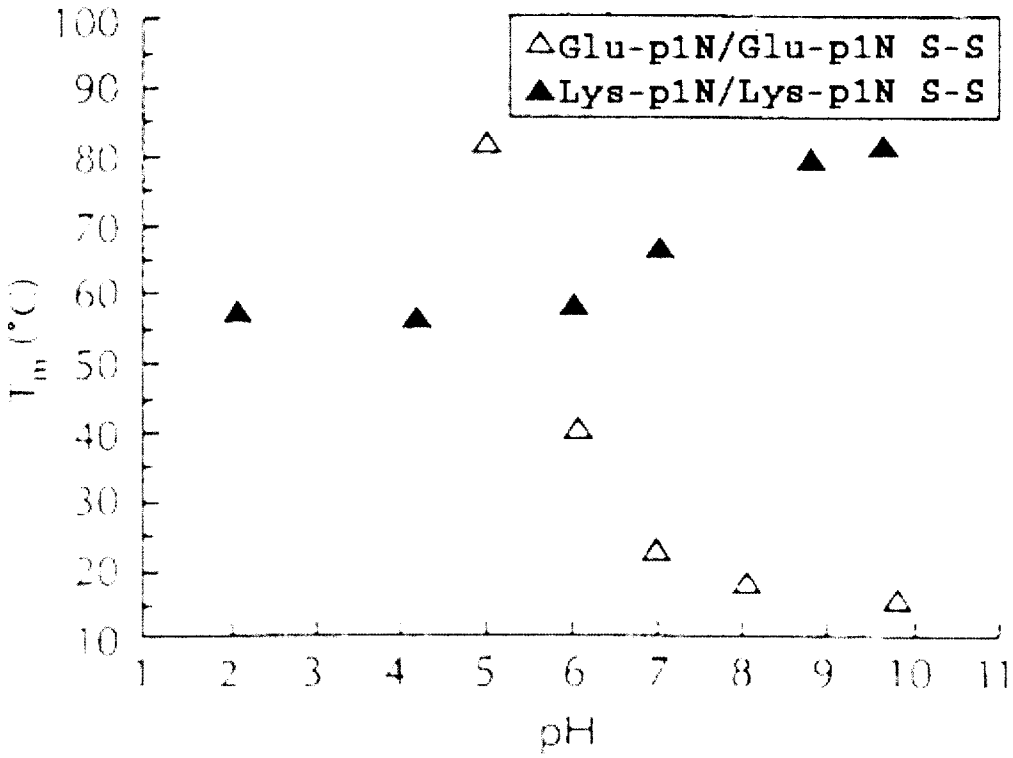

Figure 8. pH dependence of homodimer stability. Melting temperaturse for Acid and Base homodimers at varying pH. (Figure from O'Shea *et al.*, 1993)[12]

Covalently linked homo and heterodimers were synthesized to demonstrate an active role for the hydrophilic interface in peptide assembly. In fact, Acid and Base homodimers showed significant increases in thermal stability at low and high pH extremes respectively (Figure 8). This strongly supported the hypothesis that poor

homodimer stability at neutral pH was purely the result of repulsive electrostatic interactions. The heterodimer also displayed an increase in thermal stability at low pH (where Glu is fully protonated) indicating an absence of salt bridge stabilization as a factor in overall coiled coil stability. This idea of destabilizing certain assemblies to favor others has been termed negative design and has proven quite powerful for coiled coil composition specificity. Coupled with core oligomerization specificity, one can simply maximize electrostatic repulsion in unwanted complexes to access the intended strand arrangement.

Using a similar strategy, Alber and coworkers successfully prepared a heterotrimeric coiled coil derived from a theoretical model which maximized the number of favorable interhelical ion pairs in the proposed structure while unfavorable interactions were maximized in all competing structures.[13] The result was three complementary peptides that, when combined, gave a melting temperature approximately 30 to 40 degrees higher than any of the isolated components. Equimolar mixtures of any two of the three strands yielded melting temperatures significantly below that for the designed heterotrimer indicating highly specific formation of the intended complex.

More recently, Hodges and coworkers created a small library of heterodimeric coiled coils all of which displayed favorable electrostatics at the hydrophilic interface reminiscent of the "peptide Velcro" system described above.[14] Complexes varying in hydrophobic core composition and solvent-exposed residues were constructed to produce a range of stabilities for protein engineering and biomedical applications (Figure 9). Free energies ranging from 6.8 to 11.2 kcal/mol were extracted from simple chemical

denaturation experiments. This study demonstrates the versatility of combining multiple recognition domains to access a variety of related structures.

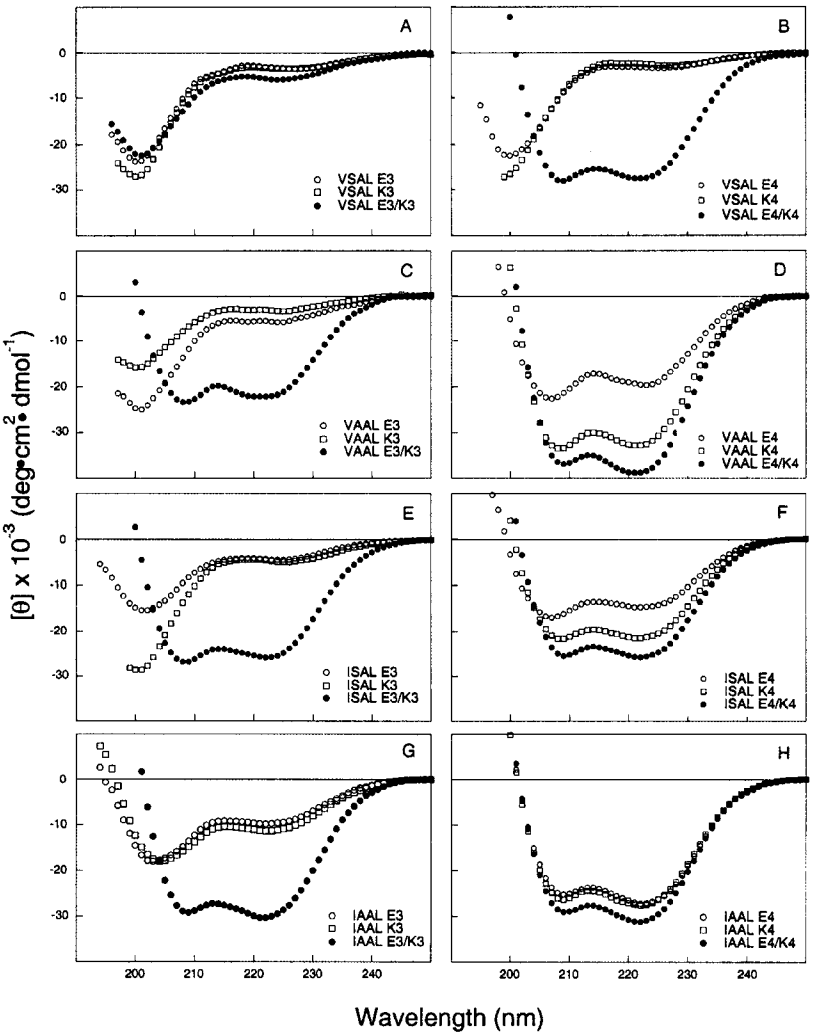

Figure 9. CD spectra of a variety of 1:1 heterodimers and individual components. The nomenclature reflects repeating *a-d* sequences (i.e. VSAL), and the number indicates the peptide length in heptads. E/K denotes the heterodimer formed from Acid (E) or Base-like (K) strands. (Figure from Litowski and Hodges, 2002)[14]

1-4: Coiled Coil Design – Orientation

The relative positioning of N and C termini, or strand orientation, in coiled coils has received much attention recently as a growing number of structurally characterized proteins have been shown to contain antiparallel assemblies.[15] As with oligomerization specificity, researchers have employed both hydrophobic and hydrophilic elements to address this design challenge.[16] Coupled together, oligomerization and orientation specificity will allow access to the entire range of native-like coiled coil structures.

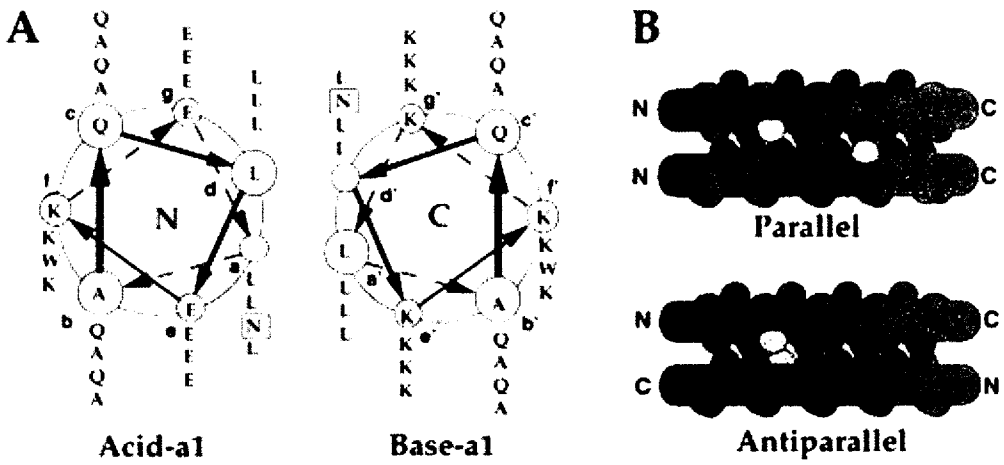

Figure 10. Antiparallel heterodimer design. (A) Helical wheel of the designed heterodimer. (B) Schematic diagram of the orientation specificity mechanism: Core Asn residues are depicted as light grey spheres. (Figure from Oakley and Kim, 1998)[17]

Kim and coworkers were initially able to direct strand orientation in a model GCN4 system by appropriate placement of a buried polar residue.[17] Specifically,

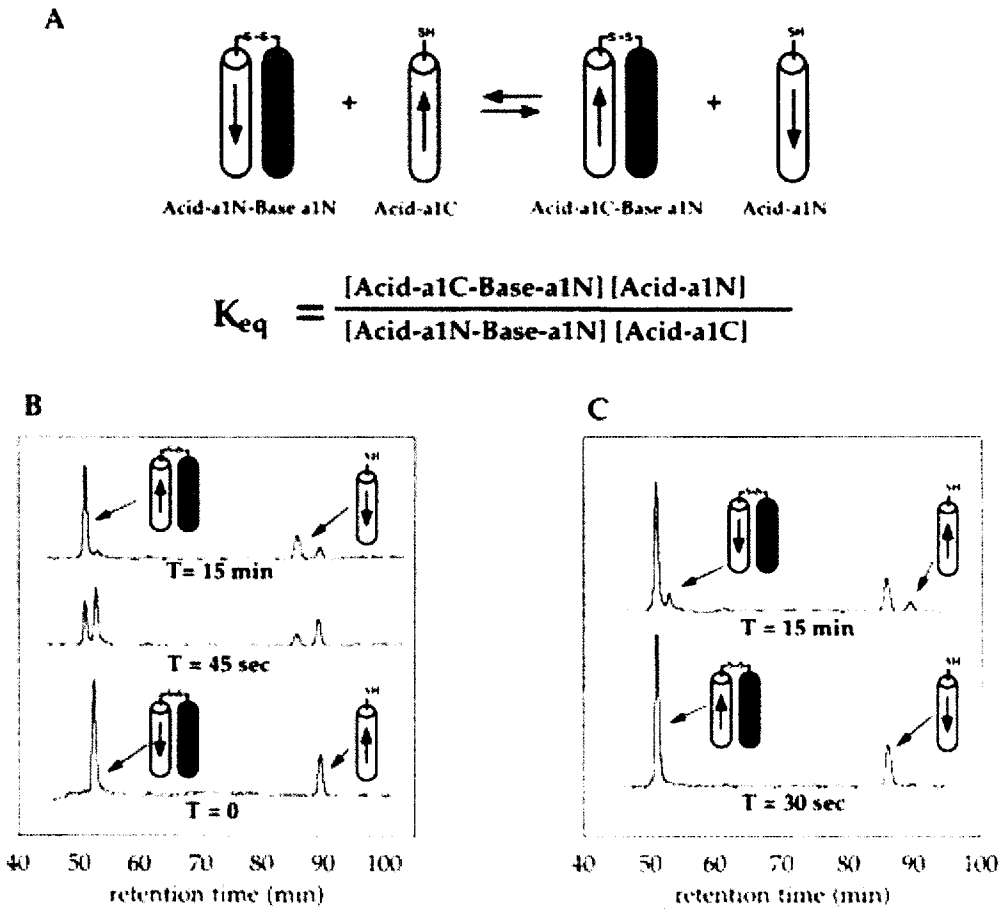

Figure 11. Orientation preference experiment. (A) Equilibrium equation between competing parallel and antiparallel heterodimers (Acid-a1N = N-termimal cysteine on the Acid peptide, etc.). (B) HLPC analysis of orientation preference starting with the parallel heterodimer. (c) HLPC analysis of orientation preference starting with the antiparallel heterodimer. (Figure from Oakley and Kim, 1998)[17]

introduction of asparagine at opposite ends of a designed heterodimer forced an antiparallel arrangement which avoided destabilizing interactions between leucine and asparagine in the hypothetical parallel orientation (Figure 10). Peptide strands modified

with either N or C terminal cysteines were prepared and oxidized to form both the N to C and N to N heterodimers. Upon subjection of either covalent assembly to an appropriate thiol-containing monomer under thermodynamic conditions, only the N to C species was observed after fifteen minutes, indicating a strong preference for the antiparallel arrangement (Figure 11). Circular dichroism spectroscopy confirmed the presence of a highly helical, highly stable entity. This work demonstrated a remarkable orientation dependence on primary amino acid sequence. However, although a preference was observed for antiparallel, the heterodimer existed as a mixture of possible orientations in the absence of a covalent linkage. Given the stability penalty associated with buried polar residues, one could not simply introduce multiple asparagines for added specificity.

More recently, Oakley and coworkers have addressed this issue by combining polar and nonpolar core components in the formation of a homodimeric antiparallel coiled coil.[18] It was previously discovered that a single charged core residue could specify a dimeric structure at a lower stability cost than two aligned asparagines.[19] The homodimer was designed bearing a single arginine at *d* position to promote dimer formation. Orientation specificity resulted from favorable electrostatic interactions in the antiparallel arrangement coupled with properly "size-matched" hydrophobic sidechains in the core (Figure 12). Alanine and isoleucine residues were strategically placed such that the parallel species suffered from poorly accommodated alanine-alanine and isoleucine-isoleucine core layers. In contrast, the antiparallel species bore alanine-isoleucine interactions similar to those observed in naturally occurring antiparallel coiled coils.

Hodges and coworkers developed a similar strategy for formation of antiparallel tetramers.[20] In their system, alternating pairs of alanine and leucine at central core

positions directed strand orientation by avoiding all alanine core layers. Each relevant level consisted of an Ala-Leu-Ala-Leu core composition. Interestingly, this system displayed degenerate electrostatic interactions in the two competing strand orientations indicating that the preference for the antiparallel arrangement was entirely the result of differences in hydrophobic core organization.

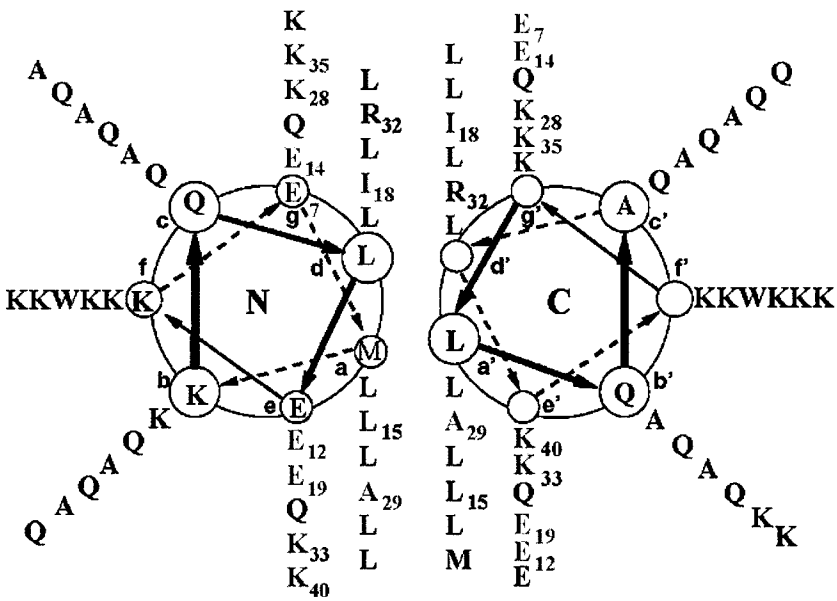

Figure 12. Helical Wheel of a designed antiparallel homodimer. Matched electrostatic interactions are shown in red and blue. "Size-matched" hydrophobic residues are depicted in green. (Figure from Gurnon *et al.*, 2003)[18]

In an attempt to prepare a parallel dimer, Degrado and coworkers serendipitously discovered that placement of large tryptophan residues at an N-terminal *a* position could direct strand orientation.[21] The designed complex existed in a non-cooperative monomer-dimer-trimer equilibrium in solution. However, when crystallized at low pH, they found that the peptides assembled to form an antiparallel trimer (Figure 13). It was proposed

that the three large indole side chains were poorly accommodated in the parallel arrangement forcing the antiparallel strand orientation. In addition, crystallization at low

Figure 13. Antiparallel trimeric coiled coil structure. Peptide backbones depicted as colored ribbons. Essential tryptophan residues are shown in red. Exterior residues have been omitted for clarity.

pH lessened the effects of electrostatic repulsion at the hydrophilic interface. This group was later able to optimize the ionic interactions at these positions which led to a stable and specific heterotrimer at neutral pH.[22]

1-5: The Alber Model System

Research in the Kennan group began with a simple question: Could one specify for oligomerization state, composition, and orientation using side chain size complementarity in the hydrophobic core? To begin our work in this area, we needed an appropriate model system to test the viability of this mechanism. Luckily, Alber and coworkers had discovered a system that, when slightly modified, would properly serve this purpose.

As experts in the area of hydrophobic core manipulation strategies, the Alber group was interested in allosteric stabilization of an unoptimized GCN4 core mutant. Replacement of the native central core asparagine of GCN4 with alanine resulted in a

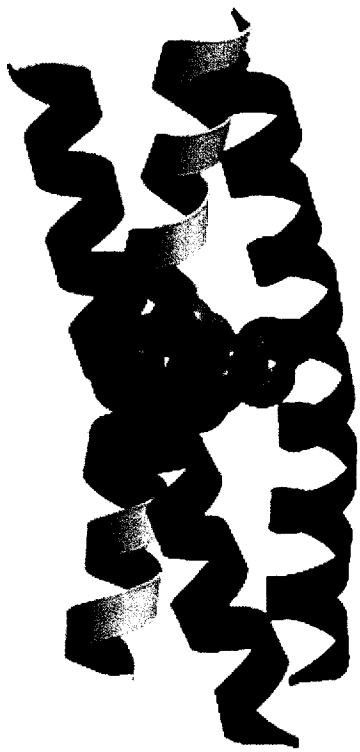

Figure 14. Crystal structure of GCN4 alanine core mutant. A single benzene molecule (grey spheres) binds tightly in the trimer core surrounded by three *a* position alanine residues (colored spheres). Helix backbones are shown as colored ribbons. Only central alanine residues are shown for clarity.

nonspecific dimer-trimer equilibrium.[23] They hypothesized that this behavior was due to a destabilizing cavity formed by the small alanine side chains in the trimeric state. The question was posed whether a small hydrophobic molecule could bind and fill the cavity, switching the equilibrium in favor of the trimer. Addition of benzene or cyclohexane to the peptide mixture resulted in significant increase in trimer population and stability. The

more polar benzene isostere, triazine, was shown not to bind the trimer cavity indicating that this interaction was purely hydrophobic. Structural data confirmed the presence of benzene amidst the three alanine methyl groups (Figure 14).

This result has served as the backbone of research in our laboratory. Starting from a rather simple concept, we have targeted exceptionally complex assemblies requiring both hydrophobic and hydrophilic specificity elements. The ensuing chapters will describe, in detail, our progress in the area of coiled coil design.

1-6: Literature Cited

(1) (a) Winkler, J. D.; Piatnitski, E. L.; Mehlmann, J.; Kasparec, J.; Axelsen, P. H. *Angew. Chem., Int. Ed.* **2001**, *40*, 743-745. (b) Tanatani, A.; Mio, M. J.; Moore, J. S. *J. Am. Chem. Soc.* **2001**, *123*, 1792-1793. (c) Lee, H.-S.; Syud, F. A.; Wang, X.; Gellman, S. H. *J. Am. Chem. Soc.* **2001**, *123*, 7721-7722. (d) Gunther, R.; Hofmann, H.-J. *J. Am. Chem. Soc.* **2001**, *123*, 247-255. (e) Daura, X.; Gademann, K.; Schaefer, H.; Jaun, B.; Seebach, D.; van Gunsteren, W. F. *J. Am. Chem. Soc.* **2001**, *123*, 2393-2404. (f) Cubberley, M. S.; Iverson, B. L. *J. Am. Chem. Soc.* **2001**, *123*, 7560-7563. (g) Corbin, P. S.; Zimmerman, S. C.; Thiessen, P. A.; Hawryluk, N. A.; Murray, T. J. *J. Am. Chem. Soc.* **2001**, *123*, 10475-10488. (h) Cheng, R. P.; Gellman, S. H.; DeGrado, W. F. *Chem. Rev.* **2001**, *101*, 3219-3232. (i) Porter, E. A.; Wang, X.; Lee, H.-S.; Weisblum, B.; Gellman, S. H. *Nature* **2000**, *404*, 565. (j) Gellman, S. H. *Acc. Chem. Res.* **1998**, *31*, 173-180. (k) Seebach, D.; Overhand, M.; Kuehnle, F. N. M.; Martinoni, B. *Helv. Chim. Acta* **1996**, *79*, 913-941. (l) Appella, D. H.; Christianson,

L. A.; Karle, I. L.; Powell, D. R.; Gellman, S. H. *J. Am. Chem. Soc.* **1996**, *118*, 13071-13072.

(2) (a) Bilgicer, B.; Fichera, A.; Kumar, K. *J. Am. Chem. Soc.* **2001**, *123*, 4393-4399. (b) Tang, Y.; Ghirlanda, G.; Vaidehi, N.; Kua, J.; Mainz, D. T.; Goddard, W. A., III; DeGrado, W. F.; Tirrell, D. A. *Biochemistry* **2001**, *40*, 2790-2796. (c) Niemz, A.; Tirrell, D. A. *J. Am. Chem. Soc.* **2001**, *123*, 7407-7413.

(3) (a) Holmes, T. C. *Trends Biotch.* **2002**, *20*, 16-21. (b) Hartgerink, J. D.; Beniash, E.; Stupp, S. I. *Proc. Natl. Acad. Sci. U. S. A.* **2002**, *99*, 5133-5138. (c) Aggeli, A.; Nyrkova, I. A.; Bell, M.; Harding, R.; Carrick, L.; McLeish, T. C. B.; Semenov, A. N.; Boden, N. *Proc. Natl. Acad. Sci. U. S. A.* **2001**, *98*, 11857-11862. (d) Bilgicer, B.; Xing, X.; Kumar, K. *J. Am. Chem. Soc.* **2001**, *123*, 11815-11816. (e) Hartgerink, J. D.; Beniash, E.; Stupp, S. I. *Science* **2001**, *294*, 1684-1688. (f) Bong, D. T.; Ghadiri, M. R. *Angew. Chem. Int. Ed.* **2001**, *40*, 2163-2166. (g) Collier, J. H.; Hu, B.-H.; Ruberti, J. W.; Zhang, J.; Shum, P.; Thompson, D. H.; Messersmith, P. B. *J. Am. Chem. Soc.* **2001**, *123*, 9463-9464.

(4) (a) Burkhard, P.; Strelkov, S. V.; Stetefeld, J. *Trends Cell Biol.* **2001**, *11*, 82-88. (b) Lupas, A. *Trends Biochem. Sci.* **1996**, *21*, 375-382. (c) Cohen, C.; Parry, D. A. D. *Science* **1994**, *263*, 488-489.

(5) (a) Micklatcher, C.; Chmielewski, J. *Current Opinion in Chemical Biology* **1999**, *3*, 724-729. (b) DeGrado, W. F.; Summa, C. M.; Pavone, V.; Nastri, F.; Lombardi, A. *Annu. Rev. Biochem.* **1999**, *68*, 779-819. (c) Harbury, P. B.; Kim, P. S.; Alber, T.

Nature **1994**, *371*, 80-83 (d) O'Shea, E. K.; Klemm, J. D.; Kim, P. S.; Alber, T. *Science* **1991**, *254*, 539-544.

(6) Crick, F. *Acta Crystallogr.* **1953**, *6*, 689-697.

(7) (a) Phelan, P.; Gorfe, A. A.; Jelesarov, I.; Marti, D. N.; Warwicker, J.; Bosshard, H. R. *Biochemistry* **2002**, *41*, 2998-3008. (b) Chana, M.; Tripet, B. P.; Mant, C. T.; Hodges, R. S. *J. Struct. Biol.* **2002**, *137*, 206-219. (c) McClain, D. L.; Binfet, J. P.; Oakley, M. G. *J. Mol. Biol.* **2001**, *313*, 371-383. (d) Vu, C.; Robblee, J.; Werner, K. M.; Fairman, R. *Protein Sci.* **2001**, *10*, 631-637. (e) Marti, D. N.; Jelesarov, I.; Bosshard, H. R. *Biochemistry* **2000**, *39*, 12804-12818. (f) Arndt, K. M.; Pelletier, J. N.; Muller, K. M.; Alber, T.; Michnick, S. W.; Pluckthun, A. *J. Mol. Biol.* **2000**, *295*, 627-639. (g) Duerr, E.; Jelesarov, I.; Bosshard, H. R. *Biochemistry* **1999**, *38*, 870-880. (h) Kohn, W. D.; Kay, C. M.; Hodges, R. S. *J. Mol. Biol.* **1998**, *283*, 993-1012. (i) Lumb, K. J.; Kim, P. S. *Science* **1996**, *271*, 1137-1138. (j) Lavigne, P.; Soennichsen, F. D.; Kay, C. M.; Hodges, R. S. *Science* **1996**, *271*, 1136-1137. (k) Lumb, K. J.; Kim, P. S. *Science* **1995**, *268*, 436-439.

(8) (a) Campbell, K. M.; Lumb, K. J. *Biochemistry* **2002**, *41*, 7169-7175. (b) Kim, B.-M.; Oakley, M. G. *J. Am. Chem. Soc.* **2002**, *124*, 8237-8244. (c) Akey, D. L.; Malashkevich, V. N.; Kim, P. S. *Biochemistry* **2001**, *40*, 6352-6360. (d) McClain, D. L.; Woods, H. L.; Oakley, M. G. *J. Am. Chem. Soc.* **2001**, *123*, 3151-3152. (e) Zhu, H.; Celinski, S. A.; Scholtz, J. M.; Hu, J. C. *J. Mol. Biol.* **2000**, *300*, 1377-1387. (f) Eckert, D. M.; Malashkevich, V. N.; Kim, P. S. *J. Mol. Biol.* **1998**, *284*, 859-865. (g) Lumb, K. J.; Kim, P. S. *Biochemistry* **1995**, *34*, 8642-8648.

(9) Harbury, P. B.; Zhang, T.; Kim, P. S.; Alber, T. *Science* **1993**, *262*, 1401-1407.

(10) Gonzalez, L., Jr.; Woolfson, D. N.; Alber, T. *Nat. Struct. Biol.* **1996**, *3*, 1011-1018.

(11) Zhu, B., Zhou, N.E., Semchuk, P.D., Kay, C.M., Hodges, R.S. *Int. J. Pept. Res.* **1992**, *40*, 171-179.

(12) O'Shea, E. K.; Lumb, K. J.; Kim, P. S. *Curr. Biol.* **1993**, *3*, 658-667.

(13) Nautiyal, S., Woolfson, D.N., King, D.S., Alber, T. *Biochemistry* **1995**, *34*, 11645-11651.

(14) Litowski, J.R., Hodges, R.S. *J. Biol. Chem* **2002**, *277*, 37272-37279.

(15) (a) Biou, V.; Yaremchuk, A.; Tukalo, M.; Cusack, S. *Science* **1994**, *263*, 1404-1410. (b) Stebbins, C. E.; Borukhov, S.; Orlova, M.; Polyakov, A.; Goldfarb, A.; Darst, S. A. *Nature* **1995**, *373*, 636-640. (c) Uhlin, U.; Cox, G. B.; Guss, J. M. *Structure* **1997**, *5*, 1219-1230. (d) Bussiere, D. E.; Bastia, D.; White, S. W. *Cell* **1995**, *80*, 651-660. (e) Soisson, S. M.; MacDougall-Shackleton, B.; Schleif, R.; Wolberger, C. *Science* **1997**, *276*, 421-425. (f) Zuccola, H. J.; Rozzelle, J. E.; Lemon, S. M.; Erickson, B. W.; Hogle, J. M. *Structure* **1998**, *6*, 821-830. (g) Melby, T. E.; Ciampaglio, C. N.; Briscoe, G.; Erickson, H. P. *J. Cell Biol.* **1998**, *142*, 1595-1604. (h) Hopfner, K.; Karcher, A.; Shin, D. S.; Craig, L.; Arthur, L. M.; Carney, J. P.; Tainer, J. A. *Cell* **2000**, *101*, 789-800. (i) Cusack, S.; Berthet-Colominas, C.; Hartlein, M.; Nassar, N.; Leberman, R. *Nature* **1990**, *347*, 249-255.

(16) Oakley, M. G.; Hollenbeck, J. J. *Curr. Op. Struct. Biol.* **2001**, *11*, 450-457.

(17) Oakley, M. G.; Kim, P. S. *Biochemistry* **1998**, *37*, 12603-12610.

(18) Gurnon, D. G., Whitaker, J. A., Oakley, M. G. *J. Am. Chem. Soc.* **2003**, *125*, 7518-7519.

(19) McClain, D. L.; Gurnon, D. G.; Oakley, M. G. *J. Mol. Biol.* **2002**, *324*, 257-270.

(20) Monera, O.D., Zhou, N.E., Lavigne, P., Kay, C.M., Hodges, R.S. *J. Biol. Chem.* **1996**, *271*, 3995-4001.

(21) Lovejoy, B., Choe, S., Cascio, D., McRorie, D.K., DeGrado, W.F., Eisenberg, D. *Science* **1993**, *259*, 1288-1293.

22) Lombardi, A., Bryson, J.W., DeGrado, W.F. *Biopolymers* **1997**, *40*, 495-504.

23) Gonzalez Jr., L., Plecs, J.J., Alber, T. *Nat. Struct. Biol.* **1996**, *3*, 510-515.

Chapter 2

Oligomerization Specificity Through Steric Matching

The study of protein-protein interfaces has garnered much recent attention.[1] As a ubiquitous and tractable means of governing protein association, the α-helical coiled coil has been the focus of numerous investigations.[2] Although considerable data have been gathered on the structure-function relationships of natural core residues, the limited number of side chain candidates restricts the design of novel assemblies.[3] Here we introduce core diversity in the form of an unnatural hydrophobic side chain, and demonstrate its use in the formation of a specific heterotrimer. These results point toward the development of completely unnatural interfaces that will greatly expand the scope of available applications.

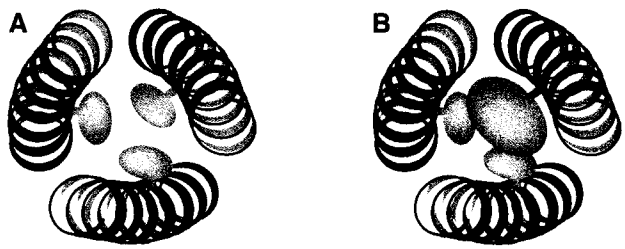

Figure 1. Heterotrimerization through steric matching. The Ala_{16} homotrimer (**A**) contains small methyl sidechains at a central *a* residue, creating a pocket in the hydrophobic core. In the 2:1 complex of Ala_{16}:Chx_{16} (**B**) the larger cyclohexylalanine sidechain partially fills the void, stabilizing the heterotrimer.

2-1: First Generation – 2:1 Heterotrimer Formation[4]

The present system describes heterotrimerization, achieved through steric matching (Figure 1). A small side chain positioned at one core position packs against the same residue on opposing strands of a parallel homotrimer. The resulting pocket should

be destabilizing, and introduction of a complementary peptide, substituted with a larger side chain, should favor heteromeric structures due to improved packing interactions. To test this principle we focused on the dimerization domain of GCN4, where the impact of natural side chain variation has been thoroughly investigated.[5,6]

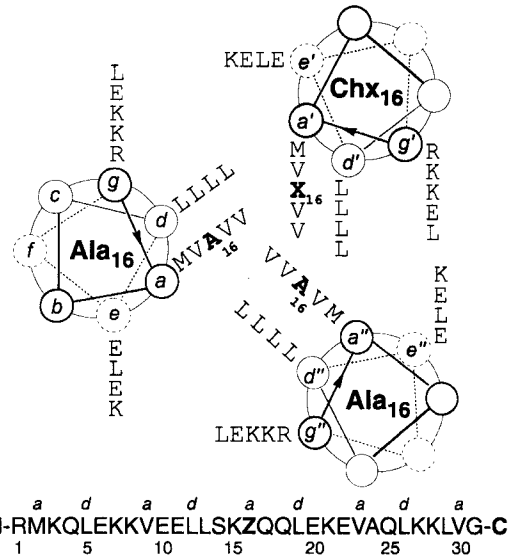

Figure 2. Helical wheel projection of the 2:1 Ala_{16}:Chx_{16} complex (viewed down the helical axis from N to C terminus). The sequence of both peptides (which differ only in the nature of **Z**) is also given. Altered core side chains are emboldened. Solvent exposed residues omitted for clarity. **X** = cyclohexylalanine.

The peptides used here, similarly derived from GCN4, contain either alanine (Ala_{16}) or cyclohexylalanine (Chx_{16}) in place of a central asparagine residue (Figure 2).[7] Since parallel coiled-coil trimers contain segregated layers of *a* and *d* residues, side chains introduced in the same *a* position should be juxtaposed in the aggregate.[8] Accordingly, it was hypothesized that a 2:1 mixture of Ala_{16}:Chx_{16} should exhibit

signatures characteristic of the heteromeric complex, rather than a superposition of weighted average component signals.[9]

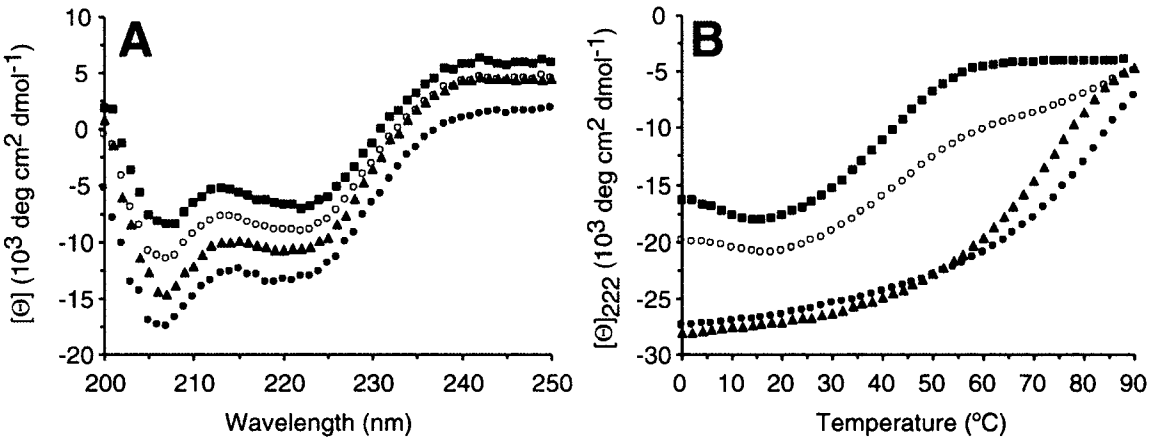

Figure 3. Circular dichroism (CD) data for solutions of: Ala_{16} (■), Chx_{16} (●), and Ala_{16}:Chx_{16} 2:1 (▲), along with calculated weighted average signals for 2:1 samples (○). (**A**) CD spectra. Samples are 1 μM total peptide concentration in PBS buffer (10 mM phosphate pH 7.5, 150 mM NaCl).[12] (**B**) Thermal melt. Samples are 10 μM total peptide concentration in PBS buffer (10 mM phosphate pH 7.5, 150 mM NaCl) containing 1.5M guanidinium hydrochloride.[11]

Samples of Ala_{16}, Chx_{16}, and 2:1 Ala_{16}:Chx_{16} all exhibit circular dichroism (CD) behavior characteristic of helical peptides (Figure 3A). Pure Chx_{16} is significantly more helical than Ala_{16} and thus also than the predicted average signal of a solution in which it is the minor component. Despite this, the 2:1 mixture has a helical content approaching that of Chx_{16}, and considerably in excess of the weighted average value.

Thermal unfolding experiments reveal cooperative behavior in each sample (Figure 3B). Again, the 2:1 mixture produces a trace similar to Chx_{16}, and radically different from the weighted average. Its melting transition is sharper than the component

ones, particularly Chx_{16}. Observed Tm values (Table 1) display the same trend.[10] Pure Ala_{16} melts markedly lower than either of the other two samples.[11]

Table 1. Apparent T_m Values Derived from CD Data[a]

Sample	T_m (°C)	Sample	T_m (°C)
Ala_{16}	47	Nap_{16}	75
Chx_{16}	87	Ala_{16}:Nap_{16} 2:1	71
Ala_{16}:Chx_{16} 2:1	77		

[a] Buffer conditions as outlined in Figure 3B.

Analytical ultracentrifugation experiments were performed to investigate aggregation number. Due to the intrinsic stability of these complexes, experiments were run in buffer containing 3 M guanidinium hydrochloride to obtain meaningful data about relative aggregate stabilities (Table 2).[13] While Ala_{16} gives a weight between monomer and dimer, 2:1 Ala_{16}:Chx_{16} exists as a trimer. Further work is required to elucidate the solution preferences of pure Chx_{16}, but behavior of the 2:1 mixture is consistent with specific interactions.[14]

Table 2. Molecular Weights from Analytical Ultracentrifugation[a]

Sample	MW_{obs}[b]	MW_{calc} dimer[c]	MW_{calc} trimer[c]
Ala_{16}	6436	7650	11475
Chx_{16}	12790	7814	11721
Ala_{16}:Chx_{16} 2:1	11215		11557[d]
Nap_{16}	11443	7902	11853
Ala_{16}:Nap_{16} 2:1	9302		11601[d]

[a] Samples were run in PBS buffer containing 3M GdnHCl (see text). [b] Average values obtained at two different speeds and three different concentrations for each sample [c] Except where noted molecular weights are calculated for homodimers and homotrimers. [d] Calculated weight of 2:1 heterotrimer.

More direct evidence for specific heterotrimer formation was obtained from an affinity tagging experiment. An analogue of Chx_{16} was prepared with an N-terminal $(His)_6GlyGly$ sequence (Chx_{His}), which binds tightly to Ni-nitrilotriacetic acid (Ni-NTA) agarose beads.[15] A 3:1 solution of Ala_{16}:Chx_{His} was exposed to Ni-NTA beads. HPLC analysis of bound material revealed a molar ratio of 0.62:0.38 Ala_{16}:Chx_{His}. Since Ala_{16} has no tag sequence, retention of approximately two of the three equivalents available provides additional support for a specific complex.

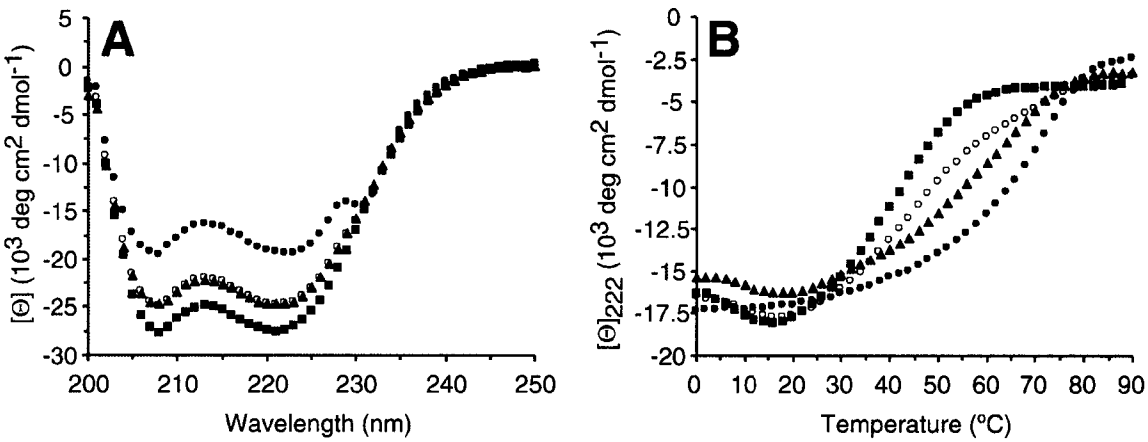

Figure 4. Circular dichroism (CD) data for solutions of: Ala_{16} (■), Nap_{16} (●), and Ala_{16}:Nap_{16} 2:1 (▲), along with calculated weighted average signals for 2:1 samples (○). (**A**) CD spectra. Samples are 10 μM total peptide concentration in PBS buffer (10 mM phosphate pH 7.5, 150 mM NaCl). (**B**) CD signal at 222 nm as a function of temperature. Samples are 10 μM total peptide concentration in PBS buffer (10 mM phosphate pH 7.5, 150 mM NaCl) containing 1.5M guanidinium hydrochloride.[11]

To further verify specificity for cyclohexylalanine, a control peptide was prepared with naphthylalanine at the central *a* position (Nap_{16}). The bulky naphthalene should be too large for even the reduced volume layer created by alanines on opposing strands. CD studies reveal that pure Nap_{16} indeed exhibits reduced helicity compared to either Ala_{16}

or Chx_{16}, while the 2:1 Ala_{16}:Nap_{16} trace overlays almost perfectly with the calculated weighted average (Figure 4A). Similarly, the 2:1 sample displays a broad melting transition whose curve shape mimics that of the weighted average (Figure 4B). Analytical ultracentrifugation of a 2:1 Ala_{16}: Nap_{16} sample gave an observed molecular weight (9302) well below that calculated for the trimer (Table 2).[16] Tagged Nap_{16} (Nap_{His}) was dramatically less efficient than Chx_{His} at retaining Ala_{16} on Ni-NTA agarose beads.[17]

The demonstrated lack of specific interaction between Ala_{16} and Nap_{16} was ascribed to a steric mismatch, due presumably to the overly bulky naphthalene group. To

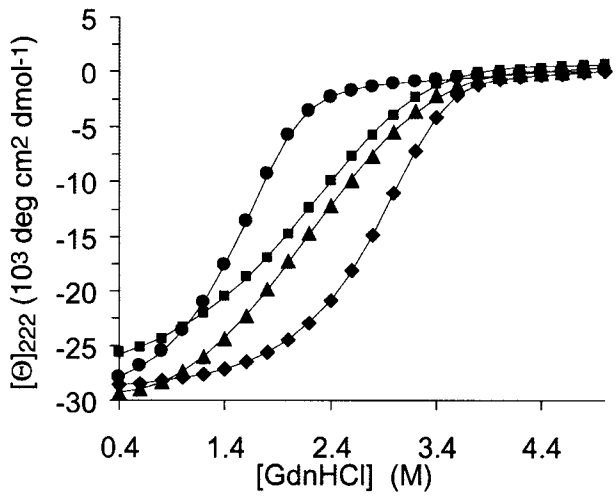

Figure 5. Guanidine hydrochloride denaturation profiles of: **Ala_{16}** (circles), 2:1 **Ala_{16}:Nap_{16}** (squares), 2:1 **Ala_{16}:Cyp_{16}**(triangles), and 2:1 **Ala_{16}:Chx_{16}** (diamonds). Lines are fits to data (see text). All solutions are 10 μM total peptide, in PBS buffer at 25°C

further verify the specific suitability of cyclohexylalanine, the alternative mismatch, in which the partner side chain is too small to complement the alanine pocket, was explored in the form of a cyclopropylalanine-containing peptide (Cyp_{16}). The results parallel those

observed with Nap_{16}, and confirm that the 2:1 Ala_{16}/Cyp_{16} complex is unstable. Both wavelength and thermal denaturation circular dichroism (CD) spectra of the 2:1 mixture overlay well with the weighted average of the pure component signals, suggesting a lack of interaction. The apparent solution molecular weight obtained from sedimentation equilibrium experiments (8515) is well short of that calculated for the heterotrimer (11473).

Table 3. Unfolding Free Energies

Sample	ΔG_{unf} (kcal/mol)
Ala_{16}	18.1 ± 0.17
2:1 **Ala_{16}**: Chx_{16}	22.6 ± 0.04
2:1 **Ala_{16}**: **Nap_{16}**	16.6 ± 0.33
2:1 **Ala_{16}**: **Cyp_{16}**	15.0 ± 0.31
Chx_{16}	24.7 ± 0.08
Nap_{16}	23.5 ± 0.13
Cyp_{16}	22.7 ± 0.31

Relative stabilities of both matched and mismatched complexes were established by chemical denaturation with guanidine hydrochloride. Unfolding free energies at 25 °C were calculated by least-squares fitting to a monomer-trimer model that assumes both folded and unfolded baselines are linear functions of denaturant concentration (Figure 5).[18] The 2:1 Ala_{16}/Chx_{16} mixture is 4.5 kcal/mol more stable than pure Ala_{16}, while the corresponding 2:1 Ala_{16}/Nap_{16} and 2:1 Ala_{16}/Cyp_{16} complexes are 1.5 and 3.1 kcal/mol less stable, respectively (Table 3). Pure Chx_{16}, Nap_{16}, and Cyp_{16} solutions are more resistant to denaturation than any of the mixed complexes. These trends are well

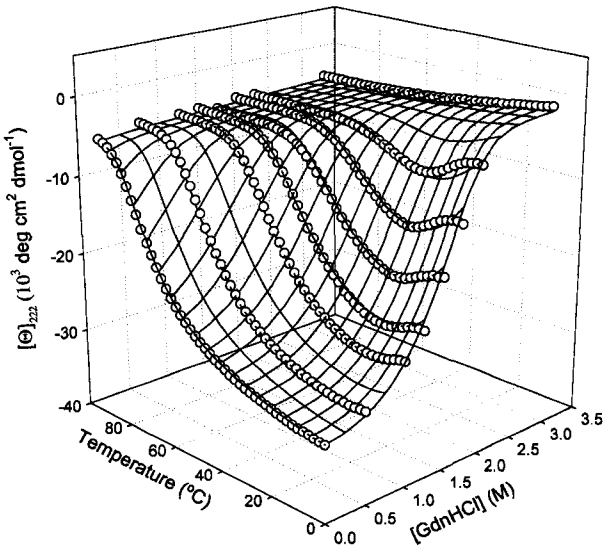

Figure 6. Global thermodynamic analysis of **Ala_{16}**. Solid line mesh depicts simultaneous fit to data (open circles) from eight thermal denaturations. Peptide is 10 μM in PBS buffer with varying concentrations of added guanidine hydrochloride.

correlated with those observed previously via thermal denaturation and sedimentation equilibrium experiments.

Table 4 Thermodynamic Parameters

Sample	ΔH_m (kcal/mol)	T_m (°C)	ΔCp (kcal/mol K)
Ala_{16}	61.6	71	1.06
2:1 **Ala_{16}:Chx_{16}**	83.5	96	1.01

More detailed thermodynamic information was obtained by global analysis of thermal denaturation data from Ala_{16} solutions containing variable concentrations of guanidine hydrochloride (Figure 6).[19] A similar analysis of the matched 2:1 Ala_{16}/Chx_{16} mixture was performed on data from both thermal denaturations with variable guanidine concentrations and guanidine denaturations at variable temperature (Figure 7). In each

case, reasonable estimates were obtained for the unfolding enthalpy at the melting temperature (ΔHm), the melting temperature itself (Tm), and the change in heat capacity (ΔCp) upon unfolding (Table 4). The value of ΔCp is of particular interest as a probe of efficient core packing. Although literature values for well-packed coiled coil structures are somewhat variable, those observed for both Ala_{16} (10.9 cal/(mol K) per residue) and 2:1 Ala_{16}/Chx_{16} (11.4 cal/(mol K) per residue) are within the expected regime.[20]

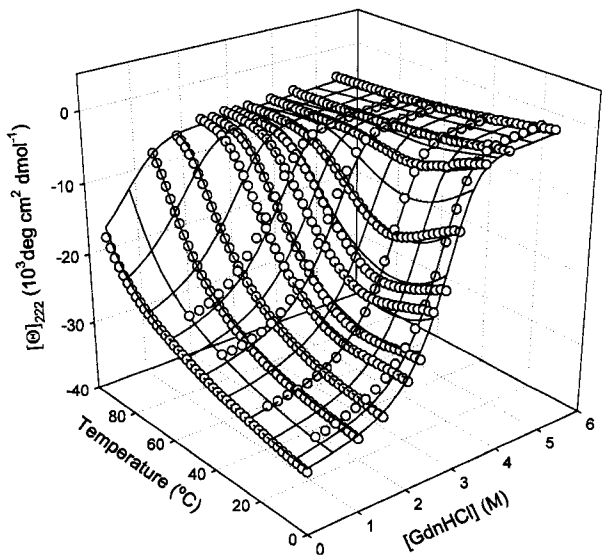

Figure 7. Global thermodynamic analysis of 2:1 **Ala_{16}:Chx_{16}**. Solid line mesh depicts simultaneous fit to data (open circles) from eleven thermal and four chemical denaturations. Total peptide concentration is 10 μM in PBS buffer with varying concentrations of added guanidine hydrochloride.

2-2: Second Generation – The Tris System[21]

Although 2:1 Ala_{16}/Chx_{16} heterotrimer formation validates the principle of steric matching as a means to specificity, the designed system remains less stable than the

Chx_{16} homotrimer. To further discourage alternate assemblies, trisubstituted systems were investigated. However, replacement of three consecutive core *a* residues with alanine (TrisAla) or cyclohexylalanine (TrisChx) did not achieve the desired effect. Both wavelength and thermal denaturation CD spectra of a 2:1 TrisAla/TrisChx mixture are well predicted by averaging the component signals, and only TrisAla suffered the anticipated reduction in homotrimer stability. Coupled with the observed stability of Chx_{16} outlined above, these data suggest that in these systems core layers with steric voids are more damaging than those with steric repulsions.

2-3: A Cooperative Approach – Peptide Tic-Tac-Toe

To capitalize on the apparent sensitivity to all-alanine core layers, a new set of peptides was prepared in which three sequential *a* residues are replaced, two with alanine

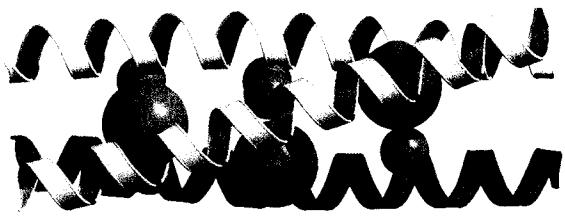

Figure 8. Specificity through multiple interactions. Large core *a* sidechains pack against small ones at the same positions of other strands.

and one with cyclohexylalanine. An equimolar mixture of peptides with cyclohexyl side chains at each possible position should form a parallel 1:1:1 heterotrimer, with each contributing the cyclohexyl group for one core layer (Figure 8). The resulting three-

dimensional arrangement somewhat resembles the outcome of a tic-tac-toe game, with three X groups along the diagonal (Figure 9). Other possible assemblies suffer from at least one destabilizing all-alanine core layer.

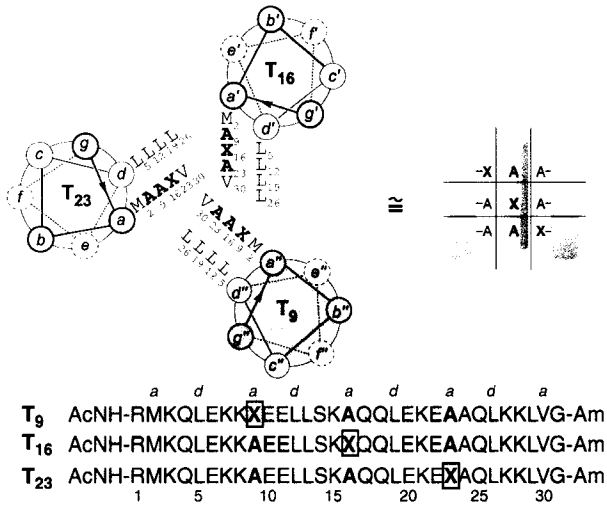

Figure 9. Helical wheel projection of the 1:1:1 T_9:T_{16}:T_{23} complex (viewed down the helical axis from N to C terminus), showing only core residues. The sequence of each peptide is also given. The tic-tac-toe arrangement of cyclohexylalanine residues **(X)** is depicted schematically at right. Ac = acetyl; Am = amide

To test the ability of cooperative steric matching to impart complex specificity, separate peptides were prepared, in which the central three *a* positions are occupied by XAA (T_9), AXA (T_{16}), or AAX (T_{23}) residues. The remaining sequence is based on the first generation system, derived in turn from GCN4 and related peptides.[22]

CD spectra of each individual peptide and the equimolar mixture argue in favor of the 1:1:1 heterotrimer as the most stable complex. All samples exhibit characteristic helical signatures, with minimum molar elipticities at 208 and 222 nm (Figure 10). The degree of sample helicity, determined by the absolute value of the molar elipticity at 222

nm, is considerably larger for the 1:1:1 mixture than for any individual peptide ($[\Theta]_{222}$)- 26200 deg cm^2 $dmol^{-1}$ for the 1:1:1 mixture versus those of individual peptides between -16200 and -21000).

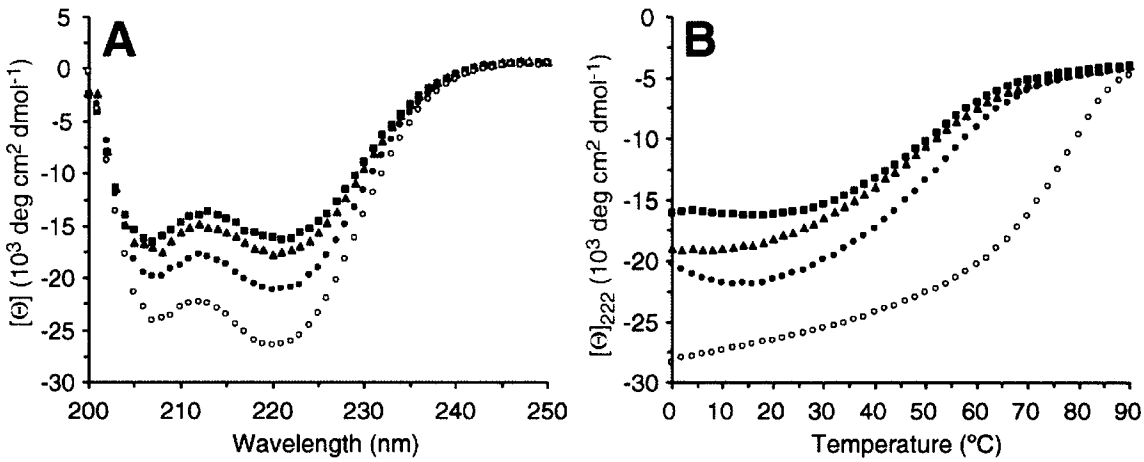

Figure 10. Wavelength scan (**A**) and thermal denaturation (**B**) CD data for solutions of: $\mathbf{T_9}$ (squares), $\mathbf{T_{16}}$ (triangles), $\mathbf{T_{23}}$ (circles), and an equimolar mixture (open circles). All samples are 10 μM total peptide in PBS buffer (10 mM phosphate pH 7.4, 150 mM NaCl).

Thermal and guanidine denaturation experiments further support enhanced stability in the designed complex. Aqueous buffer solutions of pure component strands exhibit significantly lower melting temperatures than their equimolar combination (ΔTm

Table 5. Apparent T_m Values from CD Data

Sample	T_m (°C)	Sample	T_m (°C)
T_9	61	1:1 T_9: T_{16}	63
T_{16}	59	1:1 T_9: T_{23}	71
T_{23}	59	1:1 T_{16}: T_{23}	63
1:1:1 Mixture	83		

> 20 °C, Table 5, Figure 10). The free energy of unfolding for the 1:1:1 sample, obtained by guanidine denaturation, is 19.60 ± 0.21 kcal/mol (Figure 11). In contrast to the designed system, each individual peptide failed to exhibit a cooperative unfolding transition during guanidine titration. Thus, although no quantitative information on unfolding thermodynamics is available, homoaggregates of all three component species are considerably less stable.

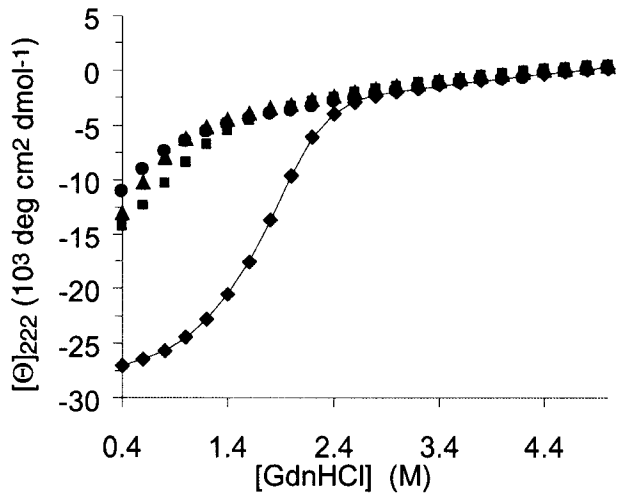

Figure 11. Guanidine hydrochloride denaturation profiles of: $\mathbf{T_9}$ (circles), $\mathbf{T_{16}}$ (squares), $\mathbf{T_{23}}$ (triangles), and an equimolar mixture (diamonds). Line is a fit to data (see text). All solutions are 10 μM total peptide, in PBS buffer at 25°C

To correlate observed helicity profiles with trimer formation, apparent molecular weights (MWapp) in PBS buffer were determined by analytical ultracentrifugation. An equimolar mixture of all three peptides gives an average value (MWapp = 10245) close to that calculated for the heterotrimer (11556), and significantly larger than that for a dimer (7704). Each of the component peptides gives a noticeably lower average, although still

in excess of the dimer value (MWapp = 9104, 9969, and 9729, for T_9, T_{16}, and T_{23}; all individual peptides have identical masses).

Complex stoichiometry was assayed using a T_{16} derivative bearing an N- terminal $(His)_6GlyGly$ affinity tag ($T_{16\text{-}His}$), which binds to nickel nitrilotriacetic acid (Ni-NTA) groups. Buffered peptide solutions are mixed with a slurry of Ni NTA-functionalized

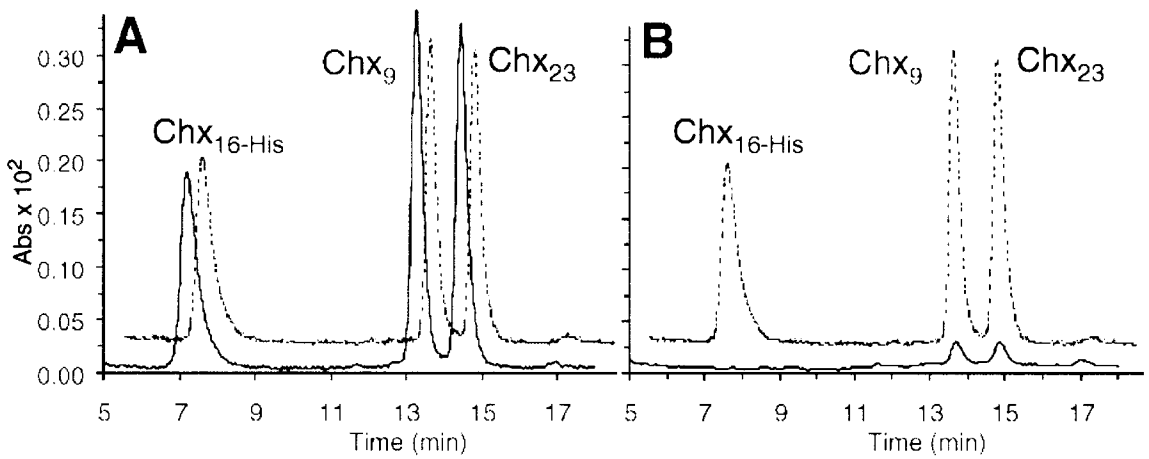

Figure 12. Ni-NTA affinity tag experiments (see text). (**A**) HPLC trace of material retained from 1:1:1 (dotted line) and 1:2:2 (solid line) mixtures of $T_{16\text{-}His}$:T_9:T_{23}. (**B**) Trace from the 1:1:1 mixture (dotted line) plotted with that from an initial solution lacking the tagged peptide (solid line). Injection volumes and extinction coefficients are identical.

agarose beads, followed by centrifugation, supernatant removal, and washing with pure buffer. Peptides bound on the beads are then eluted by treatment with imidazole buffer. Only tagged peptides and their specific binding partners are retained; thus, HPLC analysis of the material in the elution fraction reveals relative peptide concentrations. Equimolar ratios of $T_{16\text{-}His}$ and complementary untagged peptides (T_9, T_{23}) were retained from either 1:1:1 or 1:2:2 initial mixtures (Figure 12A), indicating 1 equivalent of each

peptide in the stable complex. In the absence of $T_{16\text{-His}}$, neither untagged peptide is significantly retained (Figure 12B).

As a final verification that all three peptides are required to achieve a stable complex, CD spectra and thermal denaturation curves were recorded for each of the three pairwise equimolar mixtures (Figure 13). Though somewhat more helical than the

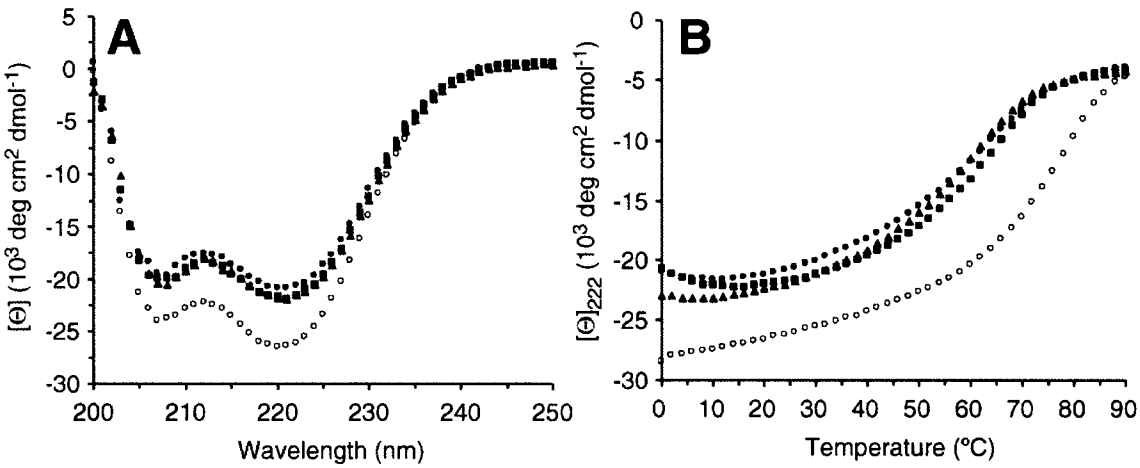

Figure 13. Wavelength scan (**A**) and thermal denaturation (**B**) CD data for solutions of: 1:1 T_9:T_{16} (squares), 1:1 **T_9:T_{23}** (triangles), 1:1 **T_{16}:T_{23}** (circles), and 1:1:1 **T_9:T_{16}:T_{23}** (open circles). Buffer conditions as in legend for Figure 10.

isolated peptides, each sample remains well short of the 1:1:1 mixture ($[\Theta]_{222}$ between -20700 and -21600 deg cm^2 dmol^{-1}). Similarly, no one pair exhibits a melting temperature within 10 deg of the designed system (Table 5). These results also support the significance of steric matching in controlling specificity. Each pairwise mixture can form equal concentrations of two possible 2:1 complexes, both of which have one matched and two mismatched core layers, with one of the mismatches being all alanine. In contrast,

the pure component solutions examined above can form only completely mismatched complexes. Thus, observance of intermediate stability in the pairwise mixtures is consistent with the design principles.

2-4: Experimental Section

Peptide Synthesis. Amino acids (including cyclohexylalanine) were obtained from NovaBiochem (San Diego). Peptides were prepared according to the in situ neutralization protocol developed by Kent,[7] except for Cyp_{16}, which was prepared by standard FMOC solid-phase methods. Each peptide was purified by reversed-phase HPLC (C-18 column, (solvent A) 1% CH_3CN in H_2O, 0.1% (v/v) CF_3CO_2H, (solvent B) 10% H_2O in CH_3CN, 0.07% (v/v) CF_3CO_2H), and the identity of purified samples was confirmed by electrospray mass spectrometry (Finnegan LCQ Duo). All peptides are C-terminally amidated and N-terminally acetylated; each contains an acetamidobenzoate group on the side chain nitrogen of Lys_7 as a spectroscopic label ($\varepsilon_{270} = 18069$).

CD Spectroscopy. All experiments were performed on an Aviv model 202 circular dichroism spectrometer, equipped with a Microlab 500 series automated titration assembly. Sample concentrations were measured by UV absorbance of the acetamidobenzoate label at 270 nm. Wavelength data are the average of three scans from 250 to 200 nm in 1 nm steps. Thermal denaturation experiments at 222 nm were run from 0 to 90 °C in 2 deg steps, at a 2 deg/min rate of increase with 1 min of equilibration and data averaging at each temperature. Tm values were obtained from the minima of the first derivatives of Θ vs 1/T plots. Guanidinium titrations were performed using the

automated titration assembly. The signal at 222 nm was recorded for solutions of constant peptide concentration with guanidine hydrochloride concentrations varied from 0 to 5 M in 0.2 M increments. Data were collected for 1 min at each step, with 10 min equilibration times (solutions were stirred during equilibration but not data collection).

Analytical Ultracentrifugation. Sedimentation equilibrium experiments were performed using a Beckman XL-I analytical ultracentrifuge equipped with an An60 Ti rotor. Data were collected using 12mm path length six-sector centerpieces at 270 nm. Samples were dialyzed against the reference buffer at 4 °C overnight. Data were collected at 38000 and 48000 rpm at concentrations spanning 17-55 μM. Samples were judged equilibrated (in all cases equilibration was complete in 12 h) when three consecutive scans taken 1 h apart were indistinguishable. Solvent densities and partial molar volumes were calculated in the manner prescribed by Laue.[23] Data were analyzed using Origin and fit to ideal single-species and appropriate monomer-oligomer models.

Ni-NTA Affinity Tag Experiments (Figure 14)**.** A 0.5 mL sample of a 50% slurry of Ni-NTA agarose (Qiagen) in an Eppendorf tube was centrifuged for 30 s, followed by removal of the supernatant. Peptide solution was added, and the tube was repeatedly inverted for 5 min. The sample was centrifuged (30 s), and the supernatant (flow-through fraction) was removed. The procedure was then repeated with 1 mL of buffer (wash fraction) and 1 mL of buffer containing 250 mM imidazole (elution fraction), except that the wash fraction was not agitated for 5 min. Solutions were analyzed by RP -HPLC. All solutions were 10 μM in total peptide, except for the 3:1 Ala_{16}:Chx_{His}, which was 13.3

μM; the 2:1:2 $T_9/T_{16\text{-}His}/T_{23}$ mixture, which was 16.6 μM; and the 1:1 T_9/T_{23}, which was 6.6 μM.

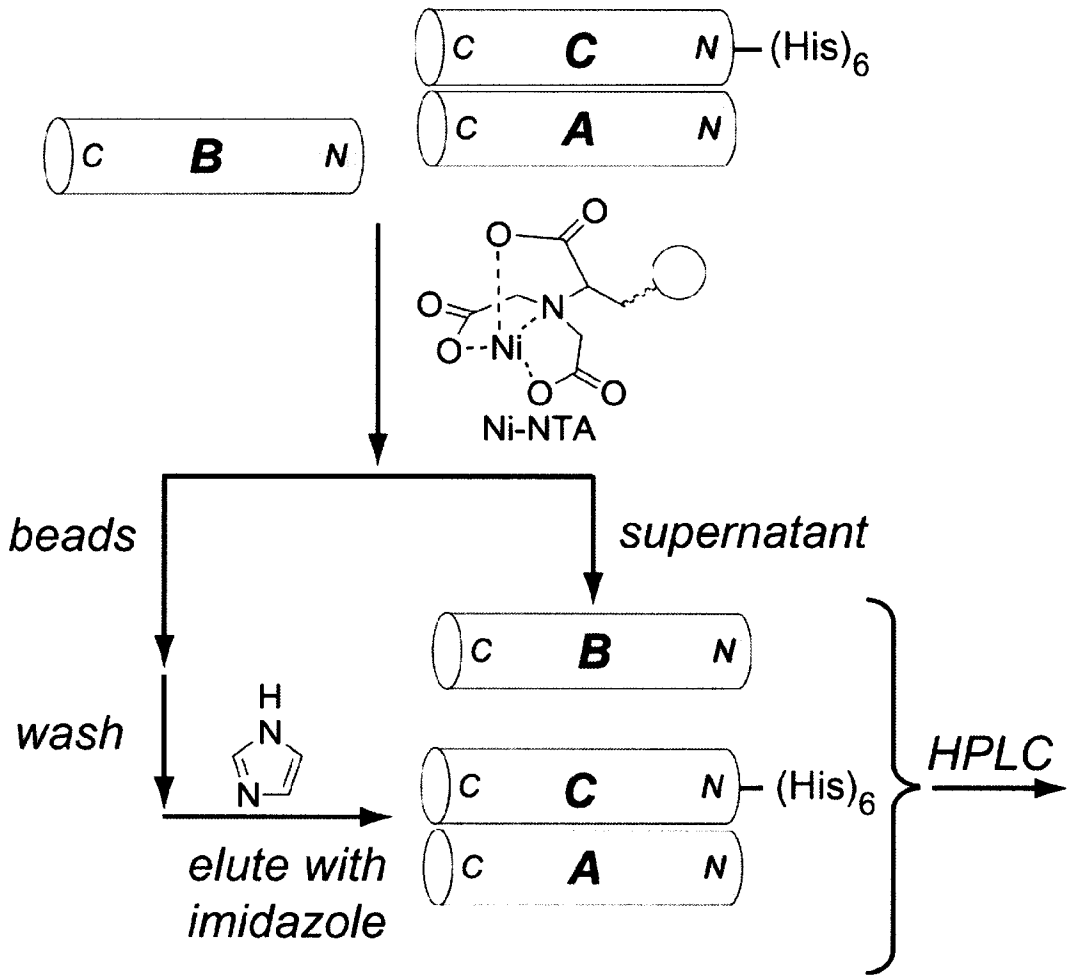

Figure 14. . Ni-NTA affinity tag analysis scheme. Initially, peptide **A** is specifically bound to **C**, which bears an N-terminal Gly-Gly-$(His)_6$ affinity tag. Upon exposure to Ni-NTA agarose beads, **C** is bound through the His tag, and **A** is bound through it's interaction with **C**. Only **B,** which does not interact with the beads or the tagged peptide, remains unbound. After supernatant removal and washing with blank buffer, bound material is eluted by treatment with imidazole or low pH (2.5). HPLC analysis reveals identity of unbound (supernatant fraction) and bound (elution fraction) material. Peptides **A** and **B** are intended to represent all binding and non-binding peptides, respectively. Thus any higher order aggregates are analyzed in the same manner.

2-5: Literature Cited

(1) Guo, Z.; Zhou, D.; Schultz, P. G. *Science* **2000**, *288*, 2042-2045. DeLano, W. L.; Ultsch, M. H.; De Vos, A. M.; Wells, J. A. *Science* **2000**, *287*, 1279-1283.

(2) (1) (a) Micklatcher, C.; Chmielewski, J. *Curr. Opin. Chem. Biol.* **1999**, *3*, 724-729. (b) DeGrado, W. F.; Summa, C. M.; Pavone, V.; Nastri, F.; Lombardi, A. *Annu. Rev. Biochem.* **1999**, *68*, 779-819. (c) Kohn, W. D.; Kay, C. M.; Hodges, R. S. *J. Mol. Biol.* **1998**, *283*, 993-1012.

(3) (a) Tang, Y.; Ghirlanda, G.; Vaidehi, N.; Kua, J.; Mainz, D. T.; Goddard, W. A., III; DeGrado, W. F.; Tirrell, D. A. *Biochemistry* **2001**, *40*, 2790-2796. (b) Hill, R. B.; Hong, J.-K.; DeGrado, W. F. *J. Am. Chem. Soc.* **2000**, *122*, 746-747. (c) Harbury, P. B.; Plecs, J. J.; Tidor, B.; Alber, T.; Kim, P. S. *Science* **1998**, *282*, 1462-1467. (d) Oakley, M. G.; Kim, P. S. *Biochemistry* **1998**, *37*, 12603-12610. (e) Harbury, P. B.; Zhang, T.; Kim, P. S.; Alber, T. *Science* **1993**, *262*, 1401-1407. (f) Gonzalez, L., Jr.; Woolfson, D. N.; Alber, T. *Nat. Struct. Biol.* **1996**, *3*, 1011-1018..

(4) Schnarr, N.A., Kennan, A.J. *J. Am. Chem. Soc.* **2001**, *123*, 11081-11082.

(5) O'Shea, E. K.; Klemm, J. D.; Kim, P. S.; Alber, T. *Science* **1991**, *254*, 539-544.

(6) Gonzalez, L., Jr.; Plecs, J. J.; Alber, T. *Nat. Struct. Biol.* **1996**, *3*, 510-515.

(7) Peptides were synthesized by standard solid phase methods, as in: Schnoelzer, M.; Alewood, P.; Jones, A.; Alewood, D.; Kent, S. B. H. *Int. J. Pept. Protein Res.* **1992**, *40*, 180-193.

(8) Lumb, K. J.; Kim, P. S. *Biochemistry* **1995**, *34*, 8642-8648.

(9) Hendsch, Z. S.; Nohaile, M. J.; Sauer, R. T.; Tidor, B. *J. Am. Chem. Soc.* **2001**, *123*, 1264-1265.

(10) T_m values were obtained according to the procedure outlined in: Cantor, C. R.; Schimmel, P. R. *Biophysical Chemistry of Macromolecules, Pt. 3*; W. H. Freeman: New York, NY, 1980, p.1132

(11) Guanidinium hydrochloride (1.5 M) had to be added to observe T_m values below 90°C for either **Chx_{16}** or the 2:1 mixture.

(12) Low concentrations were used so that differential stabilities could be assayed. The unusual curve shape presumably reflects partial unfolding in this regime. Spectra at 10 μM exhibit ~ equal minima at 208/222 nm.

(13) Initial experiments in aqueous buffer with no guanidinium hydrochloride at peptide concentrations from 15 to 55 μM demonstrated that **Ala_{16}**, **Chx_{16}**, and the 2:1 mixture are all largely trimeric.

(14) The pure **Chx_{16}** gives a MW_{obs} significantly in excess of the calculated trimer, perhaps indicative of higher-order aggregation that may also be reflected in the broader melting transition discussed above.

(15) Brown, M. B.; Sauer, R. T. *Proc. Natl. Acad. Sci. USA* **1999**, *96*, 1983-1988. **Ala_{16}** was not bound in the absence of **Chx_{His}**, but was retained from a 2:1:2 **Ala_{16}**:**Chx_{His}**:**Chx_{16}** mixture. See Supporting Information for details.

(16) The pure **Nap_{16}** sample, like that of **Chx_{16}** displays considerable self-aggregation. Although the reasons for this are not obvious, the heterotrimer is clearly disfavored.

(17) **Ala_{16}**:**Nap_{His}** ratio retained from a 3:1 mixture was less than 1:3.5.

(18) (a) Santoro, M. M.; Bolen, D. W. *Biochemistry* **1988**, *27*, 8063-8068. (b) Becktel, W. J.; Schellman, J. A. *Biopolymers* **1987**, *26*, 1859-1877. Monomer-trimer

equilibrium modeled as in: (c) Jelesarov, I.; Lu, M. *J. Mol. Biol.* **2001**, *307*, 637-656. Duerr, E.; Jelesarov, I. *Biochemistry* **2000**, *39*, 4472-4482.

(19) Kuhlman, B.; Raleigh, D. P. *Protein Sci.* **1998**, *7*, 2405-2412.

(20) Boice, J. A.; Dieckmann, G. R.; DeGrado, W. F.; Fairman, R. *Biochemistry* **1996**, *35*, 14480-14485.

(23) Schnarr, N.A., Kennan, A.J. *J. Am. Chem. Soc.* **2002**, *124*, 9779-9783.

(22) For a similar approach using natural side chains see: Kiyokawa, T.; Kanaori, K.; Tajima, K.; Tanaka, T. *Biopolymers* **2001**, *55*, 407-414. Kashiwada, A.; Hiroaki, H.; Kohda, D.; Nango, M.; Tanaka, T. *J. Am. Chem. Soc.* **2000**, *122*, 212-215.

(23) Laue, T. M.; Shah, B. D.; Ridgeway, T. M.; Pelletier, S. L. in *Analytical Ultracentrifugation in Biochemistry and Polymer Science*; Harding, S. E., Rowe, A. J., Horton, J. C., Eds.; The Royal Society of Chemistry: Cambridge, 1992; pp 90-125.

Chapter 3

Combining Orthogonal Interfaces

Although the steric matching approach to designing a single trimer was highly successful, the true potential of self-assembly will be tapped only by more sophisticated systems. In turn, the design of more intricate structures demands the simultaneous operation of multiple orthogonal recognition modes. As a first step in this direction, we were interested in exploring the use of two independent specificity mechanisms within the same peptide. Given the considerable body of literature on controlling coiled-coil specificity with *e/g* electrostatic interactions,[1] we decided to target a system that employs both the core recognition strategy we have developed, and electrostatic matching of glutamic acid (Glu)/lysine (Lys) *e/g* residues.

3-1: Matched and Mismatched Hydrophilic Interfaces – What are the Rules? [2]

Relative stabilities have been measured for core-matched complexes with one, two, or all three electrostatically matched *e/g* interfaces. Control experiments with mismatched core arrangements demonstrate that both interfaces are significant in controlling complex stability. The attendant increase in design precision is exploited in the assembly of three specific trimers from a mixture of six different peptides, a process accessible only through these methods.

The peptides used are derived from those in our previous work (Figure 1). Each parent peptide contains either XAA (T_9), AXA (T_{16}) or AAX (T_{23}) at the central three *a* positions (A = alanine, X = cyclohexylalanine). The corresponding sequences bearing either Glu (T_nE) or Lys (T_nK) at all *e/g* positions were prepared, as well as hybrids (T_nE/K) with Glu and Lys in all *e* and *g* positions, respectively. Different equimolar

combinations of these peptides give rise to complexes featuring either zero, one, or three sterically matched 2:1 Ala:Chx core layers, along with zero, one, two, or three electrostatically matched Glu/Lys *e/g* interfaces.

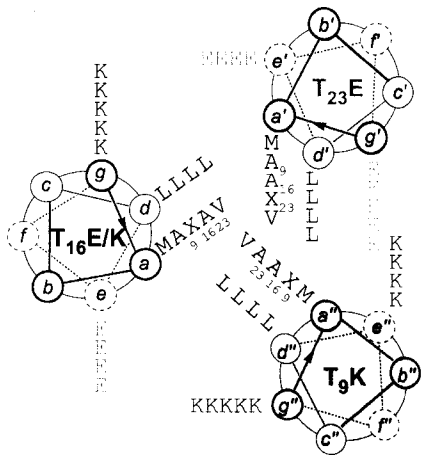

Figure 1. Peptides employed. Each sequence derives from one of three parents ($\mathbf{T_9}$, $\mathbf{T_{16}}$, $\mathbf{T_{23}}$) by replacement of all *e/g* residues with Glu ($\mathbf{T_nE}$), Lys ($\mathbf{T_nK}$), or both ($\mathbf{T_nE/K}$), as indicated. Helical wheel projection of the totally matched trimer ($\mathbf{T_9K{:}T_{16}E/K{:}T_{23}E}$) is also given to illustrate the interfaces involved. Solvent-exposed residues omitted for clarity. **X** = cyclohexylalanine. Each peptide is N-terminally acetylated (Ac) and C-terminally amidated (Am). The positions of core modification in the parent peptides are underlined.

To determine the general impact of electrostatics on these peptides, pure solutions of each new sequence were examined by circular dichroism (CD) spectroscopy. Based on literature demonstrations of like-charge repulsion at *e/g* interfaces, along with our

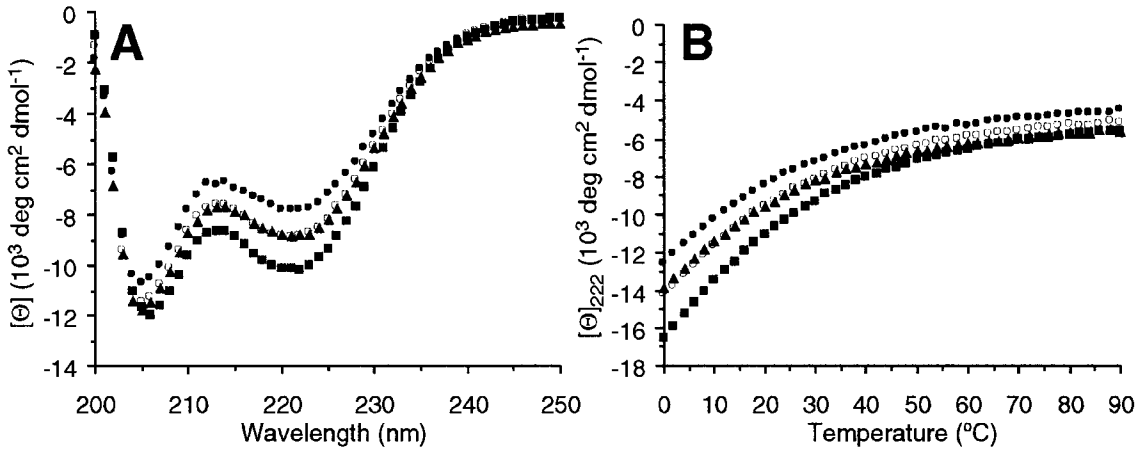

Figure 2. Wavelength scan (**A**) and thermal denaturation (**B**) CD data for solutions of: $\mathbf{T_9K}$ (circles), $\mathbf{T_{16}K}$ (triangles), $\mathbf{T_{23}K}$ (squares), and an equimolar mixture (open circles). All samples are 10 μM total peptide in PBS buffer (10 mM phosphate pH 7.4, 150 mM NaCl).

work on mismatched core sequences, we expected these homotrimers to be poor candidates for stable complex formation. In fact, the Lys-substituted basic peptides (T_nK) exhibit a somewhat helical wavelength profile, but with low absolute intensity, while thermal denaturation demonstrated a non-cooperative unfolding transition (Figure 2). Similar results were observed for the Glu-substituted acidic peptides (T_nE), which gave even weaker signals (Figure 3). The wavelength profiles are significantly distorted from helical norms, while the thermal unfolding curves afford slightly shallower and earlier transitions than for the Lys peptides. To verify that charge repulsion remains

destabilizing with matched core sequences, a requirement for orthogonal control of complex specificity, equimolar mixtures of all like-charged peptides were examined (i.e. 1:1:1 T_9K:$T_{16}K$:$T_{23}K$ and T_9E:$T_{16}E$:$T_{23}E$). In each case, CD spectra are consistent with those calculated by averaging component signals, arguing against interaction to form new stable complexes.

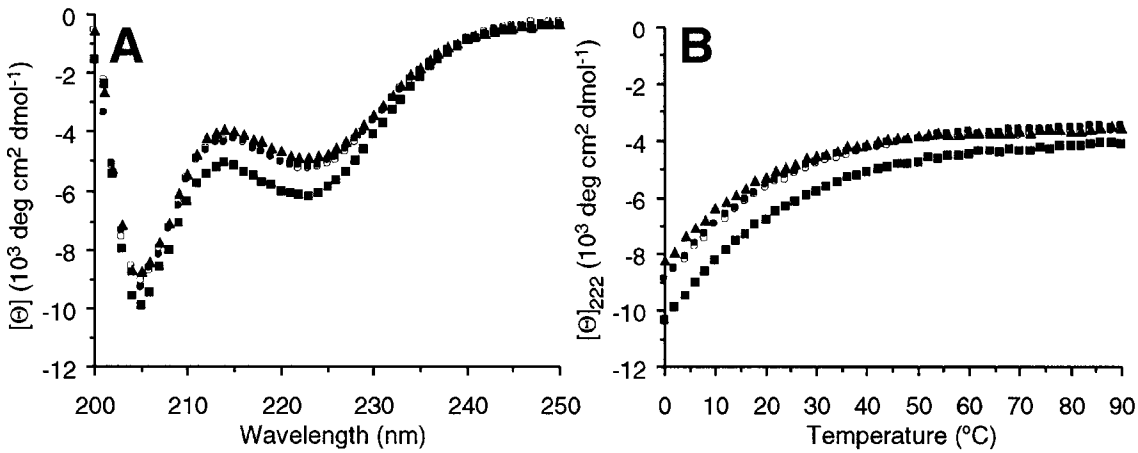

Figure 3. Wavelength scan (**A**) and thermal denaturation (**B**) CD data for solutions of: $\mathbf{T_9E}$ (circles), $\mathbf{T_{16}E}$ (triangles), $\mathbf{T_{23}E}$ (squares), and an equimolar mixture (open circles). Conditions as in Figure 2.

Having demonstrated the viability of electrostatic control in these systems, we next investigated complexes with variable numbers of matches. In all cases the hydrophobic cores were completely matched, in order to isolate electrostatic effects. Since parallel coiled-coil trimers contain three *e/g* interfaces, we examined assemblies with zero, one, two, or three matched Glu/Lys contacts. As expected, the equimolar T_9K:$T_{16}E/K$:$T_{23}E$ mixture, in which all *e/g* interfaces pair Glu against Lys, is highly

helical and thermally stable by CD ($[\Theta]_{222}$ = –28,457 deg cm^2 dmol^{-1}, Tm = 83°C, Figure 4). Sequential replacement of each Glu/Lys interface with a Lys/Lys one produced an

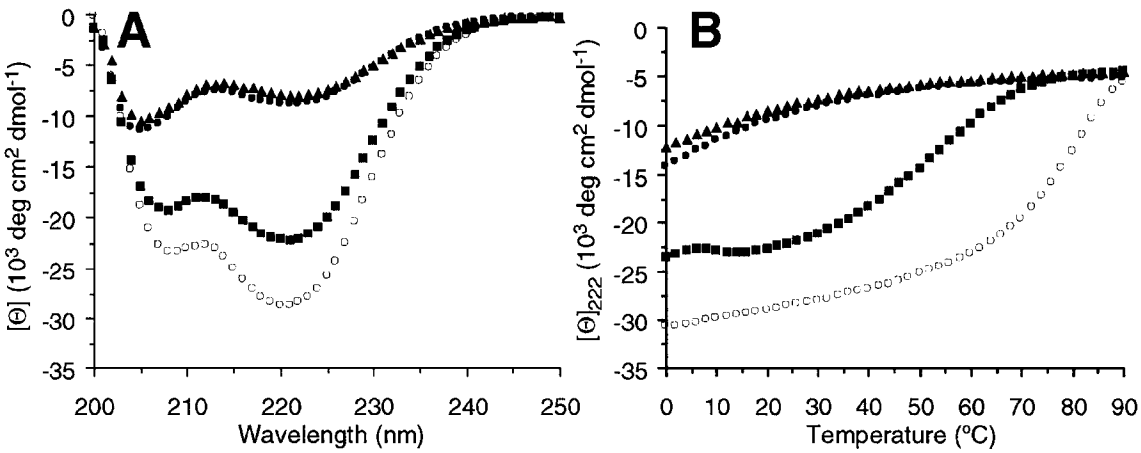

Figure 4. Wavelength scan (**A**) and thermal denaturation (**B**) CD data for equimolar solutions of: **T_9K:T_{16}K:T_{23}K** (circles), **T_9K:T_{16}E/K:T_{23}K** (triangles), **T_9K:T_{16}E:T_{23}K** (squares), and **T_9K:T_{16}E/K:T_{23}E** (open circles). Conditions as in Figure 2.

interesting result. Although the mixture with two Lys/Lys repulsive interactions (T_9K:T_{16}E/K:T_{23}K) is virtually indistinguishable from the totally mismatched system examined above, the complex with one Lys/Lys juxtaposition (T_9K:T_{16}E:T_{23}K) is reasonably stable ($[\Theta]_{222}$ = –22,098 deg cm^2 dmol^{-1}, Tm = 61°C). In contrast, when matched interfaces are replaced by Glu/Glu interactions, even a single mismatch is almost completely destabilizing (T_9E:T_{16}K:T_{23}E, Figure 5). This differential instability, observed previously in disulfide-bonded homodimers, provides another useful mechanism for controlling specificity.

To further assess relative strengths of the hydrophobic and hydrophilic recognition mechanisms, we examined complexes with only partially mismatched cores. The heterotrimer formed from an equimolar mixture of T_9K:$T_{16}E/K$:$T_{16}E$ contains 2:1,

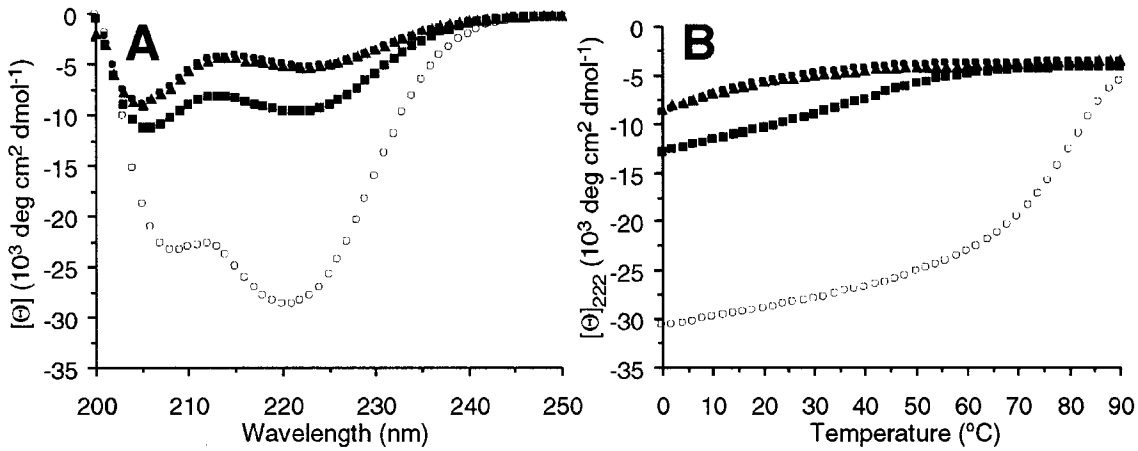

Figure 5. Wavelength scan (**A**) and thermal denaturation (**B**) CD data for equimolar solutions of: $\mathbf{T_9E}$:$\mathbf{T_{16}E}$:$\mathbf{T_{23}E}$ (circles), $\mathbf{T_9E}$:$\mathbf{T_{16}E/K}$:$\mathbf{T_{23}E}$ (triangles), $\mathbf{T_9E}$:$\mathbf{T_{16}K}$:$\mathbf{T_{23}E}$ (squares), and $\mathbf{T_9K}$:$\mathbf{T_{16}E/K}$:$\mathbf{T_{23}E}$ (open circles). Conditions as in Figure 2.

1:2, and 3:0 ratios of alanine to cyclohexylalanine at the three core layers. It thus represents an intermediate state between the fully matched and mismatched core systems, with completely matched *e/g* interfaces. Its CD profile ($[\Theta]_{222}$ = –19,593 deg cm^2 dmol^{-1}, Tm = 63°C) is comparable to that observed for the T_9K:$T_{16}E$:$T_{23}K$ system, which contains a matched core and one repulsive Lys/Lys *e/g* interface (Figure 6). The system containing two intermediate mismatches (T_9K:$T_{16}E$:$T_{16}K$), with only one 2:1 Ala:Chx layer and one Lys/Lys interface, retains little if any stability. Its CD spectra closely resemble those of systems with completely mismatched cores containing either matched

or single Lys/Lys *e/g* surfaces. The capacity of each criterion, hydrophobic or hydrophilic, to control assembly preferences seems well balanced by the other.

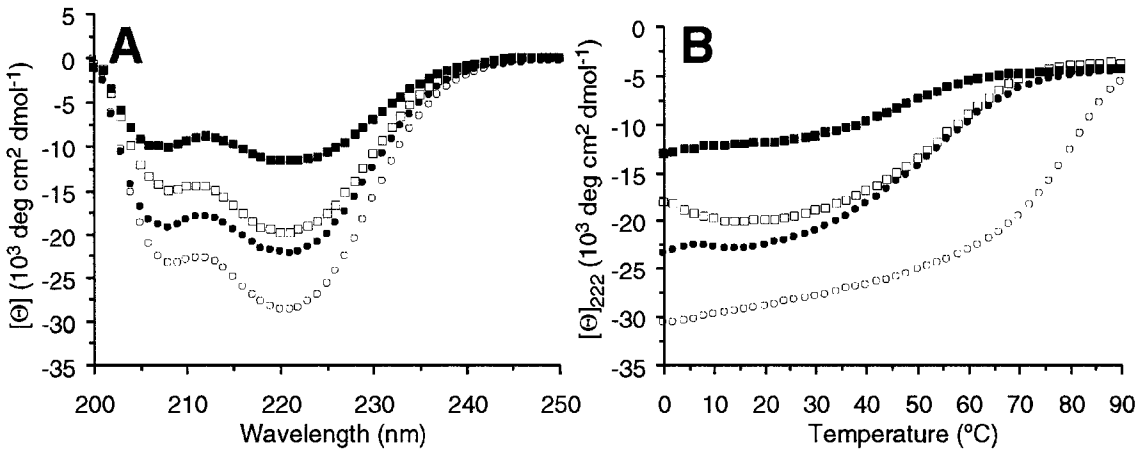

Figure 6. Wavelength scan (**A**) and thermal denaturation (**B**) CD data for equimolar solutions of: $\mathbf{T_9K}$:$\mathbf{T_{16}E}$:$\mathbf{T_{16}K}$ (squares), $\mathbf{T_9E}$:$\mathbf{T_{16}E/K}$:$\mathbf{T_{16}K}$ (open squares), $\mathbf{T_9K}$:$\mathbf{T_{16}E}$:$\mathbf{T_{23}K}$ (circles), and $\mathbf{T_9K}$:$\mathbf{T_{16}E/K}$:$\mathbf{T_{23}E}$ (open circles). Conditions as in Figure 2.

Before proceeding with the simultaneous implementation of these specificity controls, we sought to further characterize representative complexes. Since dimers, trimers, and higher oligomers of these peptides are predicted to be comparably helical, CD is not a good measure of specificity in aggregation number. Independent verification was gathered from sedimentation experiments in the analytical ultracentrifuge. Observed molecular weights in solution were obtained for systems containing matched cores and either all Glu/Lys (T_9K:$T_{16}E/K$:$T_{23}E$), one Lys/Lys (T_9K:$T_{16}E$:$T_{23}K$), or one Glu/Glu interface (T_9E:$T_{16}K$:$T_{23}E$). The completely matched system affords a value close to that calculated for the heterotrimer, and a single Lys/Lys interface lowers the observed weight only slightly (Table 1). In contrast, the Glu/Glu interaction, shown to be destabilizing by

CD, results in an observed weight closer to that of a dimer. Quantification of complex

Table 1. Molecular Weights from Sedimentation Equilibrium[a]

Sample	MW_{app}	MW_{calc}dimer[b]	MW_{calc}trimer
T_9K:$T_{16}E$/K:$T_{23}E$	11362	7709	11563
T_9K:$T_{16}E$:$T_{23}K$	10949	7706	11559
T_9E:$T_{16}K$:$T_{23}E$	8390	7712	11568

[a] Conditions as in Figure 2. [b] Average of 3 possible heterodimers

stability was obtained from guanidine hydrochloride denaturation experiments at 25°C (Figure 7). The completely matched assembly exhibits a cooperative unfolding pattern, while the single Lys/Lys complex displays an intermediate transition, and the single Glu/Glu complex is essentially uncooperative. Data from the matched system were fit

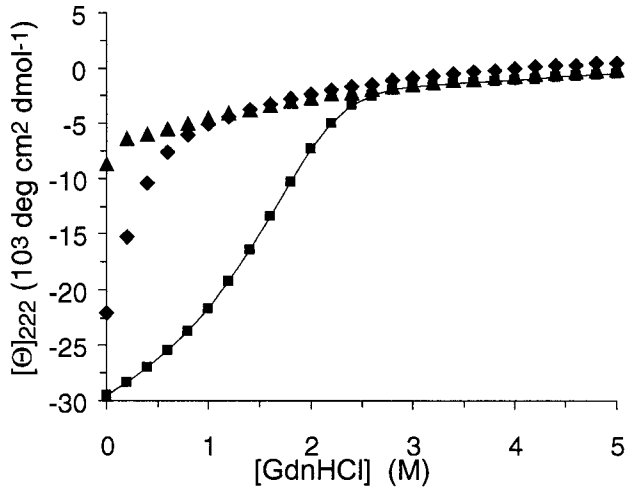

Figure 7. Guanidine hydrochloride denaturation profiles (25°C) of: **T_9K:$T_{16}E$/K:$T_{23}E$** (squares), **T_9K:$T_{16}E$:$T_{23}K$** (diamonds), and **T_9E:$T_{16}K$:$T_{23}E$** (triangles). All solutions 10 μM total peptide.

according to a monomer-trimer model that assumes both folded and unfolded baselines are linear functions of denaturant concentration.[3] The observed unfolding free energy of 17.93 ± 0.40 kcal/mol is comparable to that of the parent T_9:T_{16}:T_{23} system (19.60 ± 0.21 kcal/mol). These experiments support the viability of CD screens for reasonable complexes.

3-2: Complex Assembly – Peptide Sorting

Having established the means for independent control of complex specificity by hydrophobic or hydrophilic interfaces, we focused on its application to more complicated

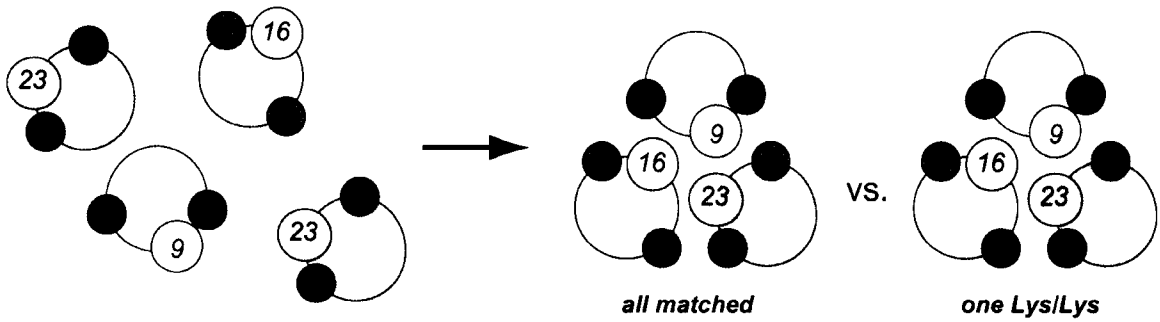

Figure 8. Competition between all Glu/Lys and one Lys/Lys interfaces. Equimolar mixture of **T_9K**, **T_{16}E**, **T_{23}E/K**, and **T_{23}K** can form two different heterotrimers. If **T_{23}E/K** is used, the complex has fully matched electrostatic *e/g* interfaces (all Glu/Lys). If **T_{23}K** is included instead, the assembly has one repulsive Lys/Lys interface.

assembly problems. Since viable complexes result from either fully matched (all Glu/Lys) or singly mismatched (one Lys/Lys) *e/g* interfaces, we sought to directly assay their relative stabilities. An equimolar mixture of T_9K, T_{16}E, T_{23}E/K, and T_{23}K can result

in formation of either heterotrimer type, depending on which T_{23} derivative is incorporated (Figure 8).

To determine relative complex stabilities, an affinity tag strategy we have previously employed proved useful.[4] A $(His)_6GlyGly$ sequence that binds Ni-nitrilotriacetic acid (Ni-NTA) functionalized agarose beads was appended to the N-terminus of $T_{16}E$ (to give $T_{16}EHis$). In the experiment, buffered peptide solutions are

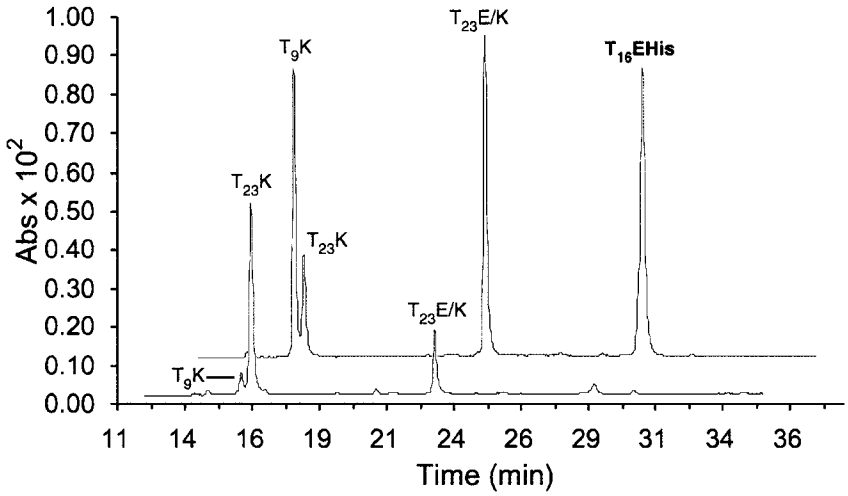

Figure 9. Ni-NTA affinity tag analysis of equimolar **T_9K**, **$T_{16}EHis$**, **$T_{23}E/K$**, **$T_{23}K$** mixture. Supernatant solution (front trace) is significantly enriched in **$T_{23}K$**, while elution fraction (back trace) contains largely the components of the fully matched heterotrimer (**T_9K**, **$T_{16}EHis$**, **$T_{23}E/K$**). See Figure 8 for schematic diagram.

mixed with a slurry of Ni-NTA beads, followed by centrifugation, supernatant removal, and washing with pure buffer. Upon subsequent elution with imidazole buffer, only tagged peptides and their specific binding partners are obtained, thus HPLC analysis of the elution fraction reveals relative peptide concentrations. In the present case, analysis of the supernatant solution is also instructive, as it should contain the rejected T_{23}

component. As expected, observed peak ratios are consistent with a significant preference for the fully matched complex (Figure 9). Specifically, the supernatant solution is enriched in $T_{23}K$, while the elution fraction is dominated by $T_{23}E/K$, the peptide required for the fully matched heterotrimer.

The preference for fully matched systems was also verified in a more complex mixture, equimolar in all nine of the new sequences (T_nE, T_nK, T_nE/K). The analysis is also more complicated, since each peptide can participate in either of two unique fully

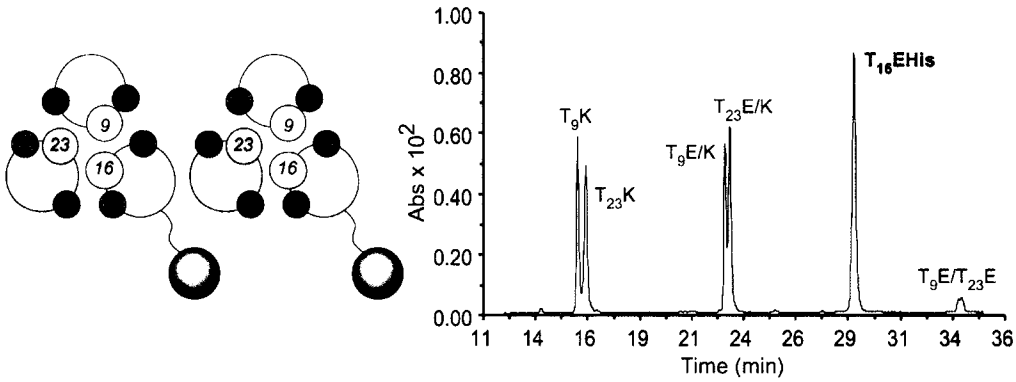

Figure 10. Ni-NTA affinity tag analysis of complex mixture. Equimolar ratios of all nine electrostatic interface peptides (**T_nE**, **T_nK**, **T_nE/K**) can afford six different fully matched complexes, with each peptide participating in two. The possibilities for **$T_{16}E$** are represented at left (black sphere indicates connection to Ni-NTA beads). At right is the elution fraction from a mixture containing **$T_{16}EHis$**, demonstrating retention of precisely the required binding partners.

matched complexes, or one of two other assemblies bearing a single Lys/Lys interface. Again the mixture was deconvoluted by the Ni-NTA method, this time by considering the results of three parallel experiments. A different acidic peptide (T_nE) was tagged in each case.

The elution fraction from one such experiment, with T_{16}EHis as the tagged peptide, again reveals a preference for fully matched systems (Figure 10). As expected, approximately equimolar ratios of the components from both possible matched complexes are observed. In addition, the roughly equal ratio of basic (T_9K, $T_{23}K$) to hybrid (T_9E/K, $T_{23}E/K$) peptides is consistent with the formation of these matched assemblies to the near exclusion of single Lys/Lys ones, as the latter necessarily require a twofold excess of basic peptides. Similar results were obtained from experiments with T_9EHis and T_{23}EHis.

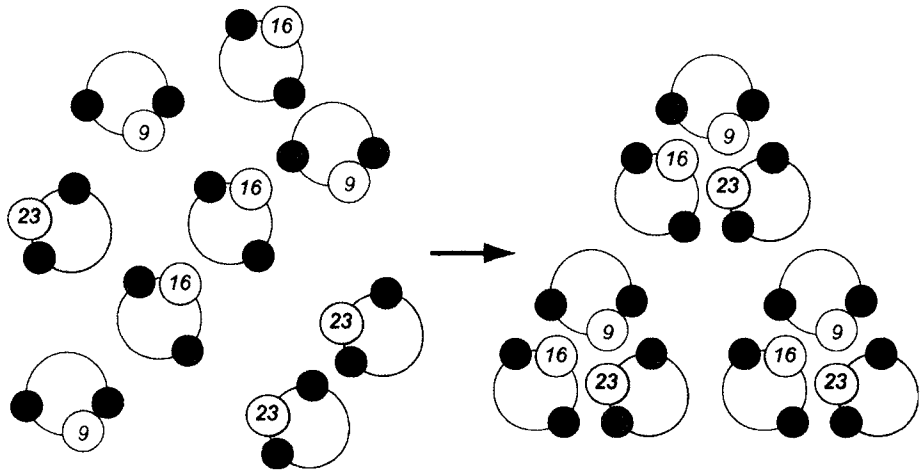

Figure 11. A more specific assembly system. Mixing two equivalents of each basic peptide (**T_nK**) with one equivalent of each acidic peptide (**T_nE**) results in formation of three specific heterotrimers starting from six different peptides. Numbers indicate location of cyclohexylalanine in the sequence.

Although these experiments demonstrated the capacity for favoring a given ensemble of structures, we were eager to identify a strategy that would allow more specific assembly control. By turning to the other viable set of interactions, complexes

with one Lys/Lys interface, we have been able to promote the specific formation of three independent heterotrimer complexes from an input of only six different peptides. From a 2:2:2:1:1:1 mixture of T_9K:$T_{16}K$:$T_{23}K$:T_9E:$T_{16}E$:$T_{23}E$ only three specific heterotrimers can be formed while maintaining the recognition requirements developed above (Figure 11). Each complex contains two basic and one acidic peptide, with the core sequence of the acidic peptide varied from one trimer to the next. Such a rapid build-up of complexity is possible only through the interaction of two distinct recognition mechanisms. The lack of such specificity associated with the fully matched systems described above also underlines the power of more diverse possible combinations.

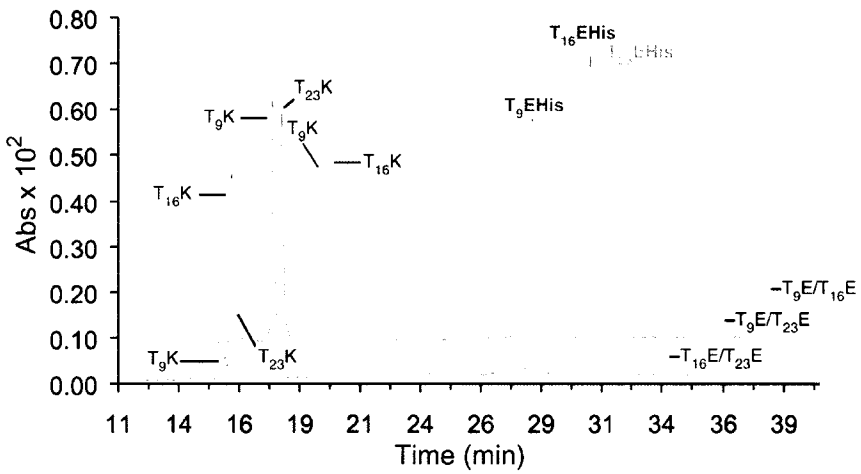

Figure 12. Ni-NTA affinity tag analysis of more complicated assembly system (see text). Traces correspond to elution fractions of experiments using: **T_9EHis** (front), **T_{16}EHis** (middle), and **T_{23}EHis** (back) as tagged peptides.

Although work on each isolated system made formation of three specific heterotrimers the only likely outcome, we sought more direct evidence of successful and specific formation of the designed complexes. To verify the presence of each specific

heterotrimer, elution fractions from three parallel Ni-NTA experiments with different tagged peptides (T_nE) were compared (Figure 12). In each case, the significant HPLC peaks are due only to the tagged peptide and its two specific binding partners. Taken together these data provide strong evidence for the designed assembly.

3-3: pH and Stability

Studies of pH sensitivity in related peptide complexes demonstrate that pH variation can alter the relative stabilities of single *e/g* interface mismatches. To verify similar effects in our heterotrimer systems, circular dichroism (CD) spectra were

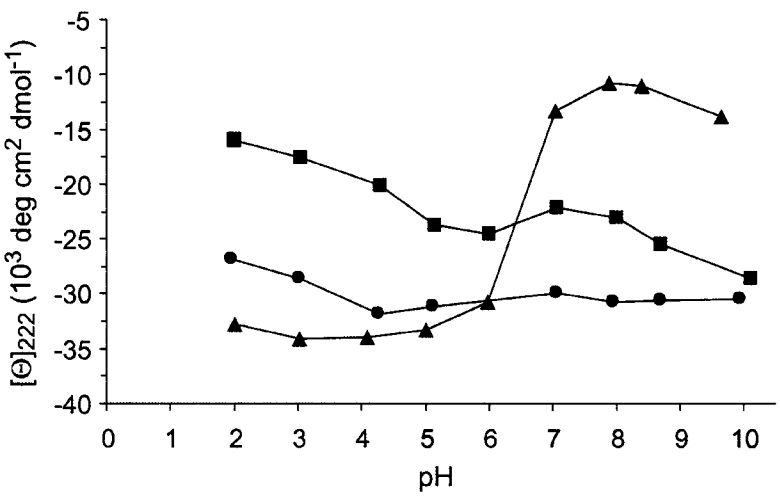

Figure 13. pH titration of heterotrimer helicity. Value of $[\Theta]_{222}$ as function of pH for equimolar solutions of: T_9K:$T_{16}E/K$:$T_{23}E$ (all matched, circles), T_9K:$T_{16}E$:$T_{23}K$ (one Lys/Lys, squares), and T_9E:$T_{16}K$:$T_{23}E$ (one Glu/Glu, triangles). All solutions are 10 μM total peptide in PBS buffer (10 mM phosphate, 150 mM NaCl)

recorded between pH 2 and 10 for complexes bearing one Glu/Glu (T_9E, $T_{16}K$, $T_{23}E$), one Lys/Lys (T_9K, $T_{16}E$, $T_{23}K$), or fully matched (T_9K, $T_{16}E/K$, $T_{23}E$) electrostatic interfaces (Figure 13). Above neutral pH the relative helicity (and hence stability) of acidic and

basic complexes is as before. In contrast, at pH 5 and below the Glu/Glu contact is preferred. The fully matched complex is relatively unaffected in this window.

3-4: Specific Strand Exchange[5,6]

These observations provide a mechanism for pH-triggered exchange of heterotrimer components. (Figure 14). A pre-formed heterotrimer bearing one Lys/Lys

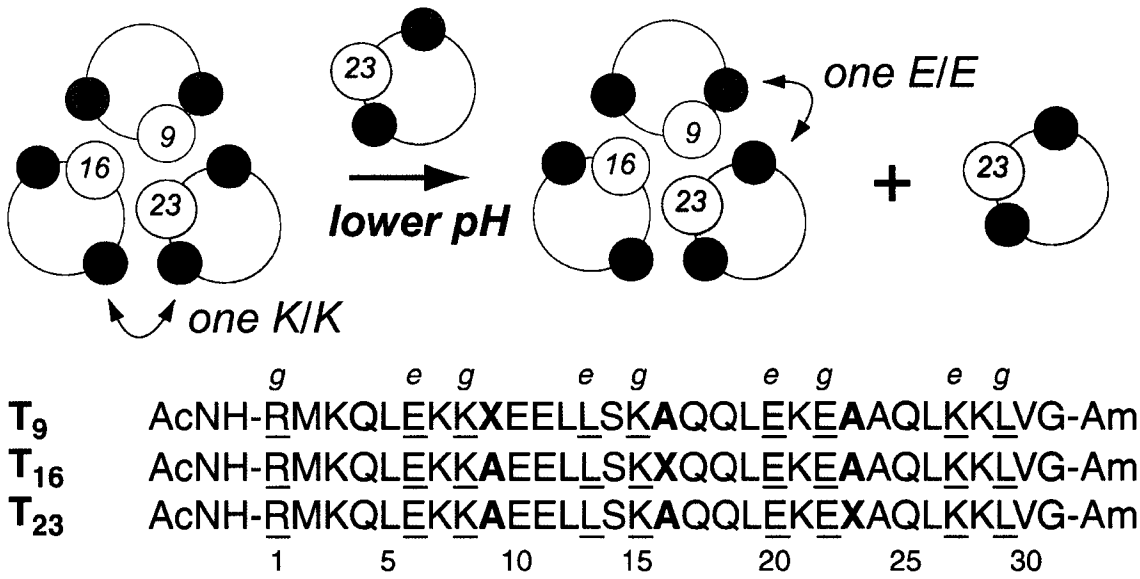

Figure 14. pH-triggered helix exchange. Initial solution favors complex with single Lys/Lys *e/g* interface. pH reduction destabilizes Lys/Lys contact compared to Glu/Glu. Simultaneous addition of suitable replacement peptide affords new specific complex. Numbers indicate position of core cyclohexylalanine (X). Parent sequences also given. Acidic (T_nE), basic (T_nK) and hybrid (T_nE/K) derivatives contain Glu, Lys, or both in all *e/g* positions (underlined). Key core positions in bold.

contact at high pH can be transformed to one featuring a Glu/Glu interface by reduction of pH and addition of a suitable new peptide. Since each complex must simultaneously maintain proper steric matching in the hydrophobic core, only one specific peptide is

replaced. This level of substitution precision is available only through the combined impact of both interfaces. More generally, any complex featuring a pH-sensitive interface is subject to the same specific replacement strategy.

To test these principles we have employed acidic (T_nE), basic (T_nK), and hybrid (T_nE/K) derivatives of our original T_9:T_{16}:T_{23} heterotrimer, whose stability profiles have

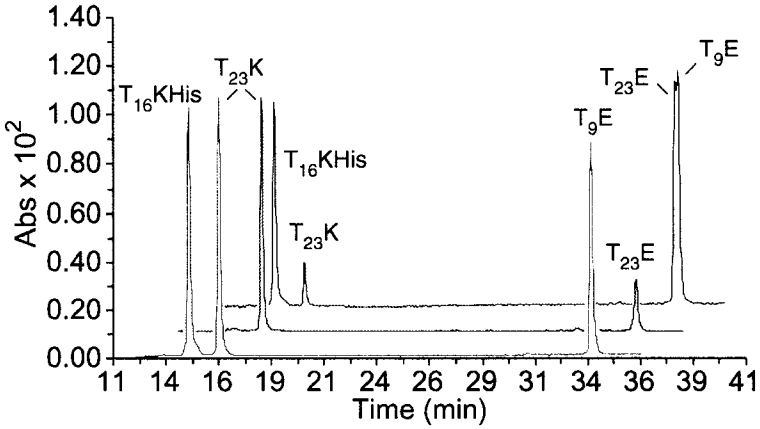

Figure 15. Affinity tag analysis of exchange experiment. Traces reflect composition of: initial 20 μM solution of T_9E:$T_{16}K_{His}$:$T_{23}K$ heterotrimer before mixing with beads (front, pH 7.7), supernatant after treatment with $T_{23}E$ (middle, pH 5.8), and material eluted from resin after $T_{23}E$ addition (back, pH 5.8). All traces normalized to same height.

been recorded at neutral pH. In keeping with the method outlined above, we reasoned that $T_{23}K$ could be displaced from a preformed 1:1:1 T_9E:$T_{16}K$:$T_{23}K$ heterotrimer (one Lys/Lys contact) by addition of $T_{23}E$ at reduced pH (Figure 14). The new complex features one Glu/Glu interface, which can be achieved in principle by replacement of either $T_{16}K$ or $T_{23}K$. The need to simultaneously maintain a sterically matched hydrophobic core engenders the additional specificity for $T_{23}K$.

Verification of the proposed process was conducted as described previously. One trimer component is functionalized with a $(His)_6$-Gly-Gly sequence that binds nickel-

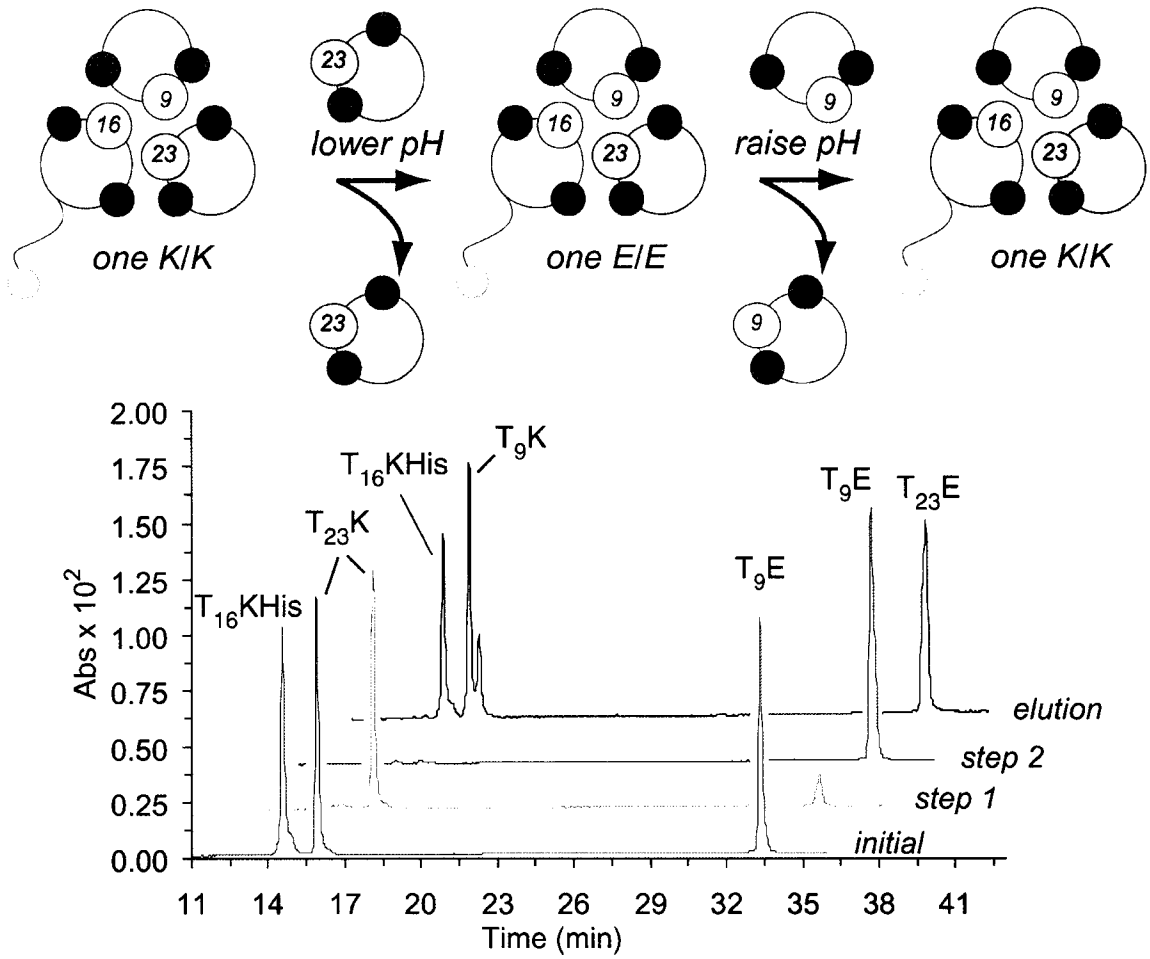

Figure 16. Two step exchange. (above) Experiment schematic. After formation of T_9E:$T_{16}K_{His}$:$T_{23}E$, addition of T_9K at pH 9.3 affords new T_9K:$T_{16}K_{His}$:$T_{23}E$ complex by specific displacement of T_9E. (below) Affinity analysis. Supernatants after steps 1, 2 contain essentially only displaced peptides. Components of final complex observed in elution fraction.

nitrilotriaceticacid (Ni-NTA) groups. When shaken with Ni-NTA agarose beads, tagged peptides and their specific binding partners are retained. Washing of the resin and

subsequent elution with imidazole buffer permits HPLC determination of bound peptides. Analysis of the original supernatant identifies unbound material. When a derivatized $T_{16}K$ ($T_{16}K_{His}$) is employed in the above experiment, observed fraction compositions are consistent with specific component displacement (Figure 15). The supernatant contains principally ejected $T_{23}K$, while eluted material is comprised of peptides from the new complex.[7]

Initial efforts at sophisticated strand exchanges targeted two sequential displacements, in which the product complex from a single exchange is subjected to a second pH adjustment in order to displace a different component of the original complex (Figure 16). After a one-step exchange from T_9E:$T_{16}K_{His}$:$T_{23}K$ to T_9E:$T_{16}K_{His}$:$T_{23}E$, a T_9K solution is added to the product complex instead of elution buffer, and the pH is adjusted to 9.3. This results in displacement of T_9E and restoration of a one Lys/Lys complex. The second supernatant trace reveals that T_9E has been selectively displaced in step 2, and the elution fraction reflects formation of the intended complex (T_9K:$T_{16}K_{His}$:$T_{23}E$). As in the one-step experiment, exclusive displacement of T_9E, rather than $T_{23}E$, emphasizes the power of dual interfaces. On simple electrostatic grounds, in the absence of the need for hydrophobic core alignment, either peptide would be a logical candidate for displacement. Conversely, the exchange process is essentially shut down under conditions that screen electrostatic interactions (e.g. 2M NaCl).

To further extend the boundaries of sequential replacement, we next focused on a three-step process, in which all of the original heterotrimer peptides are replaced. After performing the two-step process above, two independent third steps were investigated, resulting in the formation of either all-matched or one Glu/Glu complexes (Figure 17).

The all-matched complex prevents subsequent exchange, as it is relatively insensitive to further pH variation. The alternative route, which continues the oscillation between stable Lys/Lys and Glu/Glu contacts, can in principle support additional exchange. The complementary approaches to either stable or dynamic substitution products emphasize the flexibility of these methods. The latter one also results in complete inversion of each original electrostatic interface, providing access to the full continuum of relative charge arrangements.

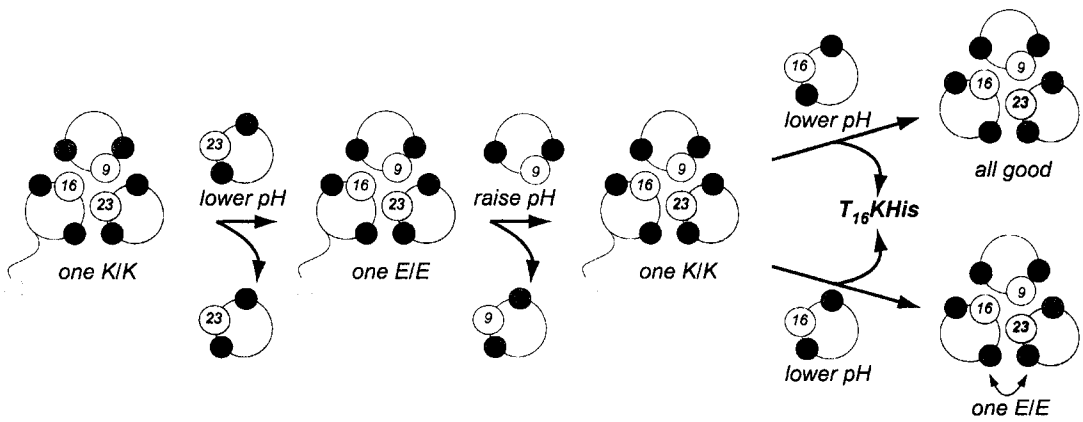

Figure 17. Three-step exchanges. Displacement of last original peptide ($T_{16}K_{His}$) from the product of two-step exchange (T_9K:$T_{16}K_{His}$:$T_{23}E$, Figure 3) can occur in two different ways. Treatment with $T_{16}E/K$ at pH 5.5 affords a fully matched complex, use of $T_{16}E$ (also pH 5.5) produces a heterotrimer with one Glu/Glu interface.

The feasibility of both three-step processes was confirmed by the usual affinity tag methods (Figure 18). After conversion to the T_9K:$T_{16}K_{His}$:$T_{23}E$ trimer as above, the bound material was treated with either $T_{16}E/K$ or $T_{16}E$ at pH 5.5, affording all-matched (T_9K:$T_{16}E/K$:$T_{23}E$) or single Glu/Glu (T_9K:$T_{16}E$:$T_{23}E$) complexes, respectively. Supernatant traces after steps 1 and 2 parallel those in previous experiments. Since the

third exchange step actually displaces the tagged peptide, the newly formed complex is now found in the supernatant of step 3. In both cases, the principal components of these traces are as expected. Elution fractions reveal largely the presence of isolated $T_{16}K_{His}$, along with residual amounts of several peptides.

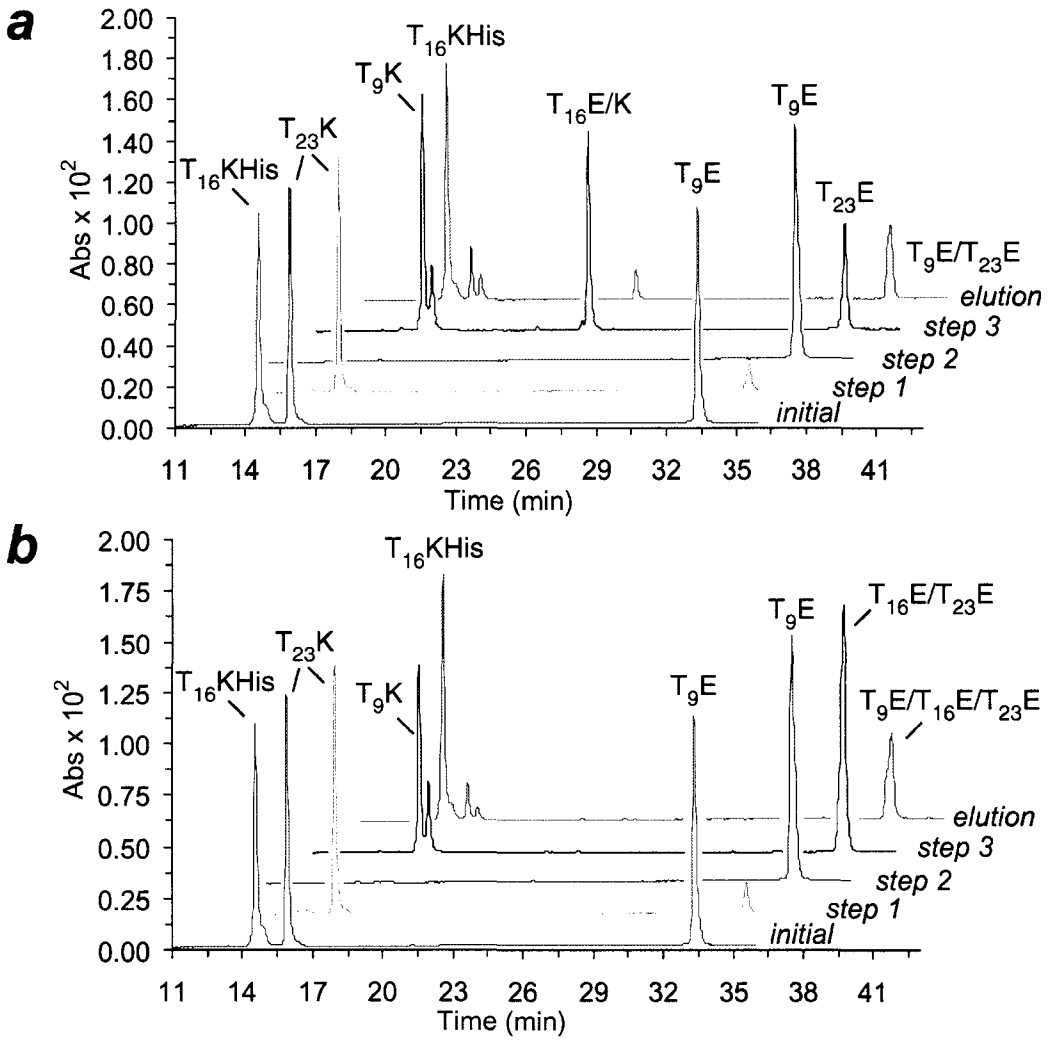

Figure 18. Three-step exchanges. Front three traces as in two-step process (Figure 3). Since tagged peptide is displaced in step three, supernatants contain components of new (a) fully matched (T_9K:$T_{16}E/K$:$T_{23}E$) or (b) single Glu/Glu (T_9K:$T_{16}E$:$T_{23}E$) complexes.

The results above demonstrate that strand exchange in isolated dual-interface heterotrimeric coiled-coils can be readily controlled. General utility of these strategies also demands that they operate in the context of heterogeneous assembly populations. Before addressing this issue directly, we sought to determine whether strand exchange in the absence of stimuli would occur amongst distinct and stable complexes. Such background changes in heterotrimer composition would of course be detrimental in systems where triggered exchange was desired.

To test for strand exchange we preformed the T_9E:$T_{16}K_{His}$:$T_{23}K$ heterotrimer (one Lys/Lys *e/g* interface), and treated it with the complex formed from T_9K:$T_{16}E/K$:$T_{23}E$ (all-matched interfaces) at pH 9. Interchange of the T_{16} derivatives between these complexes generates two new heterotrimers, but maintains the overall number of matched/mismatched interfaces (Figure 19). The experiment was performed in three slightly different ways, to avoid artifacts from the analysis method. In addition to simply adding the second complex, a version was performed in which the all-matched system contains a single His tag sequence ($T_{23}E_{His}$ instead of $T_{23}E$). If binding to the agarose beads is for some reason critical to exchange, it should be observed in this experiment. Finally, the His tag-bearing complex was pre-incubated with an independent set of Ni-NTA beads, followed by mixing of both bead populations.

The results from all of these experiments demonstrate that independent, preformed, stable complexes do not exchange in the absence of pH triggering, over the time course of these experiments (Figure 19).[8] The supernatant from the first experiment contains only the peptides from the second complex (which are expected as that complex has no affinity tag). The other components of the crossover product (i.e. T_9E, $T_{23}K$) are

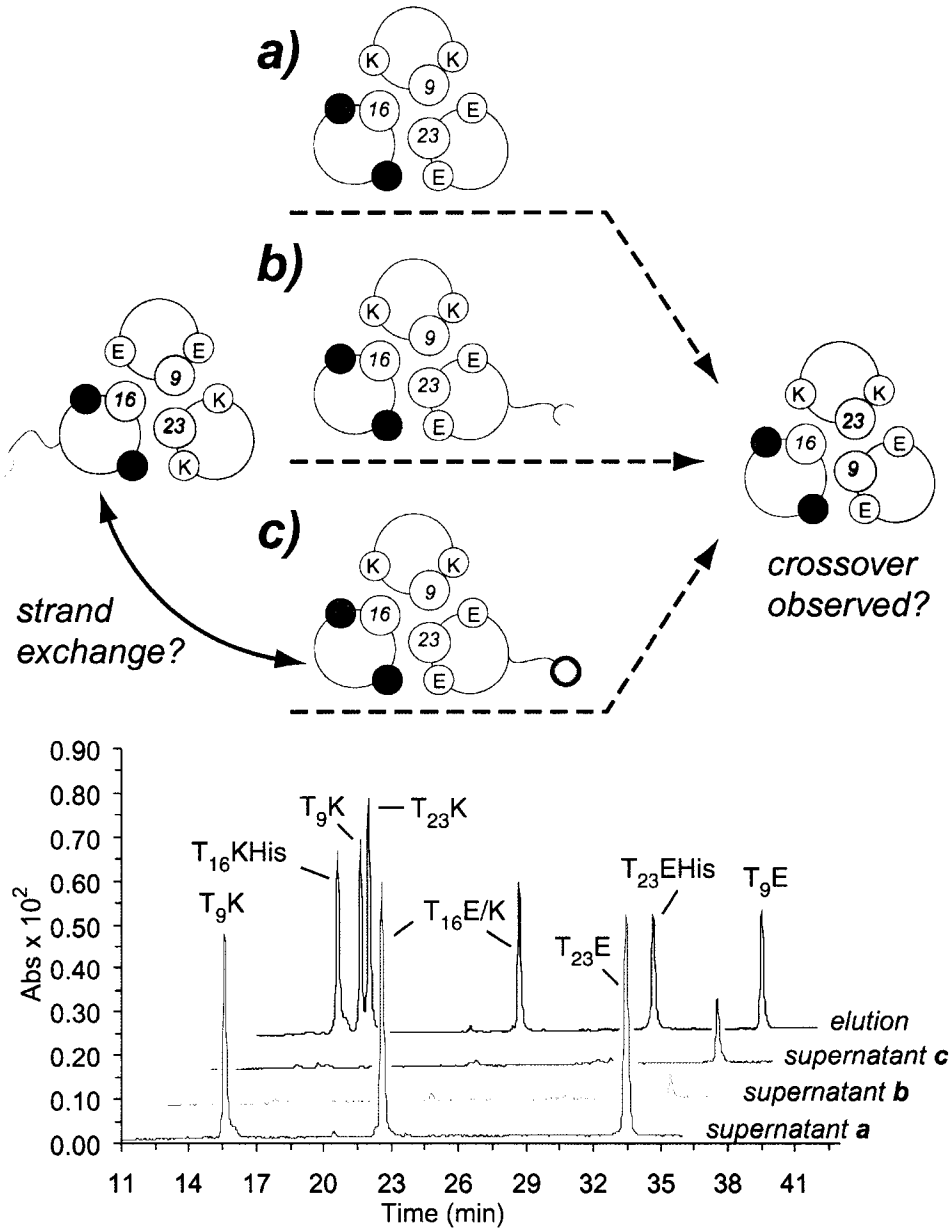

Figure 19. Crossover tests. (above) Experiment schematic. Preformed T_9E:T_{16}KHis:$T_{23}K$ heterotrimer (one Lys/Lys *e/g* interface) is treated with all-matched complexes that either: (a) bear no affinity tag, (b) have a His tag sequence, or (c) have a tag sequence and are prebound to an independent set of agarose beads. In each case, strand exchange of T_{16}KHis for $T_{16}E/K$ creates two new trimers, one of which (T_9E:$T_{16}E/K$:$T_{23}K$) contains no affinity tag. Thus appearance of T_9E and $T_{23}K$ in supernatant fractions indicates crossover. (below) Affinity analysis. In each case, supernatant traces are essentially free of T_9E and $T_{23}K$. Since the added complex in (a) has no affinity tag, its components appear in the supernatant trace. The given elution fraction is representative for traces (b), (c).

not present. In each of the other cases, where both complexes have an affinity tag, the supernatant contains little or no material. Since the crossover product does not have an affinity tag, it should be observed in the supernatant if it forms. Together these experiments suggest that once formed, independent heterotrimers can coexist without

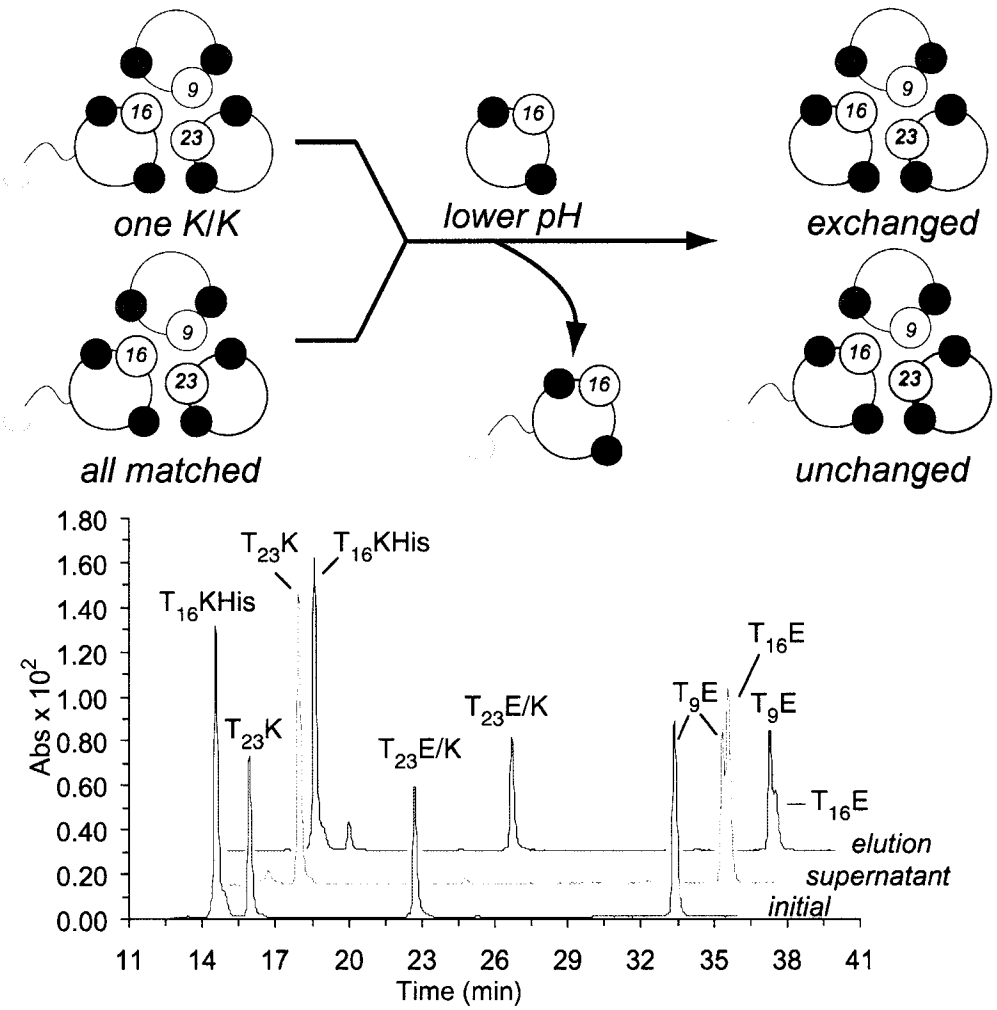

Figure 20. Strand exchange in heterogeneous systems. (above) Experiment schematic. Triggered exchange of $T_{16}E$ for $T_{16}KHis$ in only the one Lys/Lys complex results in formation of a new, soluble heterotrimer (T_9E:$T_{16}E$:$T_{23}K$). (below) Affinity analysis. Supernatant fraction contains $T_{23}K$, and essentially no $T_{23}E/K$. Thus selective displacement of $T_{16}K_{His}$ has occurred only from the desired complex. All traces are normalized to the same height.

background mixing of their components.

Having demonstrated the baseline fidelity of heterogeneous systems, we began to address selective strand replacement in these contexts (Figure 20). Given an equimolar mixture of all-matched and one Lys/Lys heterotrimers, components of the Lys/Lys complex should be selectively exchangeable, as the fully matched system is relatively unaffected by pH modulation

Affinity analysis of this more sophisticated exchange supports the intended result. A mixture of T_9E:$T_{16}K_{His}$:$T_{23}E/K$ (all matched) and T_9E:$T_{16}K_{His}$:$T_{23}K$ (one Lys/Lys) was treated with $T_{16}E$ at pH 5.5. Since replacement of $T_{16}K_{His}$ by $T_{16}E$ removes the His tagged component from either trimer, any new complexes should appear in the supernatant. In particular, the T_{23} derivatives are unique to each initial complex, so appearance of $T_{23}K$ or $T_{23}E/K$ would indicate intended (one Lys/Lys) or unintended (all-matched) exchange, respectively. The observed supernatant HPLC trace contains each component (T_9E:$T_{16}E$:$T_{23}K$) of the intended complex, and virtually no $T_{23}E/K$ (Figure 20). This result demonstrates essentially total selectivity for strand exchange in one of the two complexes. The ability to replace or ignore the *same peptide* in two different heterotrimers bodes well for more complicated future applications.

3-5: A New Method for Peptide Crosslinking

This demonstrated capability for selective replacement of a given helix can be further exploited to create more complicated crosslinked assemblies. A suitably complementary bifunctional sequence, comprised of two helical segments linked by

disulfide or other means, can in principle displace a peptide from each of two distinct heterotrimers, affording a chemically crosslinked pair of complexes (Figure 21).

These principles have now been verified. A derivative of $T_{16}E$, functionalized with an N-terminal Gly-Gly-Cys sequence, was employed as the bifunctional component. The corresponding disulfide ($T_{16}E$-SS-$T_{16}E$) was expected to displace $T_{16}K$ from a pre-formed T_9E:$T_{16}K$:$T_{23}K$ heterotrimer at low pH (Figure 21). The reverse process was also investigated.

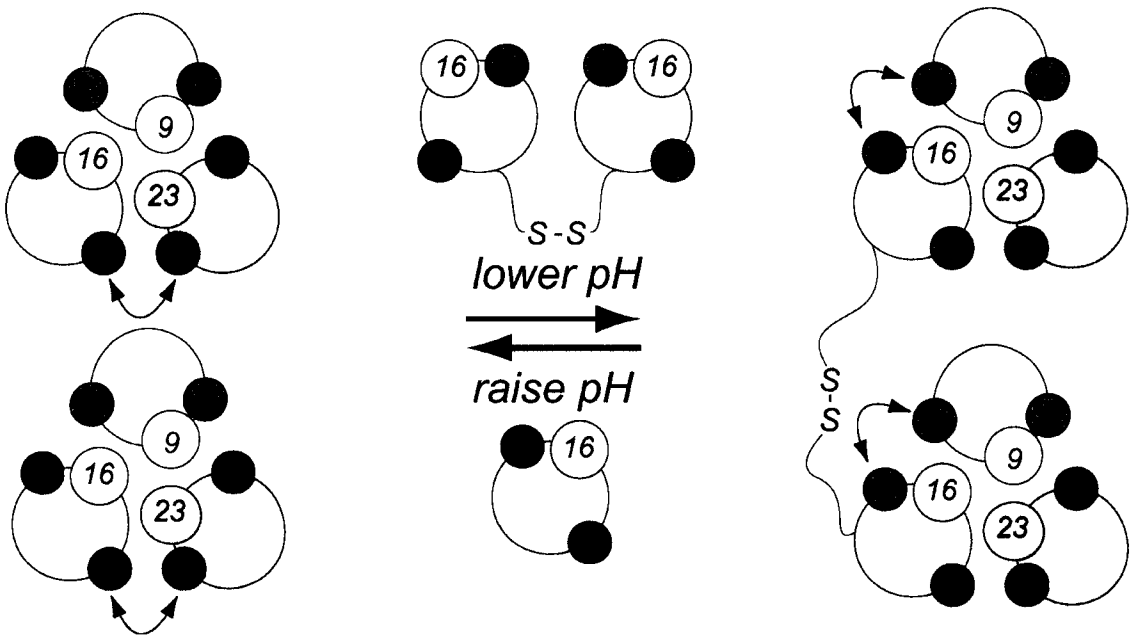

Figure 21. Peptide crosslinks. Reduction of pH destabilizes initial complex containing one Lys/Lys contact (doubleheaded arrows), and addition of bifunctional disulfide linked peptide $T_{16}E$-SS-$T_{16}E$ produces a crosslinked pair of heterotrimers bearing the now favored Glu/Glu contact. The crosslink can be dissolved by selective displacement of the bifunctional peptide at high pH in the presence of $T_{16}K$.

Before assaying the prospects for dynamic crosslinking, we sought to verify that linked complexes retain appropriate stability and aggregation profiles. Although the isolated $T_9E:T_{16}E:T_{23}K$ system was expected to be precisely analogous to previously

Table 2. Characterization of Crosslink System[a]

Sample	T_m (°C)	MW_{obs}	MW_{calc}
$T_9E:T_{16}E:T_{23}K$	89	11 881	11 559
$T_9E:T_{16}E$-SS- $T_{16}E:T_{23}K$	75	22 835	23 568

[a]All samples 10 μM in PBS, pH 5.

studied ones, no such guarantee existed for the pentameric complex formed by crosslinking the two trimers. Gratifyingly, comparison of CD (wavelength and thermal

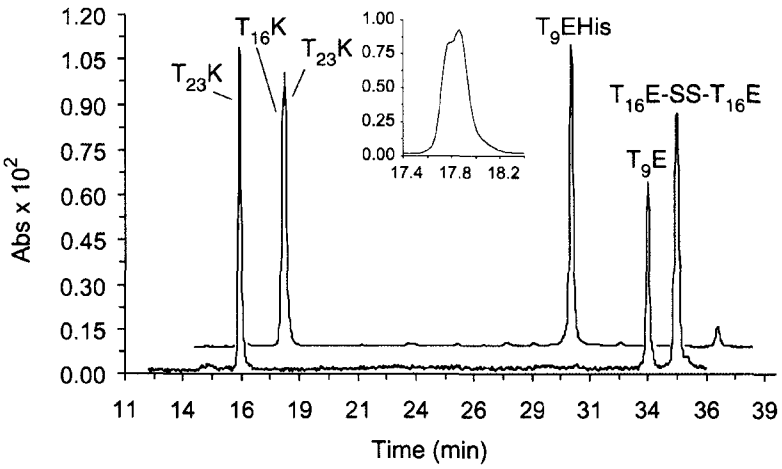

Figure 22. Affinity tag analysis of peptide crosslinking. Front trace reflects supernatant composition after treatment of 20 μM $T_9E:T_{16}K_{His}:T_{23}K$ heterotrimer with $T_{16}E$-SS-$T_{16}E$ (pH 5.4). Back trace obtained by elution of bound material after treatment of $T_9E_{His}:T_{16}E$-SS-$T_{16}E:T_{23}K$ complex with $T_{16}K$ at pH 9.1. Inset reveals presence of two peaks in 17.4-18.2 minute region (offset time scale). Traces are normalized to the same height.[7]

denaturation) and analytical ultracentrifugation data for trimer and pentamer strongly support the proposed model (Table 2). In particular, despite an apparent reduction in thermal stability, the crosslinked system exhibits the expected mass increase by centrifugation.

Having characterized viable structures, we investigated their dynamic switching. Treatment of a T_9E:$T_{16}K_{His}$:$T_{23}K$ heterotrimer with disulfide linked $T_{16}E$-SS-$T_{16}E$, followed by analysis of unbound material, reveals the expected composition (Figure 22). Conversely, beginning with the linked system (differing only in that T_9E_{His} was used in place of $T_{16}K_{His}$), addition of $T_{16}K$ at high pH results in dissolution of the crosslink. Only monofunctional components are significantly retained in the elution fraction.

To ensure the continued viability of these strategies in more intricate environments, the same initial mixture of heterotrimers outlined above (section 3-4) was treated with a disulfide-linked dimer of $T_{16}E$ ($T_{16}E_{SS}$). In principle, this peptide should also displace $T_{16}K_{His}$ from only the one-Lys/Lys complex, resulting in formation of a soluble pentameric species consisting of two crosslinked T_9E:$T_{16}E$:$T_{23}K$ heterotrimers (Figure 23).

Successful formation of the desired crosslinked system was confirmed by the Ni-NTA methods described above (Figure 23). The expected outcome in terms of supernatant versus elution composition is identical to that in the simpler experiment (Figure 20), except that $T_{16}E_{SS}$ should of course appear in place of $T_{16}E$. This is precisely what is observed. Again, the supernatant trace contains no $T_{23}E/K$, supporting the exchange selectivity

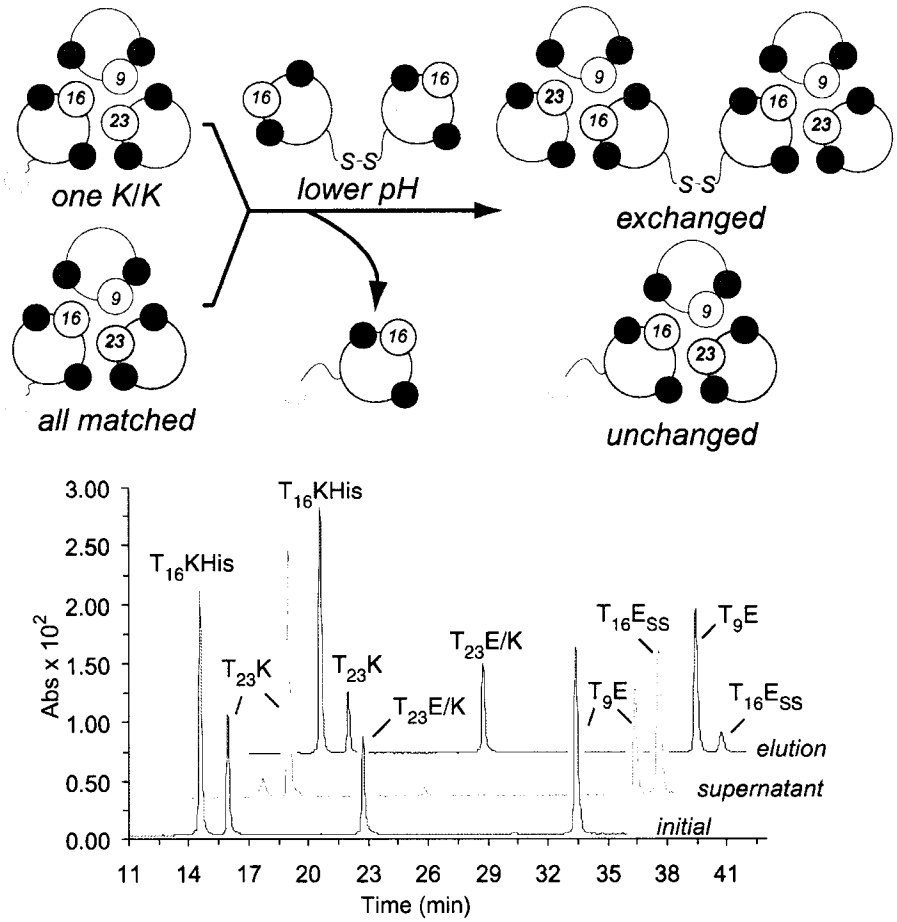

Figure 23. Selective crosslinking. (above) Experiment schematic. Displacement of $T_{16}K_{His}$ by bifunctional peptide $T_{16}E_{SS}$ should occur only in the T_9E:$T_{16}K_{His}$:$T_{23}K$ (single Lys/Lys) complex. The identical peptide in the T_9E:$T_{16}K_{His}$:$T_{23}E/K$ (fully matched) complex is left untouched. (below) Affinity analysis. Appearance of $T_{23}K$ and not $T_{23}E/K$ in the supernatant trace indicates successful selective exchange. All traces are normalized to the same height.

3-6: Experimental Section

Circular Dichroism Experiments: as described in Section 2-4.

Analytical Ultracentrifugation Experiments: as described in Section 2-4.

Ni-NTA Affinity Analysis of Exchange Experiments, General Procedure: Ni-NTA agarose slurry (1 mL) is added to a 1.5 mL Eppendorf tube and centrifuged for one

minute, followed by supernatant removal (discarded). Initial peptide solution (1 mL, 20 μM total peptide concentration) is added to the beads, followed by in situ pH adjustment with 1 M NaOH or HCl (< 1 μL). The Eppendorf tube is repeatedly inverted for five minutes, and centrifuged for one minute, followed by supernatant removal (initial fraction). The beads are then washed with 1 mL of PBS buffer (10 mM phosphate, 150 mM NaCl) of appropriate pH by repeated inversion for 30 seconds, centrifugation for one minute, and supernatant removal (wash fraction). Peptide exchange solution (1 mL, 6.66 μM total peptide concentration, PBS buffer at appropriate pH) is added and final pH is adjusted as above. Exchange is effected by repeated inversion of the Eppendorf tube for five minutes, centrifugation for one minute, and supernatant removal (supernatant fraction). The wash/exchange procedure is repeated as necessary. Following the final wash/ exchange sequence, all remaining bound peptides are eluted by addition of PBS buffer at pH 2.5 (elution fraction). In some cases where the final wash step was run at high pH (8-10), additional acid (< 1 μL 1M HCl) was needed to elute all material left on the beads. Each fraction is analyzed by reverse-phase HPLC: C-18 column, linear gradients of solvent A (1% acetonitrile in water, 0.1% v/v CF_3CO_2H) and solvent B (10% water in acetonitrile, 0.07% v/v CF_3CO_2H).

Two-step exchange. Initial solution equimolar T_9E:$T_{16}K_{His}$:$T_{23}K$ (pH 9.1). First exchange solution $T_{23}E$ (pH 5.5), second exchange solution T_9E (pH 9.3).

Three-step exchange. Initial solution equimolar T_9E:$T_{16}K_{His}$:$T_{23}K$ (pH 9.1). First exchange solution $T_{23}E$ (pH 5.5), second exchange solution T_9E (pH 9.4), third exchange solution either $T_{16}E$ (pH 5.5) or $T_{16}E/K$ (pH 5.5).

Mixed complex exchange. Initial solution 1:1 T_9E:$T_{16}K_{His}$:$T_{23}K$ to T_9E:$T_{16}K_{His}$:$T_{23}E/K$ (2:2:1:1 T_9E:$T_{16}K_{His}$: $T_{23}K$: $T_{23}E/K$, pH 9.0). Exchange solution either $T_{16}E$ (pH 5.5) or $T_{16}E_{SS}$ (pH 5.5).

Crossover experiments 1-2: Initial solution equimolar T_9E:$T_{16}K_{His}$:$T_{23}K$ (10 μM total peptide concentration, pH 9). Exchange solution 1: equimolar T_9K:$T_{16}E/K$:$T_{23}E$ (10 μM total peptide concentration, pH 9). Exchange solution 2: equimolar T_9K:$T_{16}E/K$:$T_{23}E_{His}$ (10 μM total peptide concentration, pH 9)

Crossover experiment 3: 0.5 mL of Ni-NTA agarose slurry was added to two separate 1.5 mL Eppendorf tubes, each were centrifuged for one minute, and the supernatants were discarded. Initial solution 1 (1 mL equimolar T_9E:$T_{16}K_{His}$:$T_{23}K$ 10 μM total peptide concentration, PBS buffer pH 9) was added to one set of beads, initial solution 2 (1 mL equimolar T_9K:$T_{16}E/K$:$T_{23}E_{His}$ 10 μM total peptide concentration, PBS buffer pH 9) was added to the other set of beads. Both solutions were pH adjusted to 9.3, repeatedly inverted for five minutes and centrifuged for one minute, followed by supernatant removal (discarded). PBS buffer (0.5 mL, pH 10) was added to each tube and the two sets of beads were mixed together via syringe (final pH = 9.5). The mixed beads were then repeatedly inverted for five minutes and centrifuged for one minute, followed by supernatant removal (supernatant fraction). Following a wash step (PBS buffer, pH 9), the bound material was eluted with PBS buffer (pH 2).

3-7: Literature Cited

(1) (a) Phelan, P.; Gorfe, A. A.; Jelesarov, I.; Marti, D. N.; Warwicker, J.; Bosshard, H. R. *Biochemistry* **2002**, *41*, 2998-3008. (b) Chana, M.; Tripet, B. P.; Mant, C. T.; Hodges, R. S. *J. Struct. Biol.* **2002**, *137*, 206-219. (c) McClain, D. L.; Binfet, J. P.; Oakley, M. G. *J. Mol. Biol.* **2001**, *313*, 371-383. (d) Vu, C.; Robblee, J.; Werner, K. M.; Fairman, R. *Protein Sci.* **2001**, *10*, 631-637. (e) Marti, D. N.; Jelesarov, I.; Bosshard, H. R. *Biochemistry* **2000**, *39*, 12804-12818. (f) Arndt, K. M.; Pelletier, J. N.; Muller, K. M.; Alber, T.; Michnick, S. W.; Pluckthun, A. *J. Mol. Biol.* **2000**, *295*, 627-639. (g) Duerr, E.; Jelesarov, I.; Bosshard, H. R. *Biochemistry* **1999**, *38*, 870-880. (h) Kohn, W. D.; Kay, C. M.; Hodges, R. S. *J. Mol. Biol.* **1998**, *283*, 993-1012. (i) Lumb, K. J.; Kim, P. S. *Science* **1996**, *271*, 1137-1138. (j) Lavigne, P.; Soennichsen, F. D.; Kay, C. M.; Hodges, R. S. *Science* **1996**, *271*, 1136-1137. (k) Lumb, K. J.; Kim, P. S. *Science* **1995**, *268*, 436-439. (l) O'Shea, E. K.; Lumb, K. J.; Kim, P. S. *Curr. Biol.* **1993**, *3*, 658-667.

(4) Schnarr, N.A., Kennan, A.J. *J. Am. Chem. Soc.* **2003**, *125*, 13046-13051.

(3) (a) Santoro, M. M.; Bolen, D. W. *Biochemistry* **1988**, *27*, 8063-8068. (b) Becktel, W. J.; Schellman, J. A. *Biopolymers* **1987**, *26*, 1859-1877. Monomer-trimer equilibrium modeled as in: (c) Jelesarov, I.; Lu, M. *J. Mol. Biol.* **2001**, *307*, 637-656. (d) Duerr, E.; Jelesarov, I. *Biochemistry* **2000**, *39*, 4472-4482.

(4) Method as in: Brown, B. M.; Sauer, R. T. *Proc. Natl. Acad. Sci. U. S. A.* **1999**, *96*, 1983-1988.

(5) Schnarr, N.A., Kennan, A.J. *J. Am. Chem. Soc.* **2003**, *125*, 6364-6365.

(6) Schnarr, N.A., Kennan, A.J. *J. Am. Chem. Soc.* **2003**, *125*, 13046-13051.

(7) Due to uncertain absolute resin loading, residual excess $T_{23}E$ and T_9K are observed in the first and second supernatant traces, respectively.

(8) Significantly longer equilibration times do lead to considerable exchange (up to ~ 33% after 24 hours).

Chapter 4

Orientation Specificity Through Steric Matching

We have demonstrated the power of size complementarity to direct oligomerization in a variety of complex assemblies. The question remained whether steric matching could reliably effect strand orientation specificity. Previous work with 2:1 alanine/cyclohexylalanine core layers led exclusively to parallel complexes where all core modifications occupied *a* positions. As the antiparallel arrangement requires mixed

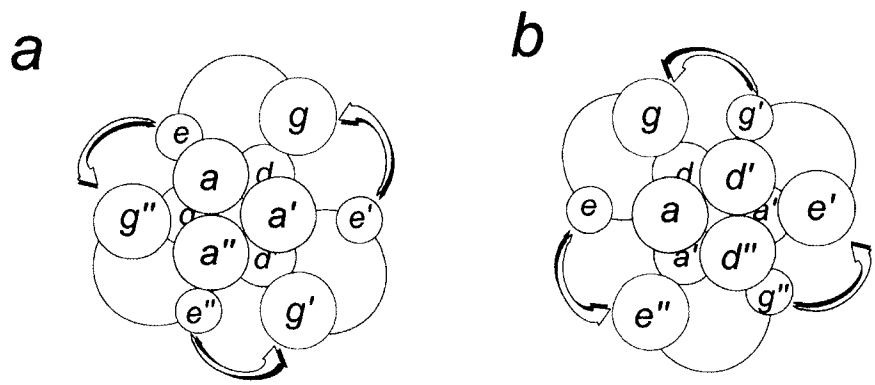

Figure 1. Packing comparisons. (a) Interstrand interactions for a parallel trimeric coiled coil. (b) Interstrand interactions for an antiparallel trimeric coiled coil. Arrows indicate potential electrostatic interactions at the hydrophilic interface.

(*a* interacting with *d*) layers, an altered design strategy must be employed to address this (Figure 1). Simple manipulation of existing recognition interfaces should lead to precise control over strand orientation.

4-1: Design of an Antiparallel Heterotrimeric Coiled Coil.[1] The symmetry present in the peptides from our previous work with dual interface recognition boded well for efforts at designing an antiparallel assembly. Comparison of important interactions in the

parallel and antiparallel orientation reveals discrepancies at *a*, *d*, *e*, and, *g* heptad positions. As our system contains either glutamic acid or lysine at all hydrophilic interface residues, we could simply synthesize the antiparallel strand in the reverse order to place the required alanine and cyclohexylalanine residues at *d* positions to interact with

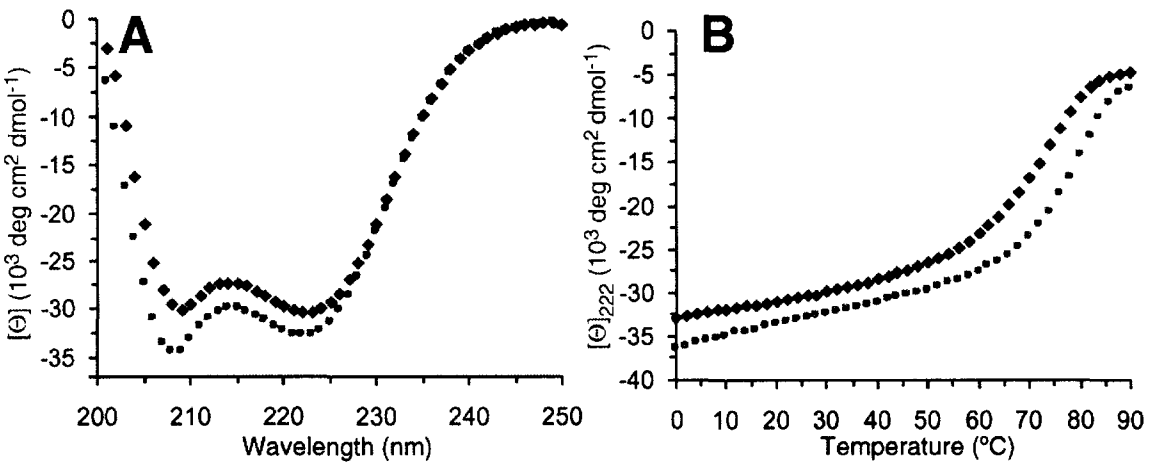

Figure 2. Wavelength scan (**A**) and thermal denaturation (**B**) CD data for solutions of: **T_9K**: **$T_{16}E_{anti}$**,:**$T_{23}E/K$** (antiparallel, Blue), and **T_9K**: **$T_{16}E$**:**$T_{23}E/K$** (parallel, Red). All samples are 10 μM total peptide in PBS buffer (10 mM phosphate pH 7.4, 150 mM NaCl).

opposing strand *a* positions. A new peptide, $T_{16}E_{anti}$, was prepared by reversing the sequence of $T_{16}E$ from our previous work.

Initial efforts focused on development of an antiparallel coiled coil bearing fully matched hydrophilic interface residues. The antiparallel T_9K:$T_{16}E_{anti}$:$T_{23}E/K$ and parallel T_9K:$T_{16}E$:$T_{23}E/K$ complexes were prepared for direct comparison. Both species exhibited strong helical signatures and cooperative thermal denaturation profiles by CD (Figure 2). A slight improvement in melting temperature was observed for the parallel over the antiparallel orientation (Tm_{para} = 81°C , Tm_{anti} = 77 °C). Chemical denaturation

experiments again revealed cooperative denaturation profiles consistent with the relative order of thermal stability (Figure 3).

To assess the complex stoichiometry of the designed antiparallel trimer, an

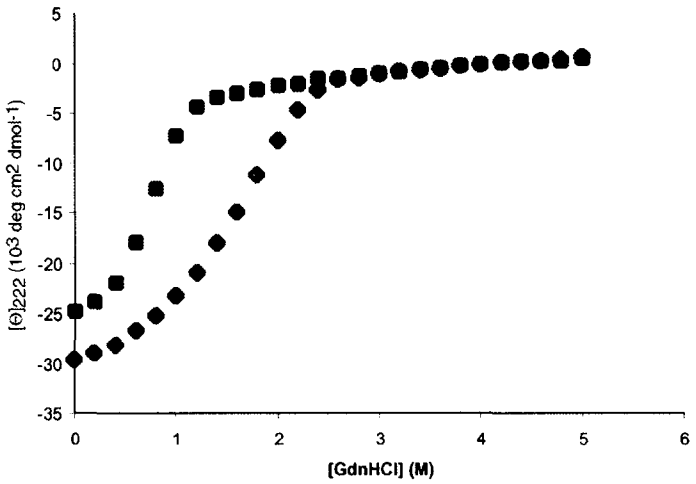

Figure 3. Guanidine hydrochloride denaturation profiles of **T_9K: $T_{16}E_{anti,}$:$T_{23}E/K$** (antiparallel, Blue), and **T_9K: $T_{16}E$,:$T_{23}E/K$** (parallel, Red). All samples are 10 μM total peptide

equimolar mixture of T_9K, $T_{16}E_{anti}$, and $(His)_6$-Gly-Gly functionalized $T_{23}E/K_{His}$ was subjected to Ni-NTA resin as before. The bound material was eluted and its contents analyzed by RP-HPLC. The presence of a roughly 1:1:1 ratio of the three component peptides indicated that the intended antiparallel complex was the dominant species in solution.

Orientation preference has been previously evaluated in dimeric systems using thiol-containing peptides for complexation-induced disulfide formation.[2] We sought to employ a similar strategy to assess the relative orientation of any two strands in the

designed trimer. Two new peptides based on $T_{16}E_{anti}$ were prepared containing a Cys-Gly-Gly sequence at either the N ($T_{16}E_{anti}$Ncys) or C ($T_{16}E_{anti}$Ccys) terminus. In addition, a single T_9K analog bearing an N-terminal thiol (T_9KNcys) was constructed. Parallel and antiparallel heterodimers, $T_{16}E_{anti}$Ncys-SS-T_9KNcys and $T_{16}E_{anti}$Ccys-SS-T_9KNcys, were isolated by RP-HPLC upon air oxidation of T_9KNcys with $T_{16}E_{anti}$Ncys and $T_{16}E_{anti}$Ccys, respectively.

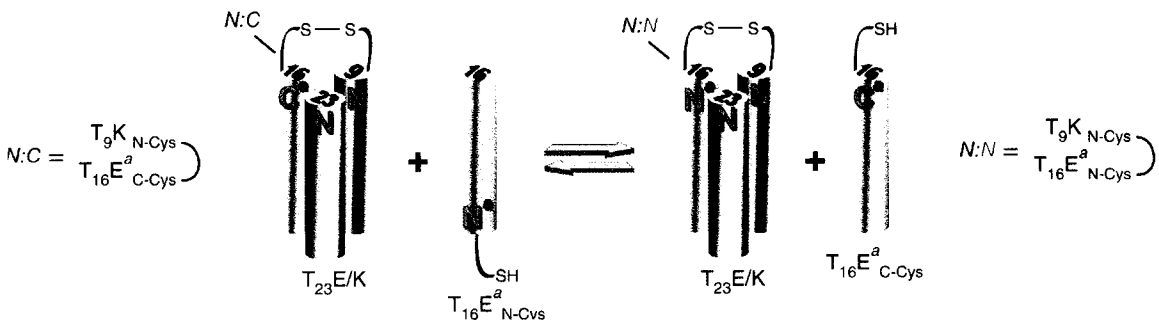

Figure 4. Schematic diagram of antiparallel disulfide exchange. Beginning with either preformed N:C or N:N dimer, addition of a complementary thiol-containing peptide under equilibrium conditions allows for free exchange to the preferred orientation. Grey C and N indicate peptide termini. Superscript *a* denotes a designed antiparallel strand

To assess strand arrangement in our designed trimer, an equimolar mixture of $T_{23}E/K$ and $T_{16}E_{anti}$Ncys-SS-T_9KNcys was treated with one equivalent of $T_{16}E_{anti}$Ccys under anaerobic conditions to allow for equilibration to the preferred orientation (Figure 4). A strong antiparallel preference was observed as nearly all material converted to the $T_{16}E_{anti}$Ccys-SS-T_9KNcys heterodimer after 7 hours (Figure 5). Further support was acquired in a complementary experiment where a mixture of $T_{23}E/K$ and $T_{16}E_{anti}$Ccys-SS-T_9KNcys was subjected to $T_{16}E_{anti}$Ncys. Little change in heterodimer composition was

observed after 24 hours indicating an equilibrium state strongly favoring the antiparallel assembly (Figure 5).

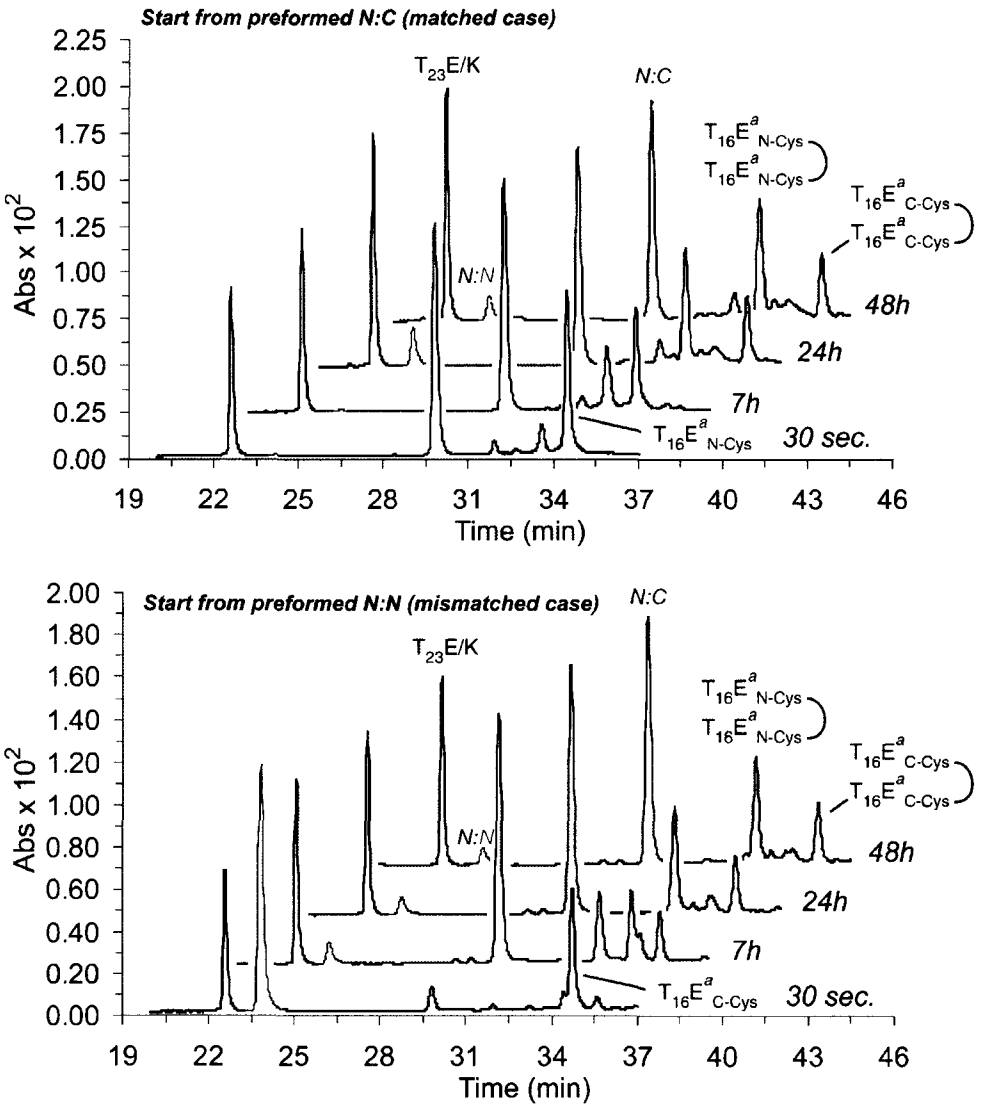

Figure 5. HPLC analysis of antiparallel disulfide exchange experiment (see Figure 4). (Top) Starting with N:C dimer, addition of $T_{16}E_{anti}$Ncys results in little change in dimer population. (Bottom) Starting with N:N dimer, addition of $T_{16}E_{anti}$Ccys results in rearrangement to N:C dimer indicating strong preference for the antiparallel orientation. Superscript *a* denotes antiparallel strand.

Control experiments employing the parallel system were executed in a similar fashion. The N and C-terminal thiol-containing peptides, T_{16}ENcys and T_{16}ECcys, were prepared and combined with T_9KNcys to form heterodimers analogous to those above. An equimolar mixture of T_{23}E/K and T_{16}ECcys-SS-T_9KNcys was treated with one equivalent of T_{16}ENcys under anaerobic conditions as before (Figure 6). A strong parallel preference was observed in this case as nearly all material converted to the

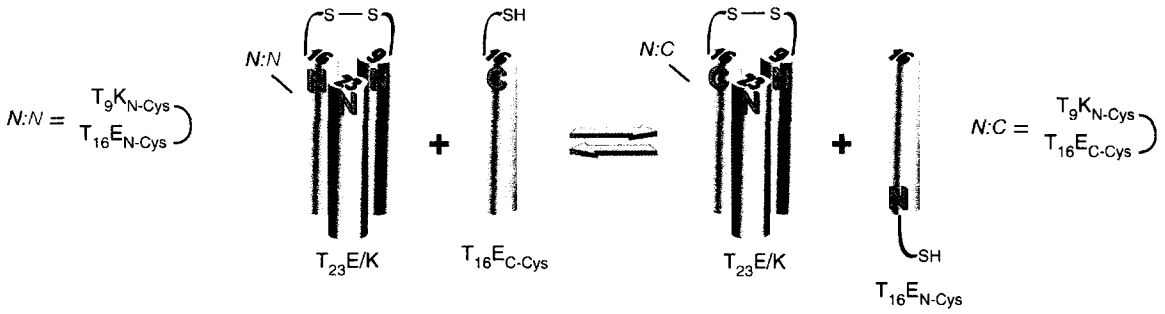

Figure 6. Schematic diagram of parallel disulfide exchange. Beginning with either preformed N:C or N:N dimer, addition of a complementary thiol-containing peptide under equilibrium conditions allows for free exchange to the preferred orientation. Grey C and N indicate peptide termini.

T_{16}ENcys-SS-T_9KNcys heterodimer after 7 hours (Figure 7). Again, further support was acquired in a complementary experiment where a mixture of T_{23}E/K and T_{16}ENcys-SS-T_9KNcys was subjected to T_{16}ECcys. Little change in heterodimer composition was observed after 24 hours indicating an equilibrium state strongly favoring the parallel assembly (Figure 7).

To directly assess any intrinsic preference for one orientation over the other, a competition experiment was devised using the affinity-tagging protocol from previous work. A 1:1:1:1 mixture of T_9K, T_{16}E, $T_{16}E_{anti}$, and $T_{23}E/K_{His}$ peptides was prepared in

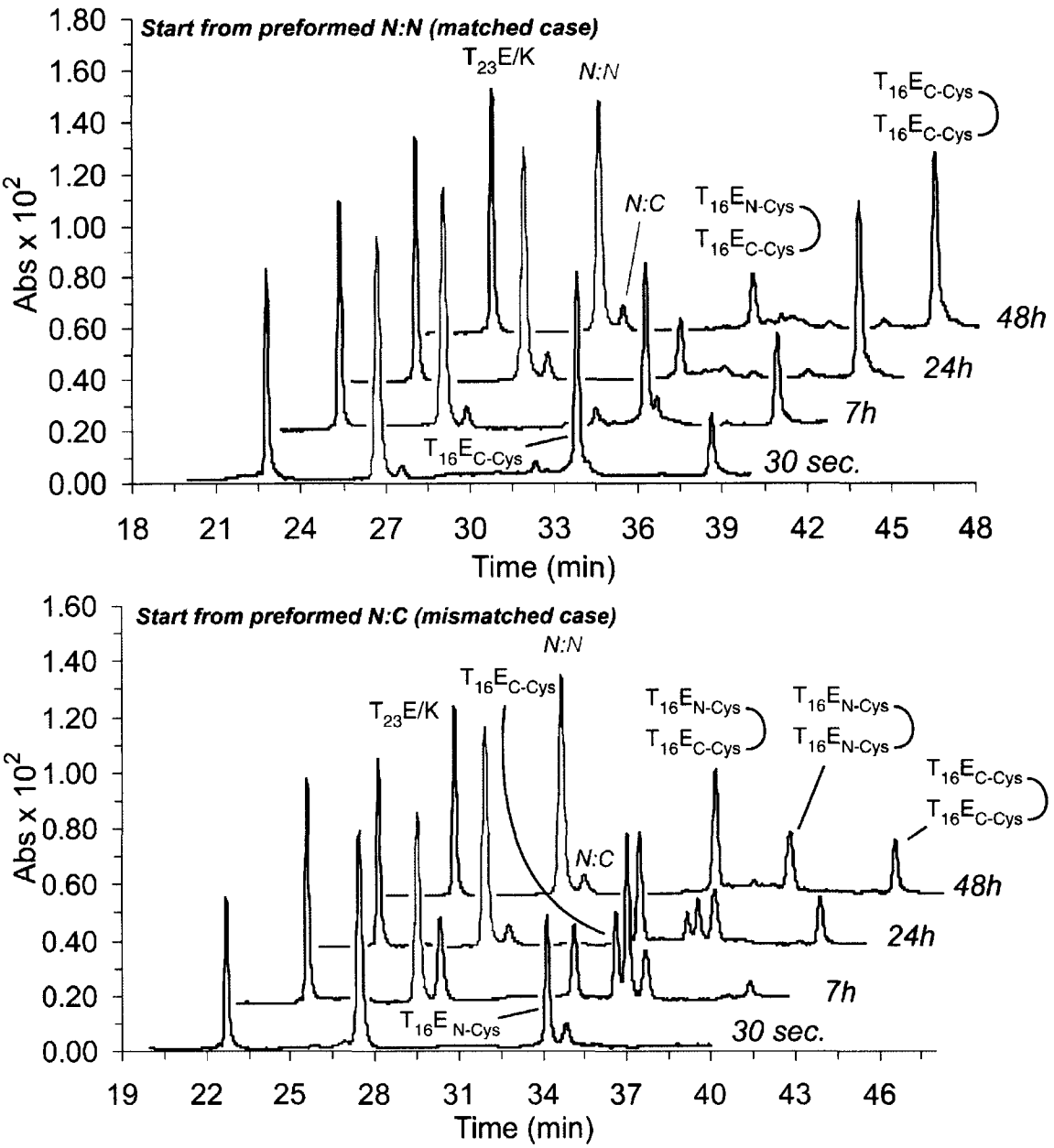

Figure 7. HPLC analysis of parallel disulfide exchange experiment (see figure 6). (Top) Starting with N:N dimer, addition of T_{16}ECcys results in little change in dimer population. (Bottom) Starting with N:C dimer, addition of T_{16}ENcys results in rearrangement to N:N dimer indicating strong preference for the parallel orientation.

aqueous buffer at neutral pH. Aliquots were taken at 3, 24, 48, and 72 hours and subjected to Ni-NTA resin. The ratio of the $T_{16}E$ to $T_{16}E_{anti}$ peptides in the bound fractions provided an estimate of the relative population of parallel and antiparallel assemblies in solution (Figure 8). Initially, a kinetic preference for the antiparallel

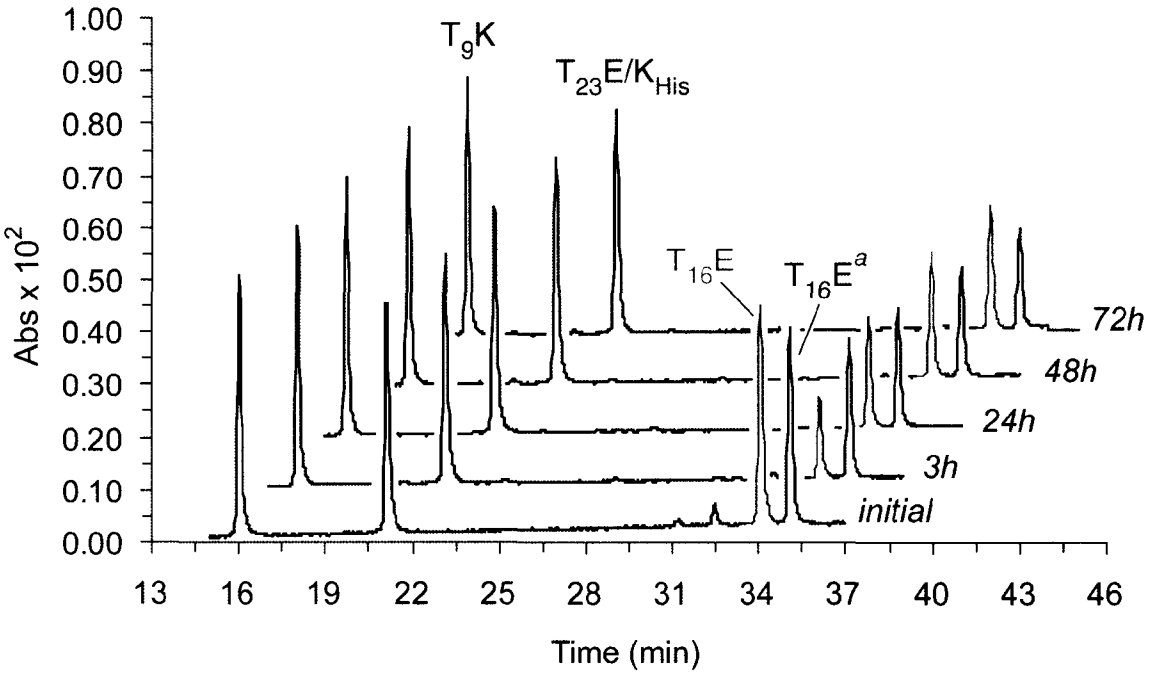

Figure 8. HPLC analysis of strand orientation competition. Bound material from Ni-NTA affinity analysis of parallel/antiparallel competition at time intervals shown. Ratio of $T_{16}E$ to $T_{16}E_{anti}$ peaks provides insight into orientation preference. The initial trace is simply the starting peptide solution and not an elution fraction from Ni-NTA analysis. Superscript *a* denotes antiparallel.

orientation was observed. However, given sufficient time to equilibrate (48 hours), a slight thermodynamic preference for the parallel arrangement developed, consistent with thermal and chemical denaturation experiments above. As the sequences of the parallel and antiparallel strands are simply reversed, kinetic and thermodynamic preferences

should result from intrinsic differences between the two competing orientations. Further analysis is required to elucidate the basis for these observations.

4-2: Experimental Section

Circular Dichroism experiments: as described in Section 2-4.

Ni-NTA affinity tagging experiment (stoichiometry): as described in Section 2-4.

Orientation Preference (general procedure): Heterodimers were formed by mixing undetermined amounts of the appropriate peptides in PBS buffer (10mM sodium phosphate, 150mM NaCl, pH = 9.4) in a 1.5 mL Eppendorf tube. Small holes were punched in the top of the tube to allow free air exchange. After 12 to 15 hours of exposure, the heterodimers were purified by reverse-phase HPLC: C-18 column, linear gradients of solvent A (1% acetonitrile in water, 0.1% v/v CF_3CO_2H) and solvent B (10% water in acetonitrile, 0.07% v/v CF_3CO_2H).

A 2.0 mL solution containing $T_{23}E/K$ and an appropriate heterodimer (10μM total peptide concentration, PBS as above, pH = 9.4) was sparged with argon for fifteen minutes in a 15 mL Falcon tube equipped with a small rubber septum and outlet needle. A specified amount of thiol-containing peptide stock solution was quickly added to the original solution (13.3μM final peptide concentration). A 0.5 ml aliquot was immediately taken for HPLC analysis (conditions as above). The tube was resealed and sparged with argon for 15 minutes. The needle was then brought well above the solvent

level and a slow, steady stream was blown through the tube until the next aliquot was taken. This process was repeated at 7h, 24h, and 48h time points.

Competition Experiment: A 1:1:1:1 mixture of T_9K, $T_{16}E$, $T_{16}E_{anti}$, and $T_{23}E/K_{His}$ peptides was prepared in PBS buffer (13.3μM total peptide conc., 10mM sodium phosphate, 150mM NaCl, pH = 7.1). A 0.5 mL sample of a 50% slurry of Ni-NTA agarose (Qiagen) in an Eppendorf tube was centrifuged for 30 s, followed by removal of the superantant. 1 mL of peptide solution was added, and the tube was repeatedly inverted for 5 min. The sample was centrifuged (30 s), and the supernatant (flow-through fraction) was removed. The procedure was then repeated with 1 mL of buffer (wash fraction) and 1 mL of buffer containing 250 mM imidazole (elution fraction), except that the wash fraction was agitated for only 30 seconds. The elution fraction was analyzed by RP–HPLC: C-18 column, linear gradients of solvent A (1% acetonitrile in water, 0.1% v/v CF_3CO_2H) and solvent B (10% water in acetonitrile, 0.07% v/v CF_3CO_2H). This procedure was repeated for 3h, 12h, and 24h time points.

4-3: Literature Cited

(1) Schnarr, N.A., Kennan, A.J. *Submitted for publication.*

(2) Oakley, M. G.; Kim, P. S. *Biochemistry* **1998**, *37*, 12603-12610.

Chapter 5

Binding Coiled Coil Surfaces

Recently, an important biological role for exposed surface residues has been discovered whereby binding of certain viral proteins to cell surface coiled coil domains is critical for viral infection. Little is known about the specific requirements that promote binding to these surfaces. Given an appropriate coiled coil model system, one can pinpoint the necessary recognition elements which should lead to more effective inhibition of viral entry. We have focused much of our recent efforts toward development of a well-behaved model system from our designed heterotrimers to address many of the issues associated with coiled coil surface binding.

5-1: HIV Entry and Inhibition

The global epidemic of HIV infection has necessitated the pursuit of effective treatments to eliminate viral entry into cells.[1] Several promising targets have surfaced that may provide viable intervention pathways. Recently, much attention has focused on the gp160 envelope glycoprotein responsible for initial interaction with the CD4 receptor.[2] A detailed understanding of this cell fusion mechanism should lead to effective inhibition of an integral and seemingly general infection mechanism.

Host-cell proteolysis of the initial gp160 protein results in direct formation of three gp120 exterior glycoproteins and three gp41 transmembrane glycoproteins. The mature gp120/gp41 complex is expressed on the surface of infected cells leading to an initial recognition event between gp120 and CD4 on the target cell (Figure 1). This induces a conformational change which allows direct binding to the chemokine receptor. The N-terminal portion of gp41 forms a stable trimeric coiled coil with deep hydrophobic

pockets on the surface which permit binding of a small number of C-terminal helix side chains upon conformational rearrangement of the intermediate loop region (trimer-of-hairpins motif). Formation of this six-helix bundle is thought to bring the viral and cell membranes in close proximity, facilitating viral entry.[3] N- and C-terminal peptide mimics have been shown to effectively inhibit this final fusogenic conformation leading to reduced infection.[4]

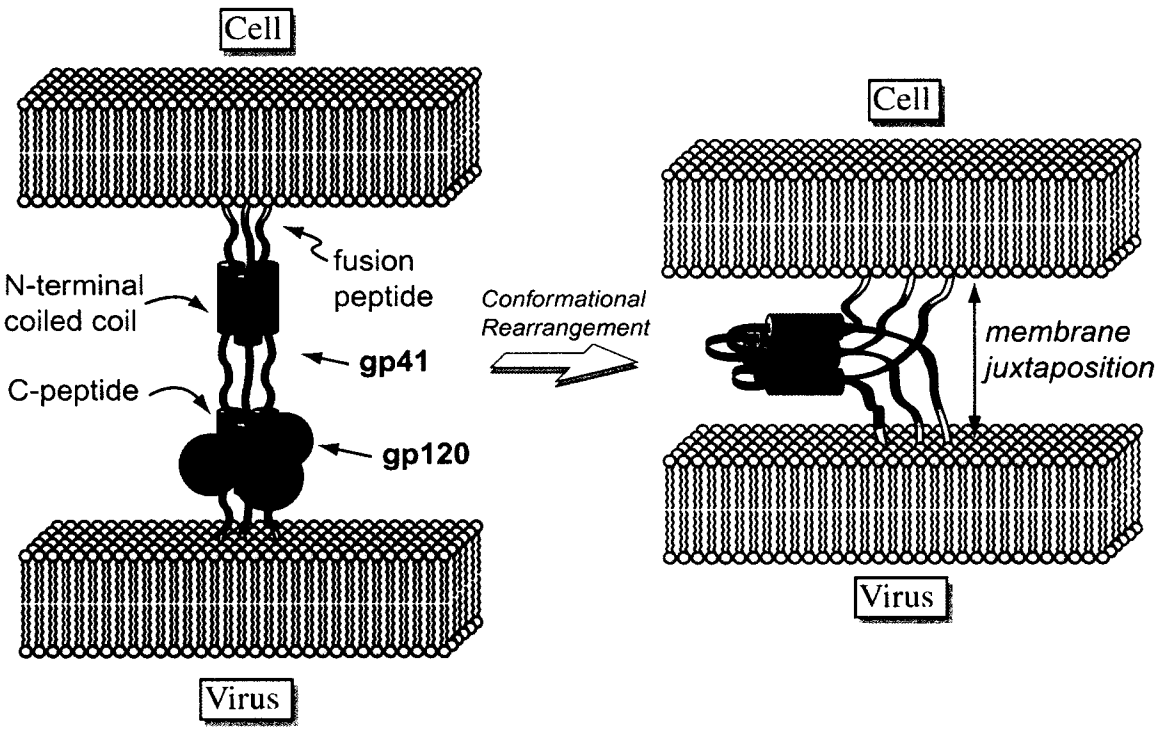

Figure 1. HIV entry mechanism. Schematic diagram of the conformational rearrangement required for cell infection. The essential six-helix bundle is formed by gp41 C-peptides binding to the surface of the N-terminal trimeric coiled coil. This trimer-of-hairpins motif is thought to bring the viral and cell membranes in close proximity.

5-2: Design of a Stable gp41 Trimer Mimic[5]

Unfortunately, in vitro experimentation on the isolated N-terminal coiled coil domain has been complicated by peptide aggregation due to the inherent hydrophobicity

of the gp41 trimer components. Several strategies have been employed to circumvent this, allowing researchers to directly study gp41 coiled coil surface binding. Wiley and coworkers constructed a chimeric N-terminal mimic where fused GCN4 based heptads were able to prevent aggregation of the gp41 coiled coil trimer.[6] More recently, Kim and

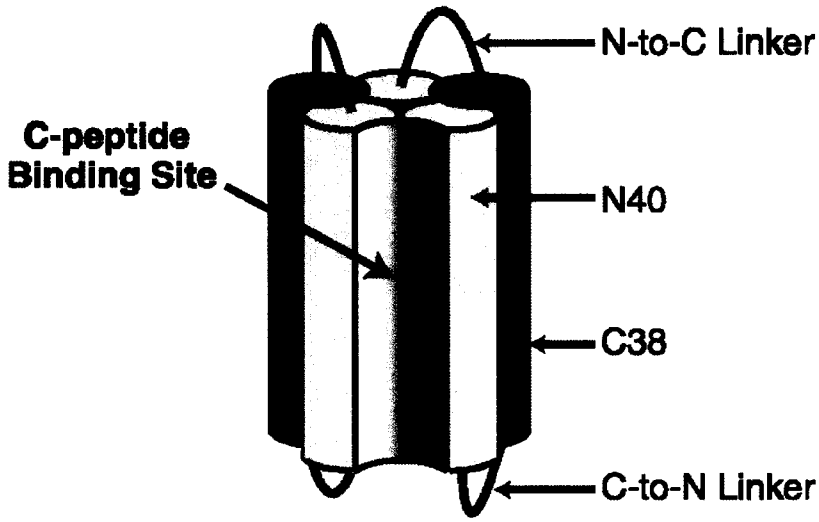

Figure 2. Schematic diagram of Kim's 5-helix bundle. N40 = peptide derived from the N-terminal portion of gp41. C38 = peptide derived from the C-terminal portion of gp41. A single hydrophobic C-peptide binding site is vacant, allowing for experiments to probe binding speicifity without significant peptide aggregation. (Figure from Root *et al.*, 2001)[8]

coworkers have used similar chimeric variants of the N-peptide region of gp41 to study viral entry inhibition.[7] In addition, they have shown that fusing N and C terminal domains of gp41 can result in a 5-helix bundle which leaves a single hydrophobic pocket open to study binding specificity without significant aggregation (Figure 2).[8]

Two groups have recently reported the use of scaffolds as an appropriate means to prevent aggregation in the gp41 coiled coil. Tam and coworkers utilized thiazolidine ligation for coupling of cysteine-containing C- or N-peptides to an aldehyde scaffold with

three arms to generate soluble gp41 mimics.[9] Similarly, Case and coworkers successfully designed an N-terminal coiled coil mimic by attaching bidentate metal-binding ligands to the N-terminus of each trimer component.[10] Addition of a metal ion such as Fe^{II} or Ni^{II} resulted in a highly stable, soluble trimer model (Figure 3). Specific binding of an isolated C-terminal gp41 peptide confirmed the suitability of this design.

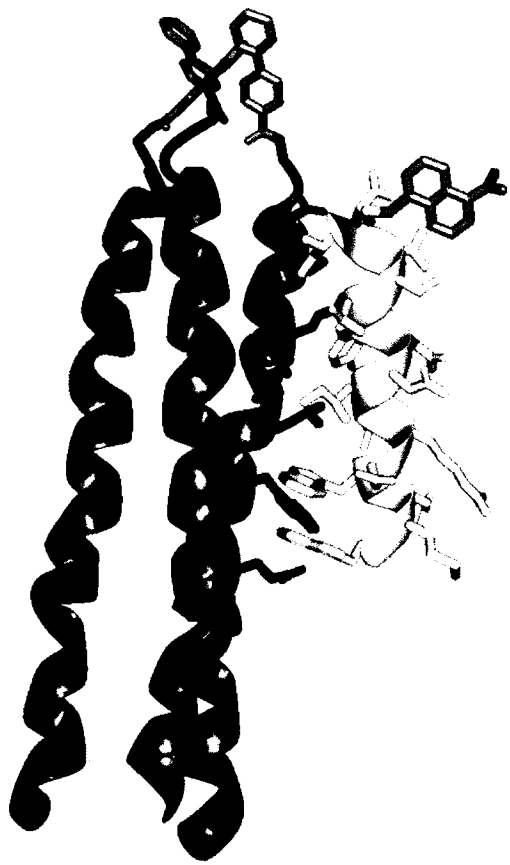

Figure 3. Metallopeptide assembly of gp41. Model of the expected interactions between metal bound N-terminal gp41 coiled coil and dansylated C-peptide ligand. Metal binding of bidentate N-terminal 2,2'-bipyridyl ligands can stabilize the trimeric coiled coil for studying ligand binding to the hydrophobic surface. N-terminal gp41 coiled coil in dark grey. C-peptide in light grey/white. (Figure from Gochin *et al.*, 2003)[10]

Mutation studies have identified several residues on the gp41 coiled coil surface critical to six-helix bundle formation. Appropriate alignment of these residues on the

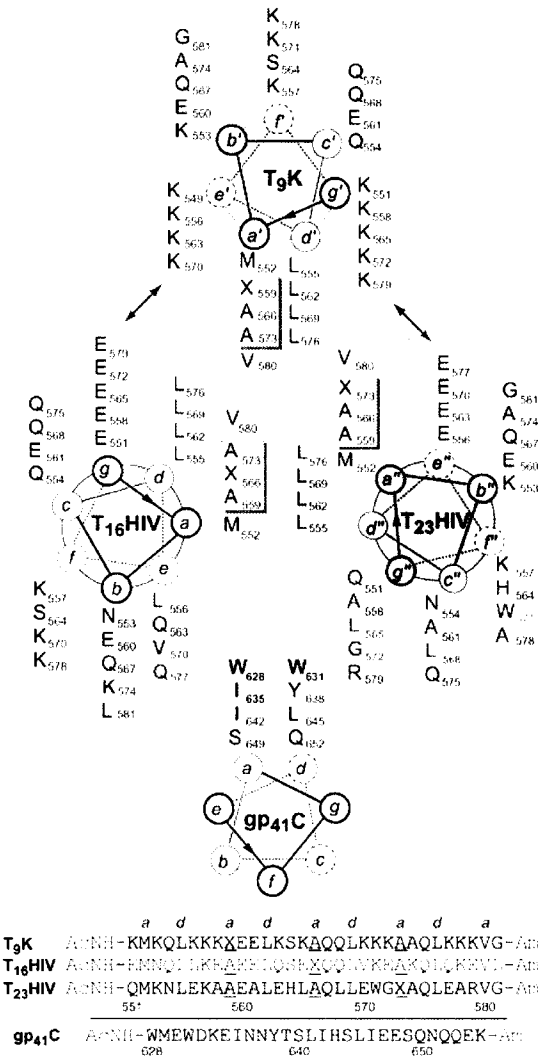

Figure 4. Heterotrimeric gp41 mimic. Complex of T_9K:T_{16}HIV:T_{23}HIV forms specifically due to core matching of 2:1 alanine/cyclohexylalanine layers (boxes). Electrostatic interfaces contain two Glu/Lys pairings (arrows) and one gp41 C-peptide binding surface. Residues from gp41 are shown in green, those that form key binding contacts are in red. An abbreviated representation of the C-terminal ligand is also given, with critical Trp628, Trp631, and Ile635 residues in blue. Sequences are given below, with core modified *a* residues underlined. Numbering as in gp160 from HBX2 strain, GenBank accession number K03455.

surface of our T_9K:$T_{16}E$:$T_{23}E/K$ heterotrimer should result in a single exposed hydrophobic binding pocket, leading to significantly decreased aggregation problems while maintaining the overall three-dimensional fold of the native gp41 coiled coil (Figure 4). A new peptide, T16HIV was derived from T16E but contains *b* and *e* residues from gp41. Similarly, T23HIV was obtained from T23EK by replacing *c*, *g*, and three key *f* residues with those from gp41.

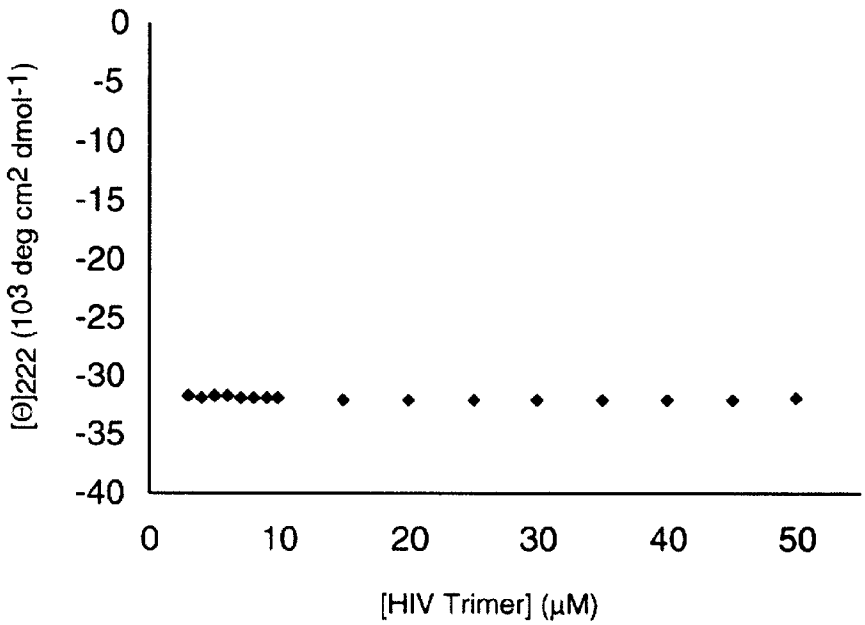

Figure 5. Concentration dependence of helical structure. The CD signal at 222 nm of a mixture of T_9K:T_{16}HIV:T_{23}HIV was monitored over a total peptide concentration range of 50μM to 2μM. No change in signal over this range indicates no significant aggregation of the component peptides.

Initial efforts focused on characterization of our HIV heterotrimer, T_9K:T_{16}HIV:T_{23}HIV. An equimolar mixture of these peptides showed significant helical content and high thermal stability by CD (Tm = 85°C, Figure 6A,B). To assay

component stoichiometry, an affinity tagging experiment was employed as before. Nearly equivalent amounts of T_{16}HIV and T_{23}HIV were retained with T_9K_{His} as a binding partner, indicating specific 1:1:1 heterotrimer formation (Figure 7). However, analytical ultracentrifugation yielded a significantly higher apparent solution molecular weight (16593) for this complex than that calculated for the trimer (11463). Concerned that our complex might be aggregating, we sought to uncover any concentration dependence on helical assembly. The CD signal at 222 nm was monitored as the total trimer concentration was varied from 50 to 2μM. No significant concentration dependence of the CD signal was observed over this range, suggesting little to no peptide aggregation was taking place (Figure 5). Although no conclusions could be drawn from these two conflicting reports, we hoped that any minor aggregation would not hinder further development of this system.

Future binding experiments would require an appropriate control complex that could not effectively bind gp41 C-peptides to assess specificity and suitability of the model HIV heterotrimer. The EK heterotrimer (T_9K:T_{16}HIV:T_{23}E/K), where half of the hydrophobic pocket was replaced with polar glutamate residues was prepared and subjected to similar analyses as above. This complex displayed high helical content and thermal stability comparable to the HIV heterotrimer (Tm = 69 deg, Figure 6C,D). Analytical ultracentrifugation confirmed the presence of a discreet trimeric species. Composition stoichiometry was determined to be 1:1:1 by an affinity tagging experiment as above (Figure 7).

5-3: Proof of Principle: Surface Binding

To assess the ability of our designed HIV heterotrimer to properly bind a suitable

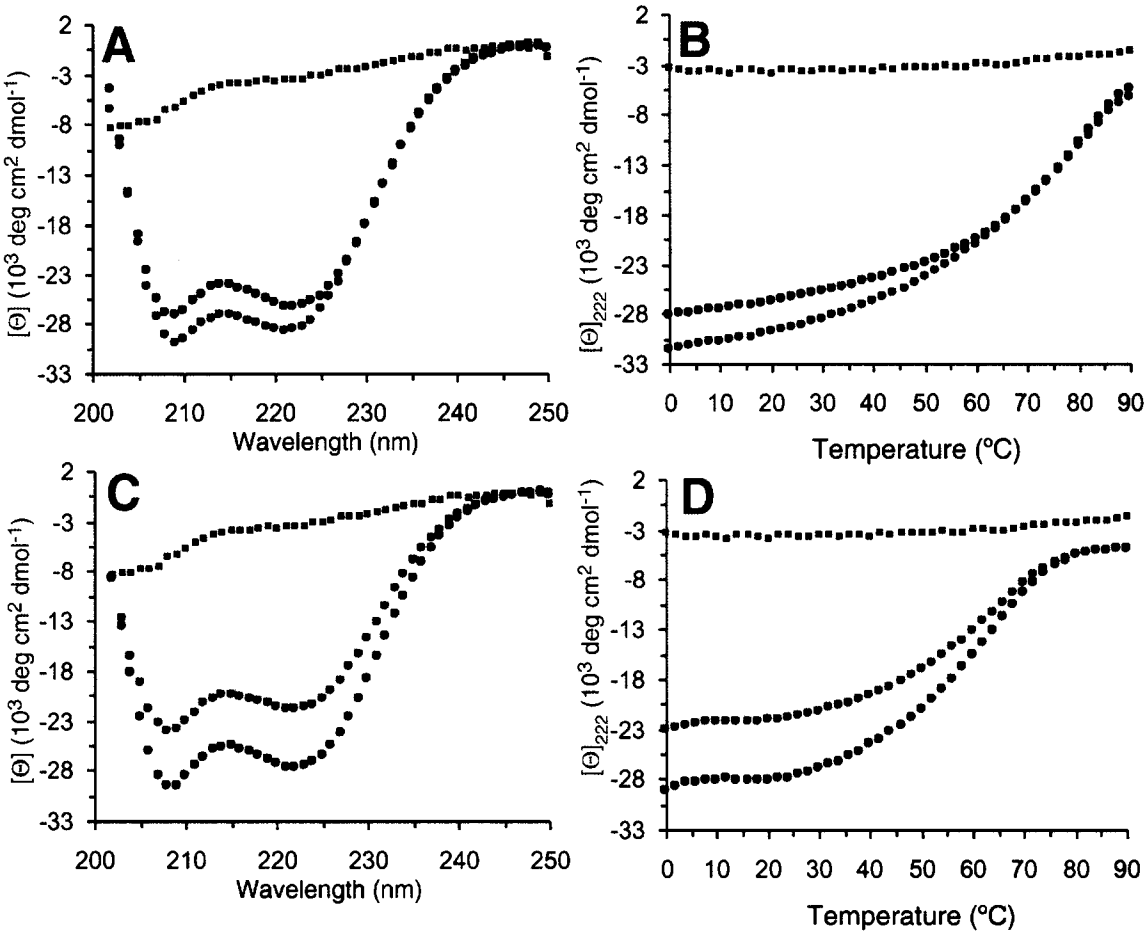

Figure 6. CD analysis of HIV mimic. Wavelength and thermal unfolding data for: (**A**, **B**) $gp_{41}C$ (black squares), 1:1:1 T_9K:T_{16}HIV:T_{23}HIV (black circles) and an equimolar mixture of the T_9K:T_{16}HIV:T_{23}HIV trimer with $gp_{41}C$ (blue circles); (**C**, **D**) $gp_{41}C$ (black squares), 1:1:1 T_9K:T_{16}HIV:T_{23}E/K (black circles) and an equimolar mixture of the T_9K:T_{16}HIV:T_{23}E/K trimer with $gp_{41}C$ (blue circles). In all four traces red open circles represent the calculated weighted average of pure trimer and ligand signals.

ligand, a peptide based on the C-terminal portion of gp41 (gp41C) was prepared. The binding propensity of the HIV and EK heterotrimers was initially probed by CD. A solution of T_9K:T_{16}HIV:T_{23}HIV:gp41C displayed increased helicity and similar thermal

stability relative to the isolated HIV trimer (Tm = 83 deg, Figure 6A,B). In contrast, CD spectra for the analogous T_9K:T_{16}HIV:T_{23}E/K:gp41C aligned perfectly with the calculated average of the component signals (EK trimer and gp41C) indicating no specific interaction between species (Figure 6C,D). Together, these results strongly suggested a site-specific binding event between the designed HIV trimer and gp41C. In addition, control experiments lacking the T_9K peptide confirmed that all heterotrimer components were required for effective ligand binding. A pairwise mixture of T_{16}HIV and T_{23}HIV showed sample helicity and thermal stability significantly less than the intact HIV heterotrimer. The T_{16}HIV:T_{23}HIV:gp41C mixture behaved similarly to the EK complex in the presence of gp41C, confirming the inability to bind the ligand in the absence of T_9K.

Ni-NTA affinity tagging experiments provided further evidence of binding propensity by simple substitution of T_9K_{His} for T_9K. An equimolar mixture of HIV trimer and gp41C was subjected to Ni-NTA resin. HPLC analysis of the bound material showed a full equivalent of gp41C along with the three expected trimer components, indicating a tight and specific binding event (Figure 7). To test for binding-site competition from possible higher order aggregation, a related experiment was conducted where the HIV trimer was subjected to the resin prior to addition of the ligand. A single equivalent of gp41C was added to the bound trimer and the resulting material was eluted from the resin. The gp41C peptide displayed similar affinity for the designed complex as in the preformed case above, indicating that, even in the absence of ligand, blockage of the binding site by HIV trimer aggregation was not an issue.

The control experiment where the HIV heterotrimer was substituted with the EK heterotrimer was implemented to demonstrate binding specificity. A mixture of T9K, T_{16}HIV, T_{23}E/K, and gp41C was subjected to the Ni-NTA resin as above. As the EK heterotrimer presents only half of the hydrophobic binding surface from the HIV complex, we expected to see significantly decreased retention of the gp41C peptide.

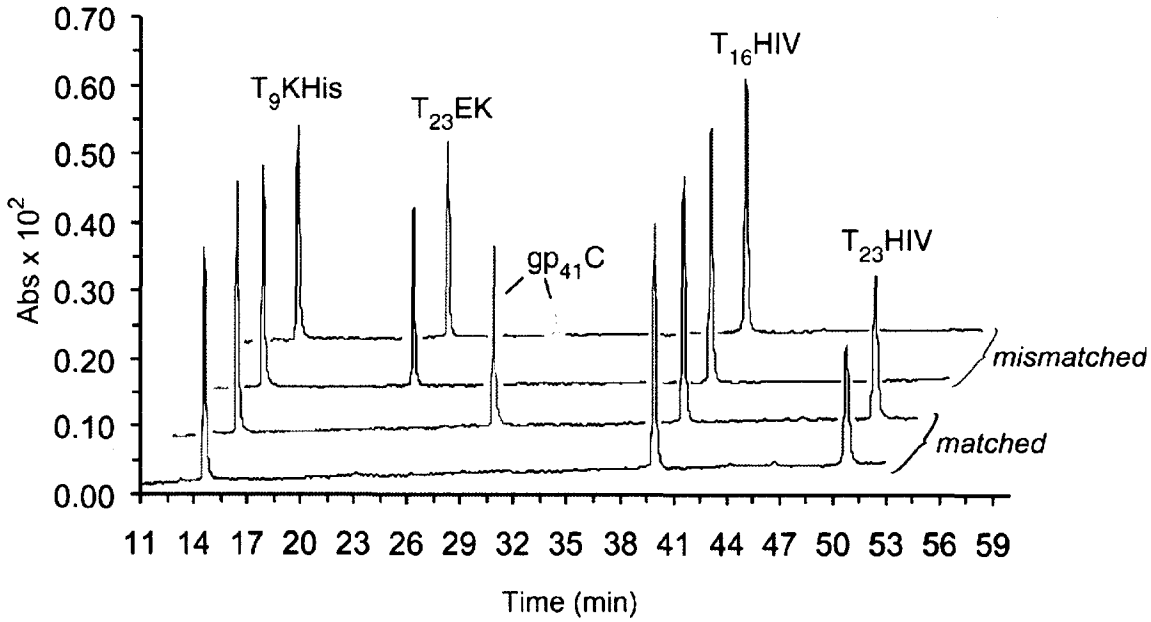

Figure 7. Ni-NTA analysis of HIV mimic. Elution fractions from four parallel experiments demonstrate that 1:1:1 T_9K_{His}:T_{16}HIV:T_{23}HIV forms a trimer (front trace), which is capable of binding gp_{41}C (blue peak, second trace); and that while a 1:1:1 T_9K_{His}:T_{16}HIV:T_{23}E/K mixture also forms a trimer (third trace), that complex has lost its affinity for gp_{41}C (red peak, fourth trace).

Analysis of the bound material reveals the near absence of gp41C amidst three EK trimer components (Figure 7).

Despite apparent oligomerization discrepancies in the HIV heterotrimer, analytical ultracentrifugation analysis of the T_9K:T_{16}HIV:T_{23}HIV:gp41C mixture gave an

apparent solution molecular weight (MWapp = 14208) consistent with that calculated for the expected tetrameric species (MWcalc = 15159). In contrast, the T_9K:T_{16}HIV:T_{23}E/K:gp41C yielded an apparent solution molecular weight (MWapp = 9345) considerably less than the calculated hypothetical tetramer (MWcalc = 15310).

These experiments confirmed that gp41C was specifically bound to the designed hydrophobic pocket of the HIV complex. As previously hoped, any aggregation that existed in the HIV heterotrimer was not an inhibitory factor in binding gp41C. This system will function as a viable model for elucidating specific interactions necessary for binding coiled coil surfaces. Facile peptide manipulation and analysis should lead to novel and effective inhibitors for a number of important viruses that employ similar entry mechanisms.

5-4: Experimental Section

Circular Dichroism Experiments: as described in Section 2-4.

Analytical Ultracentrifugation Experiments: as described in Section 2-4.

Concentration-Dependent CD: An equimolar solution of T_9K:T_{16}HIV:T_{23}HIV was prepared in PBS buffer (100μM total peptide concentration, 10mM sodium phosphate, 150mM NaCl, pH = 7.1). The solution was titrated with PBS buffer from 100 to 10μM in 5μM increments and from 10 to 2μM in 1μM increments using a Microlab 500 series automated titration assembly. Data was collected at 222nm with 60 second averaging

time following a 10-minute stir at each concentration. Data points from 100 to 55μM were discarded as the CD signal exceeded the limits of the spectrometer.

Affinity Tagging Experiments

Premixed Binding Partners: A 0.5 mL sample of a 50% slurry of Ni-NTA agarose (Qiagen) in an Eppendorf tube was centrifuged for 30 s, followed by removal of the supernatant. 1 mL of an equimolar solution (in PBS buffer, 26.6 μM total peptide concentration) of either T_9K:T_{16}HIV:T_{23}HIV:gp41C or T_9K:T_{16}HIV:T_{23}E/K:gp41C solution was added, and the tube was repeatedly inverted for 5 min. The sample was centrifuged (30 s), and the supernatant (flow-through fraction) was removed. The procedure was then repeated with 1 mL of buffer (wash fraction) and 1 mL of buffer containing 250 mM imidazole (elution fraction), except that the wash fraction was not agitated for 5 min. Solutions were analyzed by RP –HPLC: C-18 column, linear gradients of solvent A (1% acetonitrile in water, 0.1% v/v CF_3CO_2H) and solvent B (10% water in acetonitrile, 0.07% v/v CF_3CO_2H).

Addition of gp41C to Bound Trimer: Ni-NTA agarose slurry (1 mL) was added to a 1.5 mL Eppendorf tube and centrifuged for one minute, followed by supernatant removal (discarded). Initial T_9K:T_{16}HIV:T_{23}HIV solution (1 mL, 20 μM total peptide concentration) was added to the beads and the Eppendorf tube was repeatedly inverted for five minutes, and centrifuged for one minute, followed by supernatant removal (flow through fraction). The beads were then washed with 1 mL of PBS buffer (10 mM phosphate, 150 mM NaCl, pH = 7.1) by repeated inversion for 30 seconds, centrifugation for one minute, and supernatant removal (wash fraction). The gp41C solution (1 mL,

6.66 μM total peptide concentration, PBS buffer) was added followed by repeated inversion of the Eppendorf tube for five minutes, centrifugation for one minute, and supernatant removal (addition fraction). The wash procedure is repeated. Following the final wash, all remaining bound peptides were eluted by addition of PBS buffer containing 250mM imidazole (elution fraction) Each fraction was analyzed by reverse-phase HPLC: C-18 column, linear gradients of solvent A (1% acetonitrile in water, 0.1% v/v CF_3CO_2H) and solvent B (10% water in acetonitrile, 0.07% v/v CF_3CO_2H).

5-5: Literature Cited

(1) (a) Barre-Sinoussi, F., Chermann, J. C., Rey, F., Nugeyre, M. T., Chamaret, S., Gruest, J., Dauguet, C., Axler-Blin, C., Vezinet-Brun, F., Rouzioux, C., *et al*) *Science* **1983**, *220*, 868-871. (b) Gallo, R. C., Salahuddin, S. Z., Popovic, M., Shearer, G. M., Kaplan, M., Haynes, B. F., Palker, T. J., Redfield, R., Oleske, J., Safai, B., *et al*. *Science* 1984, *224*, 500-503.

(2) (a) Markosyan Ruben, M.; Ma, X.; Lu, M.; Cohen Fredric, S.; Melikyan Grigory, B. *Virology* **2002**, *302*, 174-184. (b) Eckert, D. M.; Kim, P. S. *Ann. Rev. Biochem.* **2001**, *70*, 777-810. c) Chan, D. C.; Kim, P. S. *Cell* **1998**, *93*, 681-684.

(3) Chan, D. C.; Fass, D.; Berger, J. M.; Kim, P. S *Cell* **1997**, *89*, 263-273.

(4) (a) Gulick, R. M. *Clin. Microbiol. Infect.* **2003**, *9*, 186-193. (b) Reeves, J. D.; Gallo, S. A.; Ahmad, N.; Miamidian, J. L.; Harvey, P. E.; Sharron, M.; Pohlmann, S.; Sfakianos, J. N.; Derdeyn, C. A.; Blumenthal, R.; Hunter, E.; Doms, R. W. *Proc. Nat. Acad. Sci. USA* **2002**, *99*, 16249-16254. (c) Markosyan, R. M.; Ma, X.; Lu, M.; Cohen, F. S.; Melikyan, G. B. *Virology* **2002**, *302*, 174-184. (d) Eckert, D. M.; Kim,

P. S. *Proc. Nat. Acad. Sci. USA* **2001**, *98*, 11187-11192. (e) Chan, D. C.; Chutkowski, C. T.; Kim, P. S. *Proc. Nat. Acad. Sci. USA* **1998**, *95*, 15613-15617.

(5) Schnarr, N.A., Kennan, A.J. *Manuscript in preparation.*

(6) Weissenhorn, W., Calder, L.J., Dessen, A., Laue, T., Skehel, J.J., Wiley, D.C. *Proc. Nat. Acad. Sci. USA* **1997**, *94*, 6065-6069.

(7) Eckert, D.M, Kim, P.S. *Proc. Nat. Acad. Sci. USA* **2001**, *98*, 11187-11192.

(8) Root, M.J., Kay, M.S., Kim, P.S. *Science* **2001**, *291*, 884-888.

(9) Tam, J.P., Yu, Q. *Org. Lett.* **2002**, *4*, 4167-4170.

(10) Gochin, M., Guy, R.K., Case, M.A. *Angew. Chem. Int. Ed. Engl.* **2003**, *42*, 5325-5328.